Infrared Spectroscopy of Star Formation in Galactic and Extragalactic Regions

Grant NAG5-10659

Annual Performance Report No. 2

For the period 1 March 2002 through 28 February 2003

Principal Investigator:

Dr. Howard A. Smith

January 2003

Prepared for
National Aeronautics and Space Administration
Washington D.C.

Smithsonian Institution
Astrophysical Observatory
Cambridge, Massachusetts 02138-1596

The Smithsonian Astrophysical Observatory
is a member of the
Harvard-Smithsonian Center for Astrophysics

The NASA Technical Officer for this grant is Dr. Hashima Hasan, NASA Headquarters, 300 E Street SW, Code SZ, Washington DC 20546-0001

Table of Contents

I. Program Objectives

In this program we proposed to perform a series of spectroscopic studies, including data analysis and modeling, of star formation regions using an ensemble of archival space-based data from the Infrared Space Observatory's Long Wavelength Spectrometer and Short Wavelength Spectrometer, and to take advantage of other spectroscopic databases including the first results from SIRTF. Our emphasis has been on star formation in external, bright IR galaxies, but other areas of research have included young, low or high mass pre-main sequence stars in star formation regions, and the galactic center. The OH lines in the far infrared were proposed as one key focus of this inquiry, because the Principal Investigator (H. Smith) had a full set of OH IR lines from ISO observations. It was planned that during the proposed 2-1/2 year timeframe of the proposal other data (including perhaps from SIRTF) would become available, and we intended to be responsive to these and other such spectroscopic data sets.

The program has the following goals:

1) Refine the data analysis of ISO observations to obtain deeper and better SNR results on selected sources. The ISO data itself underwent pipeline 10 reductions in early 2001, and the more "hands-on data reduction packages" have been released. The ISO Fabry-Perot database is particularly sensitive to noise and can have slight calibration errors, and improvements are anticipated. We plan to build on these deep analysis tools and contribute to their development.

2) Model the atomic and molecular line shapes, in particular the OH lines, using revised montecarlo techniques developed by the Submillimeter Wave Astronomy Satellite (SWAS) team at the Center for Astrophysics.

3) Use newly acquired space-based SIRTF or SOFIA spectroscopic data as they become available, and contribute to these observing programs as appropriate.

4) Attend scientific meetings and workshops.

5) E&PO activities, especially as related to infrared astrophysics and/or spectroscopy.

The program since its inception has been extremely successful: We presented or submitted more than about a dozen articles, sponsored a workshop, and participated in scientific conferences. The molecular line montecarlo code has undergone important revisions for infrared lines, and has made significant predictions. No SIRTF data are of course available yet, but we have made useful contributions to pending SIRTF science observations. E&PO programs have been active, including the exhibit at Boston's Museum of Science. We anticipate progress to continue in all areas. Detailed descriptions of all these results follow below.

II. Justification for a Six-Month Grant Supplement

The third and final year of this program, as presented in our original proposal P5031-10-00 (October 2000), covered the six-month period 1 January 2003 through 30 June 2003. In proposal P5511-1-03 submitted concurrently with this report we request that this half-year's effort be supplemented to allow for a full year of effort at the same rate of $64,437 for the additional six months. This supplement will enable us bring to a thorough close all of these activities. We have three reasons for making this request:

1) As planned for this program, the PI has become involved in the SIRTF IRAC and IRS science planning activities. He is, as described below, the SIRTF lead on several "Early Release Observations," as well as an active participant in several GTO programs through his IRAC colleagues. Appendix B contains several documents pertaining to these activities. In addition Dr. Smith has been active in preparing for E&PO activities on behalf of the SIRTF/IRAC instrument team (Fazio). Dr. Smith is not receiving any support from SIRTF for any of these contributions -- all his effort is covered by this current grant. SIRTF, originally "scheduled" for launch in December

2001, has now been rescheduled for an April 2003 launch. Dr. Smith would like to be able to continue to participate at the current level for another six months, and one aspect of this grant supplement request is to enable such participation. With NASA Headquarters' consent, at the conclusion of this additional six-month period any further support for participation in SIRTF would be requested via SIRTF channels.

2) As described in more detail below, the montecarlo code used for line modeling contained several errors. Although these errors did not introduce significant problems in the results of submillimeter modeling for which the code was designed, they did generate significant errors in the far-infrared line shapes and fluxes. The analysis of IR spectra is the central goal of this project. By collaboration with other montecarlo users we were able to track down the errors and repair the code, but this effort has delayed us by more than six months in the analysis of the fluxes. This requested six-month supplement would enable us to recoup the time spent fixing the code. (The revised code has now been distributed to all code users, benefiting to various degrees numerous other projects.) The budget supplement request includes 280 hours of Dr. Smith's time.

3) Our previous collaborations with Dr. Eduardo González (University of Alcalá, Spain) have proved to be very productive. As described below this grant supported his visit to Smithsonian Astrophysical Observatory (SAO) for one week last summer, with the result that significant errors in the current montecarlo code were tracked down and fixed. In addition we note that Prof. González and his colleague Dr. Pepe Chernicharo have developed new algorithms for ISO data spectral line reduction, and we intend to take advantage of them while he is here visiting. Figure 1 shows their improved analysis of the spectrum of Arp 220, listing numerous detections of the lines of H_2O. We would like to continue to work together for a more intensive and longer interval, and Prof. González has received permission to spend four months at SAO next spring/summer. We propose using funds from the requested supplement to enable his visit to SAO. The requested supplement budget includes support for his travel (four-month visit) as well as a standard stipend.

III. Progress Report

A. ISO Data Analysis and Modeling

Last spring we submitted a paper entitled "The Far Infrared Lines of OH as Molecular Cloud Diagnostics" to the 2nd Maryland Conference on Far IR Astronomy, 2002. This analysis was based on the SWAS montecarlo code modeling of the OH lines in galaxies observed by ISO. Since that meeting last spring considerable effort has been put into improving the montecarlo code. A group of European astronomers, including Dr. Pepe Chernicharo and Prof. Eduardo González, had been performing montecarlo modeling of other molecules seen in ISO galaxies. Figure 1 shows their improved reduction of the Arp 220 ISO spectrum, which reveals numerous lines of water and other species. We began to communicate to them our results for the purpose of comparing our conclusions. The discussions proved very useful because their code had several different procedures embedded in it. After much progress, we were still unable to come to full agreement on several aspects of the modeling, and we used this grant to bring Prof. González to Cambridge for an intensive working visit. We compared the details of the codes themselves and found several small but important errors that we corrected, as well as a few assumptions that made our results differ. This work has been ongoing for the past six months, and we are now at a point where we reach essentially identical results on the same model. While this seems like it should be an obvious and easy result, montecarlo modeling is quite complex, with many random variations, and our ability to have two different codes reach similar agreement is a strong confirmation for each of us. Figure 2 is a plot modeling the twelve different lines of OH observed in one or more galaxies for an 11-shell model that we used as a template to consider the radiation from Arp 220. Note that all of the lines but two are in absorption, as is observed. Figure 3 shows a clearer view of two key lines as modeled for Arp 220 (two different MC "kernels" used for each).

We would like to have Prof. González spend a more extended period of time with us next spring -- nominally a four-month visit -- which would in part be covered by this grant supplement.

B. Other Science Results

SIRTF: SIRTF science development was a major component of this year's research. This program

supported the development of five "Early Release Objects" for SIRTF observations on which Dr. Smith was Principal Investigator or Co-Investigator. The early release program is designed to rapidly present to the public and the scientific community some exciting results from SIRTF in the first months of its operation. The SIRTF instrument and science teams submitted proposals for ERO objects, and a competitive selection process narrowed these down to a small group with exciting science and realistic observational parameters. This grant supported Dr. Smith's participation in the ERO process, including developing science goals, identifying key objects for observation, and developing the detailed AOR (observing formulae) to be use by the instruments for mapping, integrating, etc. Appendix B contains copies of those ERO programs on which we are either Principal Investigator or Co-Investigator. In addition, Dr. Smith has become involved in IRAC GO planning. Appendix B also contains a statement about the use of the IRAC surveys to detect and analyze Extremely Red Objects and Hyper-Extremely Red Objects: distant galaxies that may be either massive, dusty elliptical galaxies at z~1 from mergers of older galaxies (at least in the so-called "hierarchical models"), or more primordial objects formed at earlier epochs, subsequently evolving into the older elliptical population we see (the so-called "evolutionary models").

An Imaging Fabry-Perot: During this period we also began work on a new instrument, an IR Fabry-Perot (FP), for use on the MMT. We are still in the early stages, and have proposed to SAO for support to bring a prototype instrument to Mt. Hopkins for testing. This instrument would perform wide field infrared spectral imaging in [J], [H], and [K] bands. A principal motivation for this kind of observation is to study the form of emission-line regions, particularly where the envisioned resolution of 200 km/sec or so is good enough to provide interesting information about the kinematics of the region, by scanning the filter band across the emission line profile. It would be possible, for instance, to image the inner parts of the forbidden-line regions of active galactic nuclei and thus to sort out some of the kinematics there. The tunable filter enables observations of key lines in galaxies with any redshifts that leave features in the J, H, and K bands. This near-IR spectral information could be combined with shorter-wavelength data from HST at comparable spatial and spectral resolution to understand patterns of extinction.

An FP would provide a very strong extension of several lines of work in this area that we have done at the MMT and elsewhere. This has included spectroscopy of line profiles, early high-resolution maps from speckle techniques, study of continuum extinction and thermal emission by dust, and study of extinction with the aid of infrared spectroscopy.

Some lines that are useful are:

HI:	5-3 (Paschen beta)	1.28 microns
	7-4 (Brackett gamma)	2.16
HeI:	1s2s-1s2p	1.08
	4D-3P	1.70
H2:	1-0 S(0)	2.22
FeII:	D(7/2)-F(9/2)	1.64
SII:	2D-2P	1.03

As well as in AGNs, these lines have been used in the diagnosis of HII regions and shocks. Our proposed instrument would provide a spatial resolution of 0.1 parsec in the Orion nebula to observe bright FeII and H2 lines in bow shocks in the vicinity of proplyds and "bullet" ejecta. The narrow bandwidth will also reduce background, particularly in the K band, and enable observations to be made in clear regions between night sky OH lines. This can produce deep, uncontaminated images, with full exploitation of the properties of state-of-the-art detectors.

Other Science: Appendix A includes a copy of another article resulting from some of this effort: "IR Fine-Structure Line Signatures of Central Dust-Bounded Nebulae in Luminous Infrared Galaxies."

During this period we worked with Dr. Sarah Leeks, a new postdoctoral scientist, whose thesis we helped to supervise (see Annual Performance Report #1) to prepare a paper for publication based on those results, entitled "High Mass Star Formation Regions Observed with ISO-LWS; I. W28 A2."

C. Advising Students and Postdocs

During this period we acted as advisors to two postdoctoral scientists. The first was Dr. Lisa Kew-

ley, who worked on IRB and ULIGs. Her project proposal, "The Starburst-AGN Connection (Appendix C)," probes exactly the kinds of problems supported by this grant. Some of her results are presented in "Do Mergers Stop Monsters?" Kewley, L., Dopita, M., and Smith, H.A., B.A.A.S., **199**, 4304, 2001.

Dr. Oren Sternberg, who worked on metal mesh filters for astronomy, was also a postdoctoral scientist during this period, although not supported by this grant. The filter work has resulted in two publications in press: "Designer Infrared Filters: A Nanotechnology Fabrication Process using Stacked Metal Lattices," by H.A. Smith, M. Rebbert, and O. Sternberg (submitted to *Science*), and "A New Nanotechnology Process for Making Precise Infrared Filters using Layered Metal Mesh Grids," by H.A.Smith et al., B.A.A.S., January 2003.

D. E&PO Activities

During this period the PI gave several talks to elementary school groups, as well as to a summer camp. He also helped to prepare the E&PO program for SIRTF/IRAC. He was an advisor to the Boston Museum of Science cosmological exhibition, "Cosmic Horizons," which opened in September 2002. His paper, "Public Attitudes Towards Space Science," will appear in the upcoming issue of *Space Science Reviews*.

IV. Program Plans

During the final year of this program we intend to bring to closure the projects discussed to date:

1) Reduction of the ISO galaxy data set using the Chernicharo/González algorithms
2) Modeling the OH lines with the corrected and improved montecarlo code
3) Tightening the arguments made in our earlier article -- that there are three types of active/IRB galaxies as typified by the kinds of molecular clouds that dominate their FIR emission: large diffuse clouds as in normal IRBs; smaller, more dense clouds as in Arp 220 and other mixed AGN; and very dense small cloudlets as seen in the Seyfert galaxy NGC 1068.

We would like to bring Prof. González to Cambridge for a four-month visit to work on these modeling techniques.

We anticipate that SIRTF will finally be launched in the spring of 2003 and, depending on the date and available objects, that several of our early release objects will be observed and analyzed.

We will continue to be active in E&PO, including an aggressive IRAC/SIRTF E&PO effort associated with the first days of the mission.

In order to bring all of these projects to a successful close, we have requested that the original six-month funding be supplemented by a like amount to enable a full year of support for the programs.

V. Reportable Patents/New Technology

There have been no reportable patents/new technology made under this grant.

Figure Captions

Figure 1: The observed ISO spectrum of Arp 220, showing the reduction of Chernicharo and González. Many lines of water are now apparent, as well as the OH lines, CH, and atomic lines of CII. New montecarlo modeling enables us to calculate column densities and physical conditions for all these lines.

Figure 2: Montecarlo modeling of the OH lines in Arp 220, based on an 11-shell model. The line profiles are all in absorption, as seen in the source, with the weak exception of the 163μm line (also observed). Lines are identified by wavelength in the key box on the right of the figure.

Figure 3: A clearer view of two of the OH lines modeled for Arp 220: the 84μm line and the 119μm fundamental line. The modeling shows that there is a weak emission component at the wings, but the present ISO data are unable to resolve this. We hope that future SOFIA instruments will be able to detect such line-shape structure. In the meantime, the observations of the net line are in good agreement with the modeling, which shows them to be in absorption.

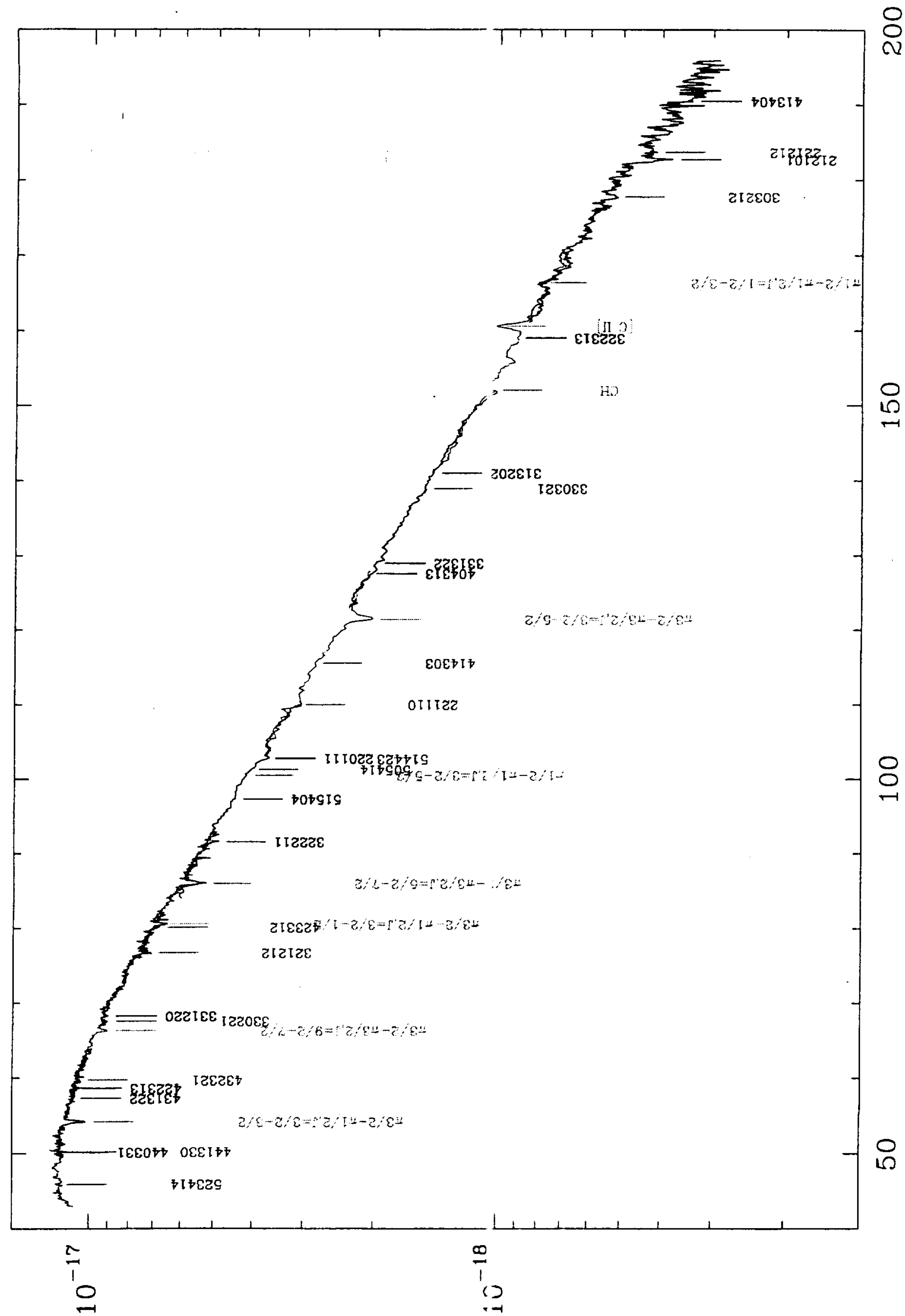

Figure 1

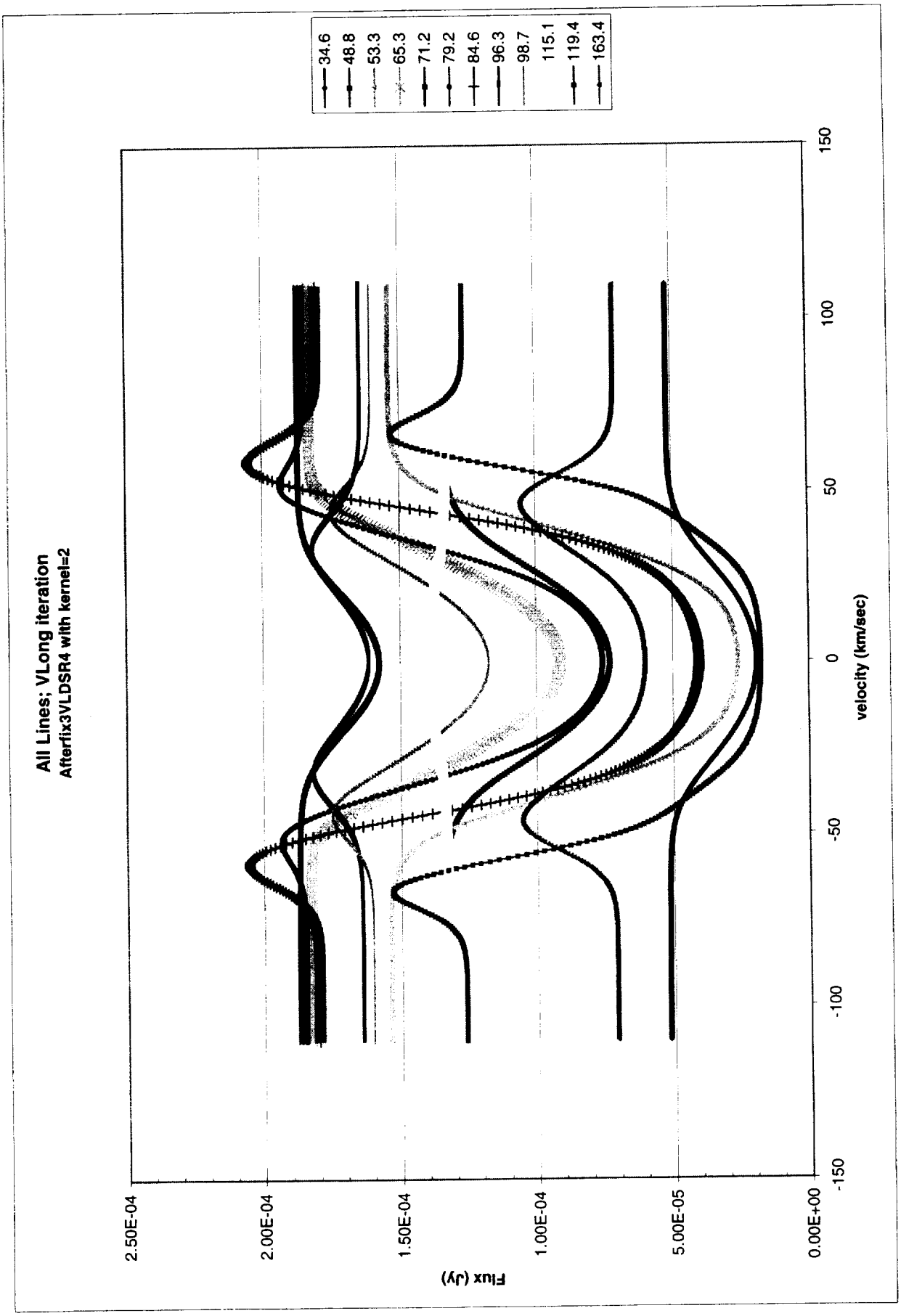
All Lines; VLong iteration
Afterfix3VLDSR4 with kernel=2
34.6
48.8
53.3
65.3
71.2
79.2
84.6
96.3
98.7
115.1
119.4
163.4
2.50E-04
2.00E-04
1.50E-04
1.00E-04
5.00E-05
0.00E+00
Flux (Jy)
150
100
50
0
-50
-100
-150
velocity (km/sec)

Figure 2

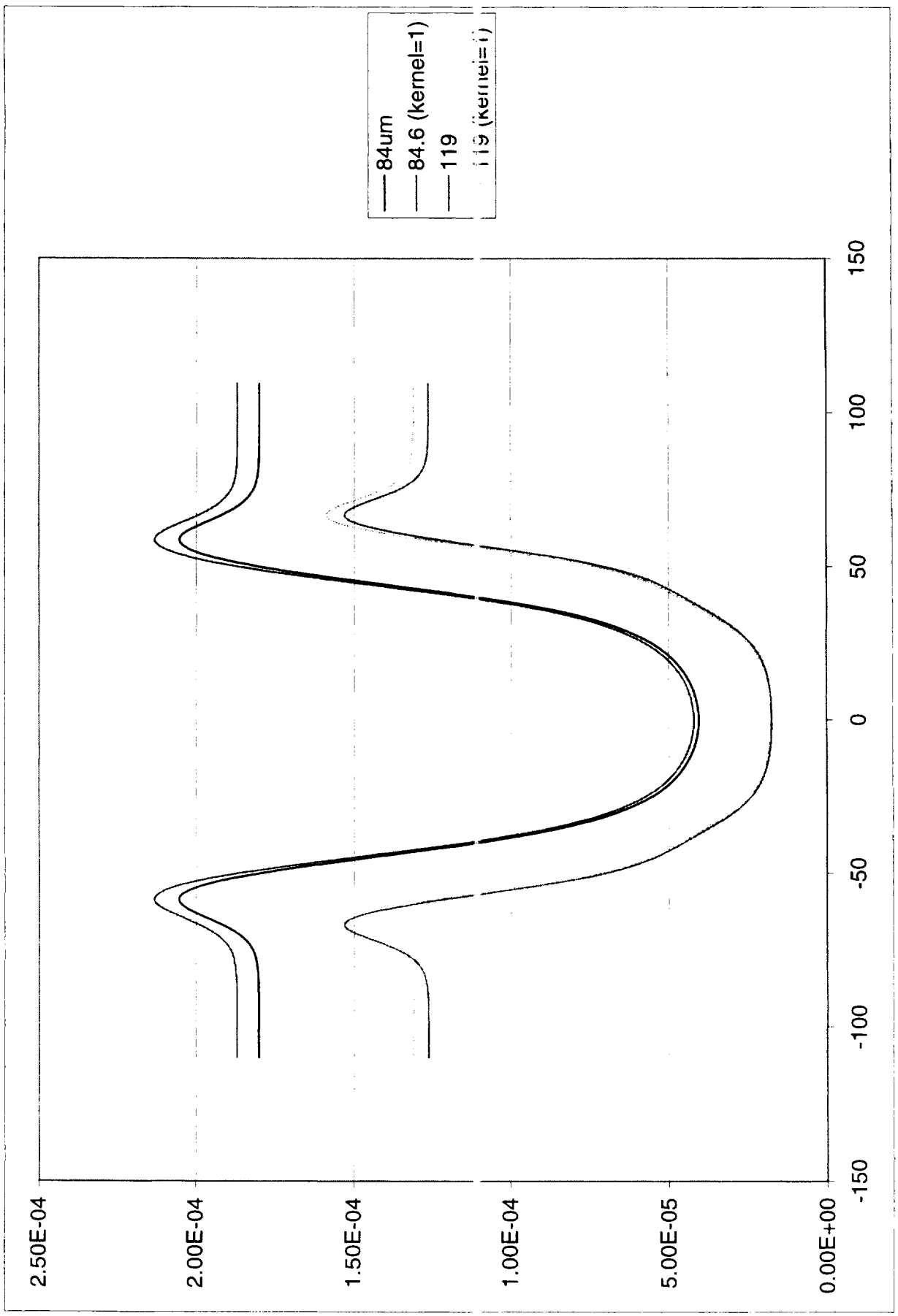
84um
84.6 (kernel=1)
119
2.50E-04
2.00E-04
1.50E-04
1.00E-04
5.00E-05
0.00E+00
150
100
50
0
-50
-100
-150

Figure 3

The far-infrared emission line and continuum spectrum of the Seyfert galaxy NGC 1068[1]

Luigi Spinoglio

Istituto di Fisica dello Spazio Interplanetario, CNR via Fosso del Cavaliere 100, I-00133 - Roma (Italy)

luigi@ifsi.rm.cnr.it

Matthew A. Malkan

Physics and Astronomy Department, University of California, Los Angeles

malkan@astro.ucla.edu

Howard A. Smith

Harvard-Smithsonian Center for Astrophysics, Cambridge, USA

Jackie Fischer

Naval Research Laboratory, Washington, USA

ABSTRACT

The prototypical Seyfert type 2 galaxy NGC 1068 has been observed with the *Long Wavelength Spectrometer* (LWS) onboard the *Infrared Space Observatory* (ISO, ESA). This provides the first complete far-infrared spectrum from 43 to 197μm. In addition to the 7 expected ionic fine structure emission lines, we also detect OH rotational lines at 79, 119 and 163μm. Unlike any other galaxy yet observed, NGC 1068 shows all these lines in emission. To increase the information on the strong ionic emission lines powered either by the Seyfert nucleus and the starburst, we have included in our analysis measurements in the 2–35μm spectral range from the ISO *Short Wavelength Spectrometer* (SWS), as well as optical and ultraviolet lines from the literature. To model the observed line intensities we have considered three emission components: the AGN component, the starburst component originated from the circumnuclear ring at $\sim$ 15 $''$ form the center and the nuclear starburst component. The nuclear emission line spectrum from the AGN was modeled using a photoionization model with a constant density of 2000 cm^{-3} and an emission region at a distance from the center of $\sim$ 30-60 pc.

We have adopted three different ionizing continua illuminating the AGN narrow line region: the first one, already suggested in the recent literature, has a large absorption dip around 4 Ryd; the second has the standard broken power-law shape generally used for NGC1068 and the third has a big blue bump peaking at $\sim$ 10 Ryd. We find that the UV to mid-IR emission line spectrum originated from the AGN cannot be used to constrain the ionizing continuum that illuminates the NLR of NGC1068, contrary to previous results. We have used the Br γ emission from the circumnuclear ring and that one originated from the nuclear region to normalize the starburst emission of the second and third component, respectively. The ionizing continua for the starburst models have been derived from starburst synthesis models.

The OH emission lines observed in NGC1068 have been modeled using.....

Subject headings: galaxies: individual (NGC 1068) – galaxies: active – galaxies: nuclei – galaxies: Seyfert – galaxies: emission lines – galaxies: starburst – infrared: galaxies.

1. INTRODUCTION

NGC 1068 is among the most studied active galaxies. It is known as the archetype Seyfert type 2 galaxy, it is nearby (distance D=15.2 Mpc, redshift z=0.0038 adopting H_0=75 km s^{-1} Mpc^{-1}), providing a scale of only $\sim$ 74 pc/″, bright ($L_{IR} = 2 \times 10^{11} L_\odot$ Bland-Hawthorn et al. 1997) and it has been extensively observed and studied in detail from X-rays to radio wavelengths. Around the active nucleus, NGC 1068 has a central nuclear star cluster extending $\sim$0.6″ (Thatte et al. 1997). Moreover, a stellar bar of 2.3kpc of size has been observed in the near-IR (Scoville et al. 1988; Thronson et al. 1989), which is surrounded by a circumnuclear starburst ring. Mapping revealed that the infrared emission in NGC 1068 was due to both the Seyfert nucleus (dominating the 10μm emission) and to the star forming regions in the bright circumnuclear ring of $\sim$ 3kpc in diameter (emitting most of the luminosity at $\lambda > 30\mu m$) (Telesco et al. 1984). A $Br\gamma$ imaging study (Davies, Sugai & Ward 1998) reveals a similar morphology. It indicates that a short burst of star formation occurred throughout the circumnuclear ring (15-16 ″ in radius) perhaps within the last 4-40 Myr. CO interferometer observations revealed molecular gas very close to the

[1]ISO is an ESA project with instruments funded by ESA Member States (especially the PI countries: France, Germany, the Netherlands and the United Kingdom) and with the participation of ISAS and NASA.

nucleus ($\sim$0.2″) suggesting the presence of $\sim 10^8 M_\odot$ within the central 25pc (Schinnerer et al. 2000).

In this article, we present the first complete far-infrared spectrum from 43 to 197μm showing both atomic and molecular emission lines (§2.). We model the far-IR continuum emission using gray body functions (§3.), we also model the composite UV- to far-IR atomic emission line spectrum, as derived by combining literature observations with our data, using photoionization models of both the active nucleus (§4.1) and the starburst components (§4.2-4.3). Moreover, montecarlo radiation transfer models have been used to account for the detected far-IR molecular lines (§5.). Our conclusions are then given in §6.

2. OBSERVATIONS

NGC 1068 was observed with the Long Wavelength Spectrometer (LWS) (Clegg et al. 1996) on board the Infrared Space Observatory (ISO) (Kessler et al. 1996), as part of the Guaranteed Time Programme of the LWS instrument team. The full low resolution spectrum (43-197μm) of NGC 1068 was collected during orbit 605 (July 13, 1997). Two on-source full scans (15,730 seconds of total integration time) and two off-source (6' N) scans of the [CII]158μm line (3,390 seconds of total integration time) were obtained. On- and off-source scans had the same integration time per spectral step. Because of the design of the LWS spectrometer, simultaneously with the 158μm data, a short spectral scan of equal sensitivity to the on-source spectrum was obtained at sparsely spaced wavelengths across the LWS range.

The LWS beam is roughly independent of wavelength and equal to 80 arcsec. The spectra were calibrated using Uranus, resulting in an absolute accuracy better than 30% (Swinyard et al. 1996). The data analysis has been done with ISAP[2], starting from the auto-analysis results processed through the LWS Version 7-8 pipeline (July 1998). To be confident that newer versions of the pipeline and calibration files did not yield different results, we have compared our data with the results obtained using pipeline 10.1 (November 2001) and we did not find significant differences on both the line fluxes and the continuum. To increase the signal-to-noise ratio, all the full grating scans taken on the on-source position

[2]The ISO Spectral Analysis Package (ISAP) is a joint development by the LWS and SWS Instrument Teams and Data Centers. Contributing institutes are Centre d'Etude Spatiale des Rayonnements (France), Institute d'Astrophysique Spatiale (France), Infrared Processing and Analysis Center (United States), Max-Planck-Insitut für Extraterrestrische Physisk (Germany), Rutherford Appleton Laboratories United Kingdom) and the Space Research Organization, Netherlands.

have been coadded, as well as the two sets of data on the off-source position. No signal was detected in the off-source position. The emission line fluxes were measured with ISAP, which fits Gaussians on top of a local continuum. In every case the observed line width was consistent with the instrumental resolution of the grating, which is typically 1000 km/sec. The integrated line fluxes measured independently from data taken in the two scan directions agreed very well, to within 10%. LWS has a known tendency for fringing to produce spurious ripples in the continuum baseline (Swinyard et al. 1998). Fortunately, these fringing ripples are hardly noticeable in our LWS spectrum, presumably because the far-IR continuum is centrally concentrated towards the center of the LWS 80 arcsec beam.

Besides the LWS observations, we also use the SWS observations presented by Lutz et al. (2000), to extend the wavelength and ionization-level coverage. Table 1 presents all the line flux measurements, including those from the SWS.

3. THERMAL CONTINUUM SPECTRUM

The 50-200μm far-infrared spectral energy distribution (SED) of NGC1068 can be fitted by the combination of different gray body functions. Fig. 1 shows a fit with the main gray body component at T=32K, a warmer component at T=65K and a cooler one at T=20K. The dust emissivity has been assumed to be proportional to the inverse square of the wavelength (i.e., the flux density is $S_\lambda = B_\lambda(T) \times \lambda^{-\beta}$ with $B_\lambda(T)$ the Planck function at the wavelength λ and temperature T and β=2). We have adopted this steep dust emissivity law because it fits better than flatter laws the 12-200 μm SED of Seyfert and starburst galaxies, as shown in Spinoglio, Andreani & Malkan (2002).

Because of the large (3) number of components used, we do not claim that the proposed fit is unique, however it fits the 50-200μm spectrum fairly well (reduced χ^2=0.40, corresponding to a probability of P>98%) and it is derived from a physically consistent view of the various dust thermal components in Seyfert galaxies (see e.g. Spinoglio, Andreani & Malkan 2002).

4. THE FINE STRUCTURE LINES

We have combined our far-infrared fine structure line measurements (Table 1) with ultraviolet, optical and infrared spectroscopic data from the literature (Kriss et al. 1992; Marconi et al. 1996; Thompson 1996; Lutz et al. 2000). However, the far-IR spectrum includes several low-ionization lines that are also produced outside the narrow line region

(NLR) of the active nucleus. For this reason, we find that no single model satisfactorily explains all the observed emission line ratios. We identify three components:

- an AGN component exciting the high ionization lines and contributing little to the low-to-intermediate ionization lines;
- a starburst component in the circumnuclear ring of the galaxy (e.g. Davies, Sugai & Ward 1998) that produces part of the emission of the intermediate ionization lines;
- another starburst component that originates from the nucleus of NGC1068.

We will also see that a photo-dissociation region (PDR), in the interstellar medium of the galaxy, has also to be added to fully model the low ionization and neutral forbidden lines.

The contributions of the starburst and PDR emission can be estimated from the CII/OI/OIII line ratio diagram, as used by Malkan et al. (2002). However, for this galaxy we can obtain a more direct measurement of the starburst/HII region components, using the high spatial resolution available from ground-based near-IR Fabry-Perot imaging and grating spectroscopy. As shown in §4.2 and §4.3, we have taken the Br_γ fluxes originated in the ring-like star forming complex and from the nuclear region of NGC 1068, respectively from Davies, Sugai & Ward (1998)and from Oliva & Moorwood (1990).

In the following of this section, we will examine separately the three components that are producing the composite fine structure emission line spectrum of NGC1068, for which we propose three different computation in §4.4. We will leave for §4.5 the estimate of the model parameters of the PDR emission produced from the ISM of the galaxy.

4.1. Modeling the AGN

The first predictions based on photoionization models of the mid to far-infrared spectrum originated from the Narrow Line Regions (NLR) of active galaxies has been done by Spinoglio & Malkan (1992), well before the observations could be collected. The specific photoionization modeling of the high ionization emission lines produced by the Seyfert nucleus of NGC1068 has been done previously by Alexander et al. (2000). We will compare their results with other models to see if their conclusions are unique or not. To model the emission from the AGN in NGC1068, we have used the photoionization code CLOUDY (Version 94.00 Ferland 2000). Following the results of Alexander et al. (2000), we have assumed a gas with a constant Hydrogen density of 2×10^3 cm^{-3} and an ionization parameter in the

range 0.03<U<0.1. Table 2 reports the results of the three models we have chosen to fit the NGC1068 spectrum, together with the observed line fluxes. The intrinsic nuclear spectrum of NGC 1068 has been inferred by Pier et al. (1994), we have modified this in the 1–100 Ryd region to model both the through derived by Alexander et al. (2000) and a *big blue bump*, as expected by the thermal emission of an accretion disk around the central black hole (ref). Specifically, model A assumes the same ionizing spectrum that was derived from the best fit model of Alexander et al. (2000), i.e. with a deep through at 4 Rydberg (log$f$ = -27.4, -29.0, -27.4, -28.2 at 2, 4, 8 and 16 Ryd, respectively). Model B assumes the original ionizing spectrum derived from Pier et al. (1994). Model C assumes a Big Blue Bump spectrum on the top of the Pier et al. (1994) ionizing continuum (log$f$ = -25.8, -25.8, -25.8, -27.4 at 2, 4, 8 and 16 Ryd, respectively). To derive the fluxes observed at Earth we have transformed the intensities given by the photoionization code assuming that the NLR clouds were at the distance of 59, 27 and 29 pc from the ionizing source for the three models A, B and C, respectively. These correspond to angular distances of 0.8 and 0.4 ″, respectively.

We can see from Table 2 that all the three models represent fairly well most of the observed line fluxes, except for the low and intermediate ionization lines, that — as we expect — are also, and sometimes mainly, produced by starburst and PDR excitation. Going into more details, we prefer model C because it predicts less emission in those intermediate ionization lines typical of HII regions/starbusrt emission, like [OIII], [NeIII] and matches the observed emission of [SIV]. We also list in Table 3 the dereddened fluxes for the ultraviolet and optical lines, assuming an E_{B-V} = 0.4 mag (Malkan & Oke 1983).

4.2. Modeling the starburst ring

NGC1068 is known to emit strong starburst emission from both its nucleus and the ring-like structure at 15-16 ″from the nucleus, traced e.g. by the Br γ emission (Davies, Sugai & Ward 1998). To model this second component, we have considered how much of the Br γ line was emitted inside the different apertures of the ISO spectroscopic observations. In the smallest ISO-SWS aperture used (14 ″ × 20 ″) no Br γ emission is detected from the ring. In the next aperture (14 ″ × 27 ″) Davies, Sugai & Ward (1998)'s regions I, J, K and L are included, for a total Br γ intensity of $\sim 10^{-14}$ erg s^{-1} cm^{-2}. The largest SWS aperture (20 ″ × 33 ″), in addition to the above regions also contains regions H, E, D and C, for a total Br γ intensity of $\sim 2.2 \times 10^{-14}$ erg s^{-1} cm^{-2}. Finally, in the large LWS aperture ($\sim$ 80 ″^{2}), all the ring-like Br γ emission is contained, $\sim 5.9 \times 10^{-14}$ erg s^{-1} cm^{-2}.

Assuming that applies "case B" recombination, we can scale the Brγ intensity into Hα intensity (from Table 4.4 of Osterbrock 1989)

$$j_{Br_\gamma}/j_{H_\alpha} = j_{Br_\gamma}/j_{H_\alpha} \cdot j_{Br_\gamma}/j_{H_\epsilon} \cdot j_{H_\epsilon}/j_{H_\beta} \cdot j_{H_\beta}/j_{H_\alpha} = 0.0097$$

For the three increasing apertures (14 $''$ × 20 $''$, 14 $''$ × 27 $''$ and 20 $''$ × 33 $''$, respectively) we have derived an Hα intensity from the starburst ring of 10^{-12}, 2.3 × 10^{-12} and 6.1 × 10^{-12}, respectively. We have used these values to derive the modeled line intensities from the CLOUDY code, that was used adopting Hα as normalizing line.

We have chosen some of the starburst synthesis models Starburst99 from Leitherer et al. (1999) as input ionizing spectra for the CLOUDY photoionization code. For the models with instantaneous star formation law, we adopted a total mass of M = 10^6 $M_\odot$, and a duration of 5 Myr, while for the models with continuous star formation law, we have chosen a star formation rate of 1 $M_\odot$ yr^{-1}. For both types of models we adopted a Salpeter IMF (α=2.35), a lower cut-off mass of 1 $M_\odot$, an upper cut-off mass of 100 $M_\odot$, abundances of Z=0.008 and nebular emission included

We report in Table 3 the results relative of two instantaneous models (SBR A and B, where SBR stands for Starburst Ring) and the four continuous models (SBR C, D, E and F).

4.3. Modeling the nuclear starburst

We have computed also the expected emission that originates from the nuclear starburst. To model this third component, we have used the Br γ intensity of 13 × 10^{-14} erg s^{-1} cm^{-2}, which was observed in a 6″× 6″aperture (Oliva & Moorwood 1990). As a first order approximation, we make the assumption that half of the Br γ intensity observed in the nuclear region is originated from the nuclear starburst, while the other half in nonthermal in origin. Then we used the two models F and E, described in the previous section. By summing up the three components we can reproduce pretty well the observed line emission spectra.

4.4. Adding the three components

Summing up the line intensities of each one of the three components, the composite spectrum of NGC1068 can be derived and compared with the observed one. We have chosen three combinations to compute the composite models, each one with a different AGN model: 1) the first one with the AGN ionizing continuum as suggested by Alexander et al. (2000)

(model AGN A), a low-ionization nuclear starburst (model SBN F) and a low-ionization starburst ring (model SBR F); 2) the second with the original Pier et al. (1994) (model AGN B), the same low-ionization nuclear starburst (model SBN F) and the same low-ionization starburst ring (model SBR F); 3) the third with the hypothetical bump (model AGN C), an high-ionization nuclear starburst (model SBN E) and the same low-ionization starburst ring (model SBR F). The results of these three composite models are given in Table 4, compared to the observed values.

4.5. Modeling the PDR

An accurate model for the PDR emission originating in the ISM of the NGC1068 galaxy is beyond the scope of the present article, however it is possible to check what are the main parameters of the PDR, i.e. far-ultraviolet field (G_0) and hydrogen density (n), just subtracting off the modeled intensities of the three components from the observed fluxes of [OI]63μm, [OI]145μm and [CII]158μm, then taking the ratios of the these lines, namely [OI]63μm/[CII]158μm and [OI]63μm/145μm and comparing them with the Kaufman et al. (1999) PDR models. Following this simple procedure, we find that for the first composite model log G_0 = 2 and log n = 3.3, while for the other two composite models log G_0 = 3 and log n = 2.5.

[.....comments here.....]

5. THE OH LINES

Figure xxx shows detailed views of the LWS spectrum around the 3 OH lines and NII 122μm.

In NGC 1068 the OH rotational lines are seen in emission, in contrast with other bright infrared galaxies, such as Arp 220 (Fischer et al. 1999), Mrk 231 (Harvey et al. 1999), NGC 253 (Bradford et al. 1999), M 82 (Colbert et al. 1999), where these lines are seen mostly in absorption. This indicates that the absorption detected at low spectral resolution in the other galaxies may actually result at an higher resolution as the combination of emission plus absorption, as seen in NGC 253 (Bradford et al. 1999).

The ISO LWS observations detected three of the far infrared OH spin-rotational lines from the ground state, and obtained useful limits on the other 8 FIR OH lines that fall into the LWS band. Table 4 lists the observed flux values. NGC1068 is a remarkable extragalactic source in its OH spectrum, because it is the only galaxy observed in which all the detected

transitions are found in *emission*. To model this behavior, we have recently begun a detailed study of all the OH lines observed by ISO. Here we report our first results on the peculiar emission from this galaxy.

We used the montecarlo radiative transfer code developed by the SWAS mission (Ashby et al., private comm). This code, a modification of the original Bernes code, adds a treatment of continuum photons from dust mixed in with the gas – a particularly essential feature for OH, which is pumped in many cases by absorption of 35 μm continuum. In addition the code corrects for some previous errors encountered at large optical depths, also an issue of importance for OH which has a very strong matrix element (1.67 Debye), and a fundamental line transition rate of about 0.1 s^{-1} – about 1000 times greater than CO rates. Finally, the code includes an ability to handle a wide range of molecules besides rigid rotors.

The montecarlo code takes an input a series of concentric shells, each of which is specified as to size, gas and dust temperature, H_2 density, velocity and velocity width, and molecular abundance relative to H_2. In addition the model as a whole requires an assumption about a dust emissivity. The montecarlo code calculates the populations of the molecular levels in each shell. The output is then fed into a radiative transfer code that calculates the line profiles as seen by an external observer looking at the cloud. The montecarlo output is not internally self-consistent; the input parameters need not conserve luminosity between shells, for example. To obtain this self consistency, and to guarantee that the final cloud model was also consistent with the observed far infrared continuum flux, we used the DUSTY code (Ivezic & Elitzur 1997) to model the continuum and generate a set of shell parameters that provided this consistency. Then we iterated the DUSTY model with the montecarlo line outputs. While we do not claim this technique gives a unique solution for the cloud structure, it does give a canonical model consistent with the observations.

The clouds that produce these lines in NGC1068 are small and dense, and heated from the inside. They are about 0.2 pc in radius, with densities of $\leq 10^4 cm^{-3}$ at the outer edges, increasing towards the center with a power law behavior of $(R/R_0)^{1.25}$. The temperature in the outer shells is about 22K, increasing inwards approximately with a power law dependence $(R/R_0)^{0.68}$. The total column density of H_2 in each cloud is $1.5 \times 10^{24} cm^{-2}$, and the relative abundance of OH in the model is 10^{-7}; OH is taken to be absent in the hotter portions of the cloud (T > 300K). The strong lines of OH are therefore very optically thick, and precise radiative transfer calculations like the present modeling are essential.

As can be seen for the table, the code accurately predicts the line flux ratios to the 119μm feature to within a factor of 40%. At a distance of 16.2 Mpc, the total number of clouds needed to produce the observed absolute flux in the lines and the continuum is $\sim 3 \times 10^7$. The limits to the observed fluxes in all the weaker lines are consistent with this

modeling. It is worth noting in this context that in some scenarios (and as observed in some other galaxies) these weaker OH lines in NGC 1068, like the 53μm line, are actually among the strongest in their respective galaxies. As for the continuum, the montecarlo code also successfully reproduces the continuum emission seen from NGC 1068, to within a factor of 2-3 in absolute flux density across the entire LWS spectrum. The dust is assumed to be 1% of the gas, and to have the same temperature as the gas everywhere in the cloud. The total mass in such an ensemble of clouds is approximately $9 \times 10^9 M_\odot$.

By way of a self-consistent check, we have also used the montecarlo code to model, independently, the emission and absorption from this series of clouds in two other species which the ISO Long Wavelength Spectrometer was able to detect: the two neutral oxygen [OI] lines at 63μm and 145μm , and the series of eleven lines from ortho-H_2O from the lower lying 8 energy levels (E < 323.8K). The results are reassuringly consistent with the observations. The [OI] 63μm and 145μm lines from these warm compact clouds are, respectively, estimated at $1.2 \times 10^{-19} W\ cm^{-2}$ and $2.6 \times 10^{-21} W\ cm^{-2}$ note that contributions from any PDRs are not included, and these are components are expected to dominate the observed strengths. The H_2O lines are highly dependent on the abundances assumed for water. Taking an abundance in these dense clouds of 10^{-7}, and noting the fact that a significant column density of material is quite warm, yields a strength of the 179μm line of about $10^{-19} W\ cm^{-2}$, in emission, with the next strongest line being the 181.6μm feature, which is about 3 times weaker. Obviously since both [OI] and H_2O have their major contributions coming from other kinds of regions - PDRs and shocks in particular - the significant conclusions to be drawn here are that the model for the OH lines is consistent with all the other observations.

Our conclusion is that NGC 1068 has a large component of relatively small, dense clouds of molecular gas and dust, heated internally. We cannot say from these data where these clouds are located in the large ISO beam, or what if any relationship they may have with the nuclear regions except that they do not appear to require either pumping or radiative effects from that region or its torus.

6. CONCLUSIONS

[.....]

The authors acknowledge the LWS Consortium, lead by Prof. Peter Clegg, for having built and operated the LWS instrument and solved many instrumental and data reduction problems. The ESA staff at VILSPA (Villafranca, Spain) is also acknowledged for the ISO mission operations. This research was supported in Italy by the Italian Space Agency (ASI).

REFERENCES

Alexander, T., Lutz, D., Sturm, E., Genzel, R. et al. 2000, ApJ, 536, 710.

Bland-Hawthorn, J., et al., 1997, ApSS, 248, 9.

Bradford, C.M., et al., 1999, Proc.of the Conference "The Universe as seeen by ISO", Paris, France, 20-23 October 1998 (ESA SP-427),p.861.

Clegg, P.E., et al. 1996, A&A, 315, L28.

Colbert, J., et al., 1999, ApJ, 511, 721.

Davies, R.I., Sugai,H., and Ward, M.J., 1998, MNRAS, 300, 388

Ferland, G.J., 2000, RevMexAA,(Serie de Conferencias), Vol.9, 153

Fischer, J., et al. 1999, Proc.of the Conference "The Universe as seeen by ISO", Paris, France, 20-23 October 1998 (ESA SP-427),p.817.

Harvey, V.I., et al., 1999, Proc.of the Conference "The Universe as seeen by ISO", Paris, France, 20-23 October 1998 (ESA SP-427),p.889.

Kaufman, M.J., Wolfire, M.G., Hollenbach, D.J., Luhman, M.L. 1999, ApJ, 527, 795.

Kessler, M.F. et al.,1996, A&A, 315, L27

Kriss, G.A. et al. 1992, ApJ, 394, L37

Ivezic, Z., & Elitzur, M. 1997, MNRAS, 287, 799

Leitherer, C., and Heckman, T.M., 1995, ApJSS, 96, 9.

Leitherer, C., et al. 1999, ApJS, 125, 489.

Lutz, D. et al., 2000, ApJ, 536, 697.

Marconi, A., et al. 1996, A&A, 315, 335.

Malkan, M. A., et al. 2002, in prep.

Malkan, M. A. & Oke, J. B. 1983, ApJ, 265, 92.

Oliva, E. & Moorwood, A.F.M., ApJ, 348, L5.

Osterbrock, D.E. 1989, Astrophysics of gaseous nebulae and active galactic nuclei, University Science Books, Mill Valley, California, p.84.

Pier, E.A., et al. 1994, ApJ, 428, 124.

Schinnerer, E., et al. 2000, ApJ, 533, 850.

Spinoglio, L., Andreani, P. & Malkan, M.A., 2002, ApJ, 572, 105.

Spinoglio, L. & Malkan, M.A.,1992, ApJ,399,504.

Scoville, N.Z., Matthews, K., Carico, D.P., Sanders, D.B. 1988, ApJ, 327, L61.

Swinyard, B.M., et al. 1996, A&A, 315, L43.

Swinyard, B.M., et al. 1998, Proc. SPIE, A.M. Fowler (Ed.), Vol.3354, P.888.

Telesco, C.M., et al., 1984, ApJ, 282, 427.

Thatte, N., et al. 1997, ApJ, 490, 238.

Thompson, R.I., 1996, ApJ, 459, L61.

Thronson,H.A. et al. 1989, ApJ, 343, 158.

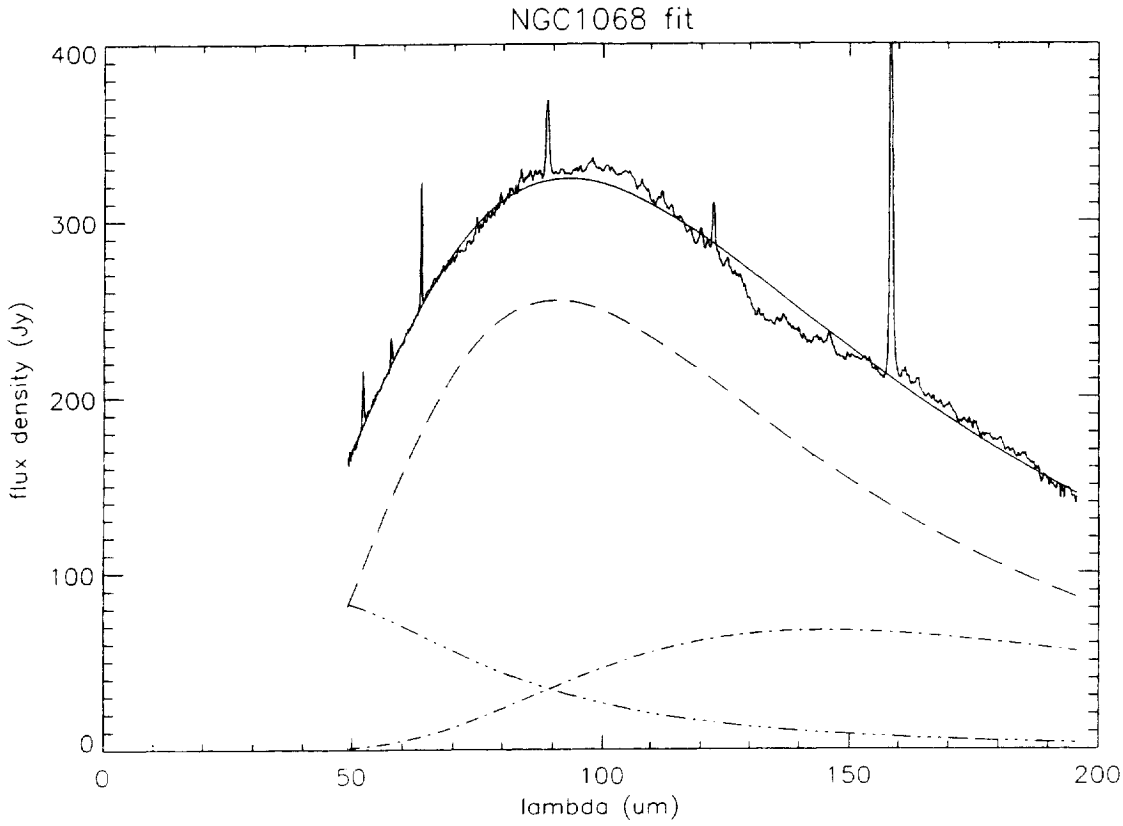

Fig. 1.— The ISO-LWS spectrum of NGC1068. The solid line, which is fitting the data (reduced χ^2=0.40, corresponding to a probability of P>98%) represents the sum of the three different grey-body functions: dashed line: main component at T=32K; dotted-dashed line: cold component at T=20K; three-dotted-dashed line: warm component at T=65K.

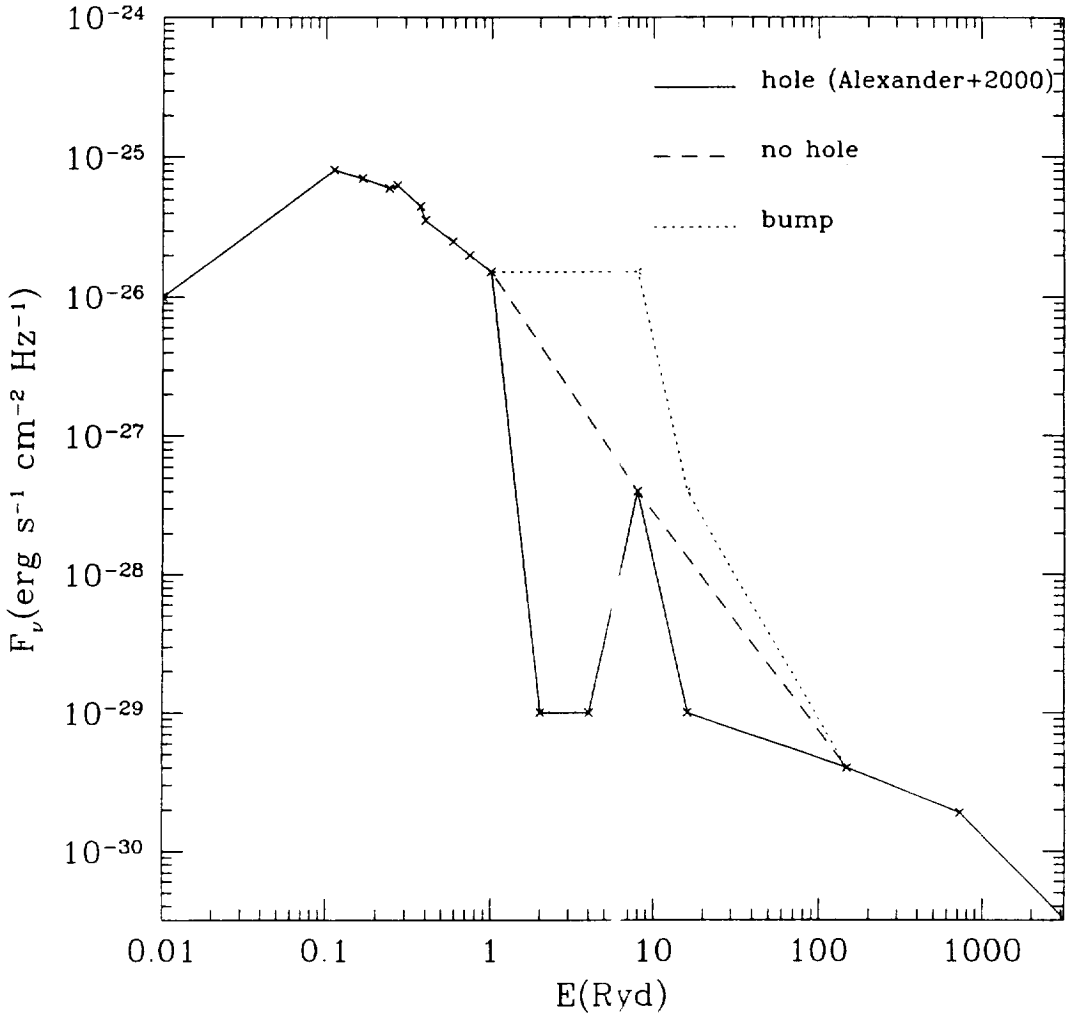

Fig. 2.— The AGN ionizing continua used as input for the photoionization models of NGC1068. The three continua differ in the frequency region between $1>E_{Ryd}>100$, while outside this region the Pier et al. (1994) spectrum was adopted. The solid line shows the continuum derived from Alexander et al. (2000); the dashed line shows a simple power law interpolation; the dotted line shows the presence of the predicted "big blue bump".

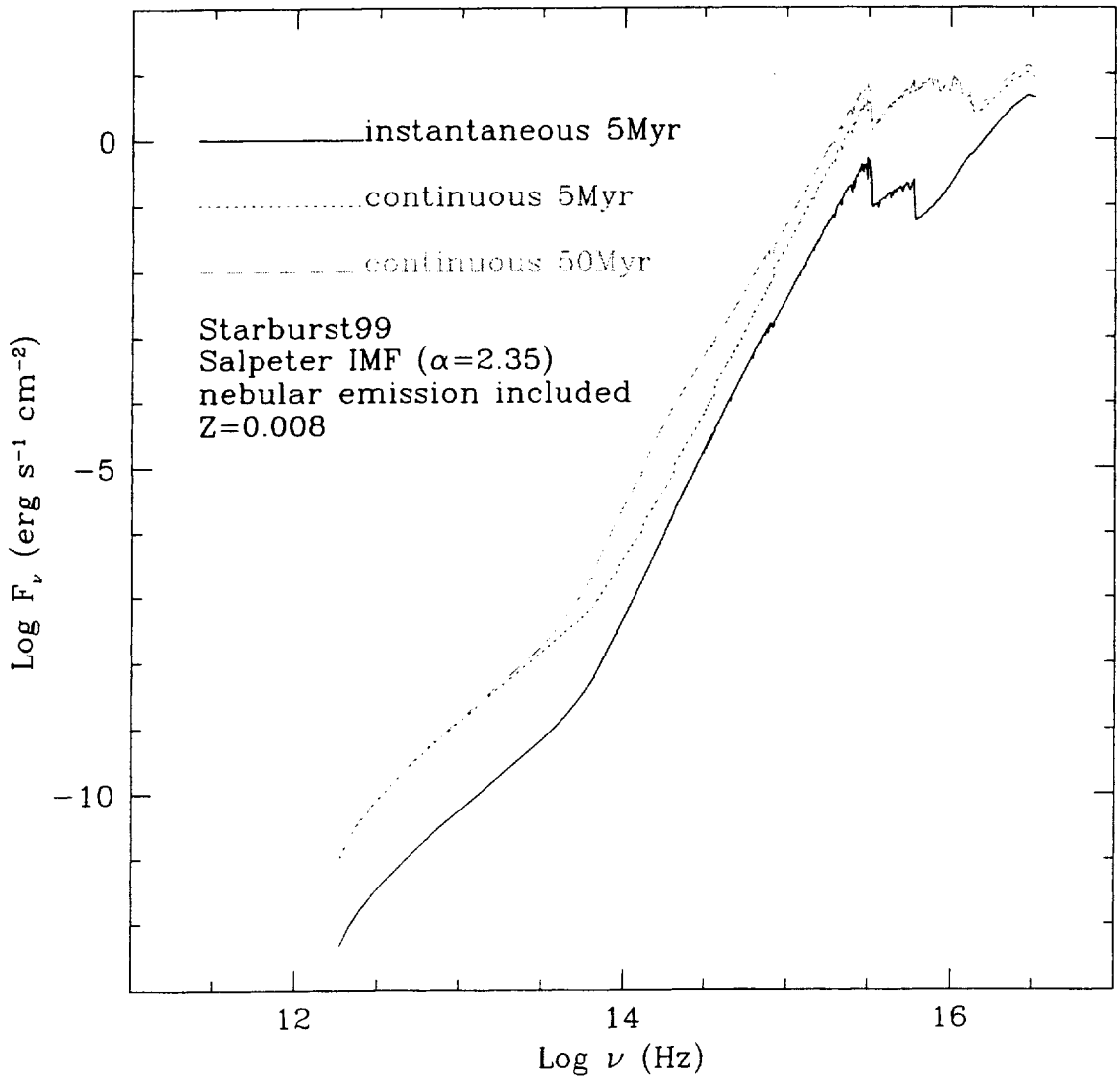

Fig. 3.— The starburst ring ionizing continua used as input for the photoionization models of NGC1068. The three continua are taken from Leitherer et al. (1999).

Table 1. Measured line fluxes from the LWS and SWS grating spectra, with 1σ uncertainties.

Line	λ (μm)	Flux (10^{-13} erg s^{-1} cm^{-2})	Aperture ($''^2$)	reference
[Si IX] $^3P_2 \rightarrow {}^3P_1$	2.584	3.0 ±	14 × 20	1
[Mg VIII] $^2P_{3/2} \rightarrow {}^2P_{1/2}$	3.028	11. ± 1.1	14 × 20	1
[Si IX] $^3P_1 \rightarrow {}^3P_0$	3.936	5.0 ± 0.6	14 × 20	1
[Mg IV] $^2P_{1/2} \rightarrow {}^2P_{3/2}$	4.487	7.6 ± 1.5	14 × 20	1
[Ar VI] $^2P_{3/2} \rightarrow {}^2P_{1/2}$	4.529	5. ± 3.	14 × 20	1
[Fe II] $^{a4}F_{9/2} \rightarrow {}^{a6}D_{9/2}$	5.340	5.0 ±	14 × 20	1
[Mg VII] $^3P_2 \rightarrow {}^3P_1$	5.503	13. ±	14 × 20	1
[Mg V] $^3P_1 \rightarrow {}^3P_2$	5.610	8. ± 2.	14 × 20	1
[Ar II] $^2P_{1/2} \rightarrow {}^2P_{3/2}$	6.985	13. ±	14 × 20	1
[Na III] $^2P_{1/2} \rightarrow {}^2P_{3/2}$	7.318	5.8 ±	14 × 20	1
[Ne VI] $^2P_{3/2} \rightarrow {}^2P_{1/2}$	7.652	110. ± 11.	14 × 20	1
[Fe VII] $^3F_4 \rightarrow {}^3F_3$	7.815	3.0 ±	14 × 20	1
[Ar V] $^3P_2 \rightarrow {}^3P_1$	7.902	< 12.	14 × 20	1
[Na VI] $^3P_2 \rightarrow {}^3P_1$	8.611	< 16.	14 × 20	1
[Ar III] $^3P_1 \rightarrow {}^3P_2$	8.991	23.0 ± 3.3	14 × 20	1
[Fe VII] $^3F_3 \rightarrow {}^3F_2$	9.527	4.0 ±	14 × 20	1
[S IV] $^2P_{3/2} \rightarrow {}^2P_{1/2}$	10.510	58. ± 6.	14 × 20	1
[Ne II] $^2P_{3/2} \rightarrow {}^2P_{1/2}$	12.813	70. ±	14 × 27	1
[Ar V] $^3P_1 \rightarrow {}^3P_0$	13.102	< 16.	14 × 27	1
[Ne V] $^3P_2 \rightarrow {}^3P_1$	14.322	97. ± 9.7	14 × 27	1
[Ne III] $^3P_1 \rightarrow {}^3P_2$	15.555	160. ± 32.	14 × 27	1
[Fe II] $^{a4}F_{7/2} \rightarrow {}^{a4}F_{9/2}$	17.936	< 10.	14 × 27	1
[S III] $^3P_2 \rightarrow {}^3P_1$	18.713	40. ±	14 × 27	1
[Ne V] $^3P_1 \rightarrow {}^3P_0$	24.317	70. ± 7.	14 × 27	1
[O IV] $^2P_{3/2} \rightarrow {}^2P_{1/2}$	25.890	190. ± 20.	14 × 27	1
[Fe II] $^{a6}D_{7/2} \rightarrow {}^{a6}D_{9/2}$	25.988	8. ±	14 × 27	1
[S III] $^3P_1 \rightarrow {}^3P_0$	33.481	55. ±	20 × 33	1
[Si II] $^2P_{3/2} \rightarrow {}^2P_{1/2}$	34.814	91. ±	20 × 33	1
[Ne III] $^3P_0 \rightarrow {}^3P_1$	36.013	18. ±	20 × 33	1
[O III] $^3P_2 \rightarrow {}^3P_1$	51.814	114. ± 3.	80	2
[N III] $^2P_{3/2} \rightarrow {}^2P_{1/2}$	57.317	71.4 ± 2.5	80	2
[O I] $^3P_1 \rightarrow {}^3P_2$	63.184	56. ± 1.	80	2
[O III] $^3P_1 \rightarrow {}^3P_0$	88.356	111. ± 1.	80	2
[N II] $^3P_2 \rightarrow {}^3P_1$	121.897	10.5 ± 1.1	80	2
[O I] $^3P_0 \rightarrow {}^3P_1$	145.525	11.9 ± 0.4	80	2
[C II] $^2P_{3/2} \rightarrow {}^2P_{1/2}$	157.741	216. ± 1.	80	2
OH $^2\Pi_{1/2}5/2$-$^2\Pi_{3/2}3/2$	34.60/34.63	< 3.	20 × 33	2
OH $^2\Pi_{1/2}1/2$-$^2\Pi_{1/2}3/2$	79.11/79.18	4.4 ± 1.5	80	2
OH $^2\Pi_{3/2}5/2$-$^2\Pi_{3/2}3/2$	119.23/119.44	1.9 ± 1.2	80	2
OH $^2\Pi_{1/2}3/2$-$^2\Pi_{1/2}1/2$	163.12/163.40	7.42 ± 0.65	80	2

Note. — (1): from Lutz et al. (2000); (2): this work

Table 2. Comparison of observed line fluxes with AGN and SBN model predictions

Line id.λ (μm)	Observed/Dereddened	Flux (10^{-13} erg s^{-1} cm^{-2}) AGN A[a]	AGN B[b]	AGN C[c]	SBN F[d]	SBN E[e]
O VI λ .1032+.1037	37.4/4334.	32.4+18.4	32.6+16.9	57.8+30.0	...	0.25+0.15
N IV] λ .1487	5.1/103.	16.6	15.0	11.1	...	...
HeII λ .1640	21.4/426.	133.	90.	116.	75.	108
[Ne V] λ .3426	15.7/95.	84.2	54.0	87.3	...	10.9
[Ne III] λ .3869+.3968	19.2/97.	38.5+11.6	87.5+26.4	33.2+10.	42.+12.	43.+13.
HeII λ .4686	6.1/27.6	18.7	12.5	16.1	11.3	16.
[O III] λ .4959+.5007	256./964.	297+861	514+1482	180+520	29.+83.	156+452
[Si VI] λ 1.96	8.0/9.2	13.7	8.2	11.1	...	...
[Si VII] λ 2.48	8.3	5.8	12.0	5.0	...	...
[Si IX] λ 2.584	3.0	0.19	4.3	.06	...	...
[Mg VIII] λ 3.028	11.	1.6	14.9	1.26	...	...
[Si IX] λ 3.936	5.4	0.37	8.3	.12	...	...
[Mg IV] λ 4.487	7.6	6.7	2.7	2.0	...	4.9
[Ar VI] λ 4.529	15.	30.	26.8	12.5	...	...
[Mg VII] λ 5.503	13.	7.1	22.4	7.8	...	...
[Mg V] λ 5.610	18.	12.	2.9	8.9	...	5.3
[Ar II] λ 6.985	13.	20.	...	.07	6.0	2.0
[Na III] λ 7.318	5.8	1.4	2.2	0.4	0.8	0.5
[Ne VI] λ 7.652	110.	100.	120.	135.	...	5.6
[Fe VII] λ 7.815	3.0	3.2	1.3	2.0	...	...
[Ar V] λ 7.902	< 12.	5.8	3.2	1.0	...	1.2
[Na VI] λ 8.611	< 16.	1.3	0.7	1.3	...	0.25
[Ar III] + [Mg VII] λ 8.991	25.	21.+9.	6.5+22.4	2.3+10.	20.+ ...	7.3+ ...
[Fe VII] λ 9.527	4.0	14.	5.6	3.7	...	...
[S IV] λ 10.510	58.	180.	298.	62.	1.3	41.6
[Ne II] λ 12.813	70.	38.	0.31	0.1	7.1	2.5
[Ar V] λ 13.102	< 16.	9.0	4.9	1.4	...	2.2
[Ne V] λ 14.322	97.	170.	101.	148.	...	43.8
[Ne III] λ 15.555	160.	145.	149.	30.	59.	38.
[S III] λ 18.713	40.	92.	14.	5.2	21.3	22.6
[Ne V] λ 24.317	70.	135.	77.	111.	...	48.
[O IV] λ 25.890	190.	280.	136.	101.	3.3	207.
[S III] λ 33.481	55.	53.	7.4	2.9	32.7	34.8
[Si II] λ 34.814	91.	90.8	1.4	1.2	155.	60.
[Ne III] λ 36.013	18.	12.3	12.8	2.6	5.2	3.4
[O III] λ 51.814	110.	180.	144.	42.5	16.7	59.
[N III] λ 57.317	51.	20.	8.9	2.0	5.9	21.2
[O I] λ 63.184	156.	39.	...	0.12	25.1	8.
[O III] λ 88.356	110.	41.	33.	10.	26.6	104.
[N II] λ 121.897	30.	2.9	...	...	7.0	2.5
[O I] λ 145.525	12.	3.9	...	...	2.4	0.8
[C II] λ 157.741	220.	5.9	...	...	67.5	38.5

Note. —

[a]AGN A parameters: Log U=-1.5, Log n=3.3, radius $\simeq$ 60 pc, ionizing spectrum from Alexander et al. (2000).

[b]AGN B parameters: Log U=-1.0, Log n=3.3, radius $\simeq$ 27 pc, Pier et al. (1994) ionizing spectrum

[c]AGN C parameters: Log U=-1.5, Log n=3.3, radius $\simeq$ 29 pc, big blue bump added (see text)

[d]SBN F parameters: Log U=-3.5, Log n=1.3, ionizing spectrum from Starburst99 continuous model with Z=.008 and duration of 50 Myr. The integration was stopped at a temperature of 50K.

[e]SBN E parameters: Log U=-2.5, Log n=0.3, ionizing spectrum from Starburst99 continuous model with Z=.008 and duration of 50 Myr. The integration was stopped at a temperature of 50K.

Table 3. Comparison of observed line fluxes with Ring Starburst model predictions

Line id.λ (μm)	Observed	Flux (10^{-13} erg s^{-1} cm^{-2}) SBR A[a]	SBR B[b]	SBR C[c]	SBR D[d]	SBR E[e]	SBR F[f]
[Ne II] λ 12.813	70.	xxx	xxx	1.0	1.2	0.3	1.1
[Ar V] λ 13.102	< 16.	...	...	...	...	0.3	...
[Ne V] λ 14.322	97.	...	...	...	...	0.6	...
[Ne III] λ 15.555	160.	11.2	11.4	8.7	8.8	5.7	9.0
[S III] λ 18.713	40.	3.9	3.7	3.2	3.0	3.4	3.2
[Ne V] λ 24.317	70.	...	...	...	...	7.3	...
[O IV] λ 25.890	190.	...	...	0.5	0.4	31.	0.5
[S III] λ 33.481	55.	13.3	12.9	11.1	11.	12.	11.3
[Si II] λ 34.814	91.	65.8	75.2	52.4	58.4	20.9	53.8
[Ne III] λ 36.013	18.	2.2	2.3	1.8	1.8	1.1	1.8
[O III] λ 51.814	110.	4.2	3.7	16.5	14.7	54.8	15.3
[N III] λ 57.317	51.	1.5	1.4	5.9	5.6	19.5	5.4
[O I] λ 63.184	156.	32.	36.6	21.7	24.3	7.3	22.
[O III] λ 88.356	110.	7.0	6.5	26.6	25.9	95.8	24.7
[N II] λ 121.897	30.	8.2	8.0	6.1	6.2	2.4	6.7
[O I] λ 145.525	12.	3.1	3.6	2.1	2.3	0.7	2.2
[C II] λ 157.741	220.	76.3	142.	60.	107.	35.	62.3

Note. — (1):

[a]SBR A parameters: Log U=-3.5, Log n=1.3, ionizing spectrum from Starburst99 instantaneous model with Z=.008 and duration of 5 Myr. The integration was stopped at a temperature of 50K.

[b]SBR B parameters: Log U=-3.5, Log n=0.3, ionizing spectrum from Starburst99 instantaneous model with Z=.008 and duration of 5 Myr. The integration was stopped at a temperature of 50K.

[c]SBR C parameters: Log U=-3.5, Log n=1.3, ionizing spectrum from Starburst99 continuous model with Z=.008 and duration of 5 Myr. The integration was stopped at a temperature of 50K.

[d]SBR D parameters: Log U=-3.5, Log n=0.3, ionizing spectrum from Starburst99 continuous model with Z=.008 and duration of 5 Myr. The integration was stopped at a temperature of 50K.

[e]SBR E parameters: Log U=-2.5, Log n=0.3, ionizing spectrum from Starburst99 continuous model with Z=.008 and duration of 50 Myr. The integration was stopped at a temperature of 50K.

[f]SBR F parameters: Log U=-3.5, Log n=1.3, ionizing spectrum from Starburst99 continuous model with Z=.008 and duration of 50 Myr. The integration was stopped at a temperature of 50K.

Table 4. Comparison of observed line fluxes with composite model predictions

Line id.λ (μm)	Flux (10^{-13} erg s^{-1} cm^{-2}) Observed/Dereddened	AGN A + SBN F + SBR F[a]	AGN B + SBN F + SBR F [b]	AGN C + SBN E + SBR F[c]
O VI λ .1032+.1037	37.4/4334.	50.5	49.5	88.2
N IV] λ .1487	5.1/103.	16.6	15.0	11.1
HeII λ .1640	21.4/426.	208.	165.	224.
[Ne V] λ .3426	15.7/95.	84.2	54.0	98.2
[Ne III] λ .3869+.3968	19.2/97.	104.	168.	99.2
HeII λ .4686	6.1/27.6	30.	23.8	32.1
[O III] λ .4959+.5007	256./964.	1270.	2108.	1308.
[Si VI] λ 1.96	8.0/9.2	13.7	8.2	11.1
[Si VII] λ 2.48	8.3	5.8	12.0	5.0
[Si IX] λ 2.584	3.0	.19	4.3	.06
[Mg VIII] λ 3.028	11.	1.6	14.9	1.3
[Si IX] λ 3.936	5.4	.37	8.3	.12
[Mg IV] λ 4.487	7.6	6.7	2.7	6.9
[Ar VI] λ 4.529	15.	30.	26.8	12.5
[Mg VII] λ 5.503	13.	7.1	22.4	7.8
[Mg V] λ 5.610	18.	12.	2.9	14.2
[Ar II] λ 6.985	13.	26.	6.0	2.1
[Na III] λ 7.318	5.8	2.2	3.0	0.9
[Ne VI] λ 7.652	110.	100.	120.	141.
[Fe VII] λ 7.815	3.0	3.2	1.3	2.0
[Ar V] λ 7.902	< 12.	5.8	3.2	2.2
[Na VI] λ 8.611	< 16.	1.3	0.7	1.6
[Ar III] + [Mg VII] λ 8.991	25.	50.	48.9	19.6
[Fe VII] λ 9.527	4.0	14.	5.6	3.7
[S IV] λ 10.510	58.	181.	299.	104.
[Ne II] λ 12.813	70.	46.2	8.5	3.7
[Ar V] λ 13.102	< 16.	9.0	4.9	3.6
[Ne V] λ 14.322	97.	170.	101.	192.
[Ne III] λ 15.555	160.	213.	217.	77.
[S III] λ 18.713	40.	116.	46.6	31.
[Ne V] λ 24.317	70.	135.	77.	159.
[O IV] λ 25.890	190.	284.	140.	308.
[S III] λ 33.481	55.	97.	51.	49.
[Si II] λ 34.814	91.	300.	210.	115.
[Ne III] λ 36.013	18.	19.3	19.8	7.8
[O III] λ 51.814	110.	212.	176.	117.
[N III] λ 57.317	51.	31.3.	20.2	28.6
[O I] λ 63.184	156.	86.	47.	30.
[O III] λ 88.356	110.	92.3	84.3	139.
[N II] λ 121.897	30.	16.6	13.7	9.2
[O I] λ 145.525	12.	8.5	4.6	3.0
[C II] λ 157.741	220.	136.	130.	84.3

Note. —

a

b

c

Table 5. Comparison of observed line fluxes with OH montecarlo model predictions

Line id.λ	Flux ($10^{-19} W cm^{-2}$) Observed	Modeled	Notes
34μm	< .5	-0.5	(absorption)
48μm	...	0.12	
53μm	< 1.2	-0.1	(absorption)
65μm	< 1.2	0.[illegible]	
79μm	0.80	1.10	
84μm	< 1.2	0.[illegible]	
96μm	...	0.[illegible]	
98μm	< 1.2	0.[illegible]	
115μm	...	.004	
119μm	1.20	1.31	
163μm	0.74	0.60	

Note. — (1):

Active Galactic Nuclei: from Central Engine to Host Galaxy
ASP Conference Series, Vol. xxx, 2003
S. Collin, F. Combes, and I. Shlosman

Mid- and far-infrared spectroscopy of Seyfert galaxies

Luigi Spinoglio

IFSI-CNR via Fosso del Cavaliere 100, I-00133 - Roma (Italy)

Matthew A. Malkan

Physics & Astronomy Dept., UCLA, Los Angeles, CA 90095, USA

Howard A. Smith

Harvard-Smithsonian CfA, 60 Garden St., Cambridge, MA 02138, USA

Jackie Fischer

Naval Research Laboratory, Code 7213, Washington DC 20375, USA

Abstract. Infrared line ratio diagrams are a powerful tool to distinguish the different emission components in galaxies. We focus here on two particular examples: the ISO LWS diagram showing the ratio [CII]158μm/[OI]63μm versus the ratio [OIII]88μm/[OI]63μm is able to separate AGNs from starburst and PDR emission. The ISO SWS diagram with the [NeVI]7.6μm/[OIV]26μm ratio versus the [NeV]14μm/[NeV]24μm ratio is a good tracer of both the ionization potential and the density in the extreme conditions of AGNs, as is shown from photoionization models.

1. Introduction

Mid- and far-infrared spectroscopy is able to distinguish among the different excitation mechanisms at work in active galaxies (see e.g. Spinoglio & Malkan 1992): high ionization and coronal lines are produced by nonthermal processes associated to the AGN; intermediate ionization lines are excited by massive young stars during violent starbursts; neutral and low-ionization lines are mostly excited in the photodissociation regions in the ISM of galaxies; emission and absorption molecular lines from species as H_2O and OH originate either in the ipothetical torii or in the nuclear ISM regions (Fischer et al. 1999). For the limited space available, we present here only two examples of diagnostic line ratio diagrams made of lines observed with the Infrared Space Observatory, while we refer to upcoming papers for a complete presentation of our results.

2. Line ratio diagrams

We show in Fig. 1 (a) the line ratio diagram of [CII]158μm/[OI]63μm versus [OIII]88μm/[OI]63μm. It appears from the figure that nearby normal galax-

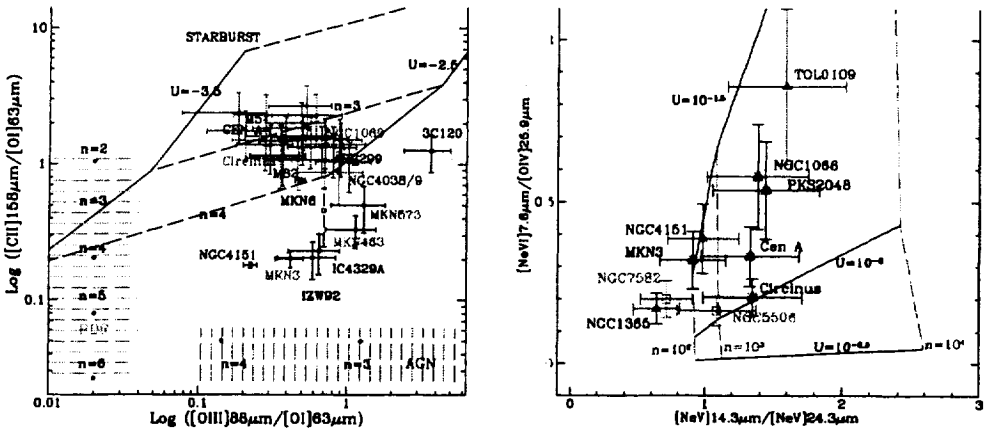

Figure 1. (a:)[CII]158μm/[OI]63μm versus [OIII]88μm/[OI]63μm. Seyfert 1's are in blue, Seyfert 2's in green and starburst galaxies in red. Pink crosses show nearby galaxies (Negishi et al. 2001). The grid shows starburst models with increasing densities (from top to bottom) and increasing ionization parameter (from left to right). The vertical hatched area shows the [CII]158μm/[OI]63μm ratio for PDR models (log n=2-6 cm^{-3} and log G_0=3). The horizontal hatched area shows the [OIII]88μm/[OI]63μm ratio for AGN models (log U=-2.5 and log n= 3, 4 cm^{-3}). (b:) [NeVI]7.6μm/[OIV]26μm versus [NeV]14μm/[NeV]24μm for 3 Seyfert 1's (NGC1365, NGC4151, Tol0109), 5 Seyfert 2's (MKN 3, Cen A, Circinus, NGC1068, PKS2048) and 2 NLXR galaxies (NGC5506, NGC7582). The grid shows AGN models with ionizing continuum of slope α=-1.0 and different densities and ionization parameters.

ies cluster together with those Seyfert's whose emission is dominated in these lines by starburst emission (e.g. NGC1068) and coincides with typical starburst galaxies photoionization models. However, at lower values of the [CII]/[OI] ratio, there is another region where only AGNs are present.

The ratios [NeVI]7.6μm/[OIV]26μm versus [NeV]14μm/[NeV]24μm constrain the main parameters (density and ionization parameter) of photoionization models of the NLRs of AGNs. These lines are produced only in the highly ionized medium of AGNs, and not from photoionization by stars. The [NeVI]7.6μm/[OIV]26μm ratio is sensitive to the ionization, while the ratio [NeV]14μm/[NeV]24μm probes the density. This line ratio diagram is shown in Fig. 1 (b). No differences are apparent among the different types of AGNs.

References

Fischer, J. et al. 1999, Ap&SS, 266, 91.

Negishi et al. 2001, A&A, 375, 566.

Spinoglio L. & Malkan M.A. 1992, ApJ, 399, 504.

Public Attitudes Towards Space Science

Howard A. Smith

Harvard-Smithsonian Center for Astrophysics, 60 Garden Street, Cambridge, MA, 02138 USA

hsmith@cfa.harvard.edu

Abstract. Astronomy and space science, including their associated basic research activities, enjoy broad popular backing. People generally support the work they do, and say that they follow their results with interest. This article summarizes some of the detailed results of public surveys in the United States, focusing on popular opinions and attitudes, and the somewhat paradoxical finding that despite being interested and supportive, people are often ignorant about the basic facts. I explore some of the reasons for the popularity of space science, and suggest ways of justifying space science research in the broader context of science research. I argue that vigorous and innovative education and outreach programs are important, and can be made even more effective.

KEYWORDS: space science education; public opinion; public understanding

This paper has not been submitted elsewhere in identical or similar form, nor will it be during the first three months after its submission to Space Science Reviews.

1. The "Judgment of the Multitude"

> "[And] though I know that the speculations of a philosopher are far removed from the judgment of the multitude - for his aim is to seek truth in all things as far as God has permitted human reason so to do -- yet I hold that opinions which are quite erroneous should be avoided."
>
> -- Nicholaus Copernicus, *De Revolutionibus*, from his letter to Pope Paul III (as cited in *Theories of the Universe* by Milton K. Munitz, 1957).

Contrary to the sentiment Copernicus expressed to Pope Paul III circa 1542, today the "judgment of the multitude" is <u>not</u> far removed from the research of astronomy and space science, nor from their other activities for that matter. The public pays for them, and the public pays attention to them. The Federal government provides billions of dollars to the space science enterprise; state and private contributors also provide substantial funding. Progress in space science therefore depends upon public dollars, although continued financial support is only one reason - perhaps not even the most important one - why we as a community of astronomers should be attentive to popular perceptions. In this article I will review our knowledge of the US public's attitudes, and will argue that vigorous and innovative education and outreach programs are important, and can be made even more effective. And, speaking as a practicing scientist, I will argue that doing so is worth our best efforts.

Space science enjoys broad popular support. People say they generally like it, and admit that they follow it with interest. Later in this article I will discuss some specific survey results, and the somewhat paradoxical finding that, despite being supportive and interested, people are often

ignorant about the basic facts. The 1985 study by the Royal Society of Britain entitled, "The Public Understanding of Science" (The Royal Society, 1985) is a landmark document in addressing the topic; in the US, the National Science Foundation's (NSF) series "Science and Engineering Indicators" (National Science Board, 2000) is an ongoing, statistical study of public attitudes from which I draw many examples. Although these studies and their data sets have come under various levels of thoughtful criticism (e.g., Irwin and Wynne, 1996), I will argue that they provide useful and relatively self-consistent statistics from which to consider the state of the public's consciousness.

Why should scientists care about these social analyses, or the statistical subtleties of the public's knowledge, interest, or "understanding," especially when the methodology of such studies has come under attack? First, despite their limitations, such surveys show that the space science community can do better at public education – in none of the important measures of public response are the results close to "saturation." And secondly, they highlight disconcerting but redeemable public attributes, prompting me to suggest the community ought to do better -- not in order to increase budgets, but because a scientifically literate society (not proficient, just literate) is essential to rational discourse and judgment in a millennium dominated by science and technology which to many people increasingly resembles sorcery. Space science, popular as it is according to all studies, is one of the most potent areas of inquiry which science has at its disposal to teach the facts and methods of modern scientific research.

The term "space science" encompasses a much wider arena of topics than simply astronomy or satellite-based research. The popular conception of the topic includes rockets and the technologies needed for rocket and shuttle launches, their control and tracking, and also the technologies for new instruments; the results of the Smithsonian Institution's National Air and Space Museum (NASM) survey (Section 2) confirm this. The term rightly includes the manned aspects of space exploration,

from the Apollo-to-the-Moon missions to future manned missions to Mars, as well as earth-orbiting space stations. Some of the surveys I will discuss make explicit distinctions between these various areas, but most often they do not.

2. All the Surveys Say that People are Interested

For over fifteen years the National Science Board of the National Science Foundation has taken "science indicator surveys" of the US public's relationships with science (*Science and Engineering Indicators - 2000,* National Science Board, 2000), asking people about their attitudes towards a wide range of science topics, including in particular space exploration, and also medicine, nuclear power, environment, and technology. While this limited breakdown of science topics constrains some of our conclusions, it is adequate for most of the discussion. There have been ups and downs in the numbers over time, reflecting, for example, concerns after the explosion of the space shuttle Challenger, or budget deficits, but the general conclusions have been roughly the same: a huge number of Americans -- 77% in 1997 -- say they are very interested or moderately interested in space exploration. A majority of people also say they are interested in "new scientific discoveries"- - 91% -- so space science is not unique in its appeal, but it is remarkable in that it does not involve the immediate practical concerns of the other queried science topics like heath, the environment, or nuclear power. Indeed the second highest "not interested" response was to "space exploration" – 22% in 1997 (agricultural and farm issues was the highest at 26%). The largest difference in responses between male and female respondents, 30% was for space exploration. Also noteworthy is the fact that expressed interest is about 50% greater in people with graduate degrees than in those who have not completed a high school education. By comparison, the 1998 survey done by the

European Space Agency of the 14 ESA countries found that about 42% of the public said they were interested or very interested in space exploration.

During the period I was the chairman of the astronomy program at the Smithsonian Institution's National Air and Space Museum in Washington, D.C., from 1988 to 1996, the museum undertook a survey of its approximately 8 million annual visitors in an effort to understand why they came, and what they liked. It is useful to this inquiry because it broke down the broad category of "space science" into sub topics. Most people came to the museum to see a bit of everything, but of those who came particularly to see an artifact or gallery (and excluding the IMAX movie theater), 45% came for aviation-related subjects, and 35% came for the spacecraft, or astronomy galleries, or the planetarium shows. Those people who came with no specific special interest in mind were asked upon leaving what they had found the "most interesting." Forty-three percent said they found space science topics (spacecraft/astronomy/planetarium) "the most interesting," with the spacecraft artifacts being by far the most popular of these, by about 3:1. Forty-four percent said they found the aviation exhibits most interesting. The NASM artifacts are spectacular and inspirational, so it is perhaps not surprising that people want to see them; we will see below that space technology and manned exploration bring excitement to the whole space science endeavor. What is interesting from the study is the very strong showing of non-artifact based space science.

•

3. Space Science News is Generally Good News

The Pew Research Center for the People and the Press (quoted in *Science and Engineering Indicators - 2000*) has for over 15 years tracked the most closely followed news stories in the US. There were 689 of them from 1985 to 1999, with 39 having some connection to science (including medicine, weather, and natural phenomena.) To an overwhelming degree these 39 science stories

told bad news -- earthquakes or other calamities of nature, nuclear power, AIDS, or medical controversies. Virtually every *good news* science story, however, was about space science: John Glenn's shuttle flight, the deployment of the Hubble, the Mars Pathfinder mission, and the cosmic microwave background. (The only positive, *non*-space, science news story was on Viagra, while only the negative space stories were the explosion of the Shuttle Challenger, and troubles with the Mir space station.) The most recent results from the Pew Center (for the years 2000 and 2001) conform to this same pattern.

3.1 FIVE REASONS FOR THE APPEAL OF SPACE SCIENCE

Space science, as these news items suggest, makes people feel good about themselves; no doubt this is one reason why people say they like it. There are at least four other reasons which I believe are unique to astronomy in particular and space science in general, and which set the field apart from others in science like physics, chemistry or biology. They are worth explicitly listing because effective education and outreach efforts can build on their inherent appeal. (1) Universal access to the skies: everyone can look up in wonder at the heavens. Creation myths, developed by many diverse cultures, make the sky a simple yet nearly universal natural reference frame, while those people who have more interest can easily become familiar with the constellations or planets using only their eyes. Reports of the latest discoveries, for example, protoplanetary disks in the Orion nebula, can be made more immediate to people by pointing out their positions in the sky. (2) Issues of personal meaning: there are religious/spiritual overtones in space science research. Questions about the universe lead naturally to questions of origins -- the creation of the universe, and the creation of life. These matters, far from being esoteric philosophical debates about matters that happened perhaps 13 billion years ago, are taken personally. They directly affect the spiritual perspectives of at least the Western religions. But even for nonreligious people these are matters

of spirit and meaning, and so they are both important as well as interesting. The vigorous and sometimes acrimonious debate in the US over Darwinian evolution is a biological echo of these spiritual sensitivities. (3) Ease of understanding: the profound questions are simply put. Developments in physics today are exciting - in quantum mechanics, the nature of elementary particles, and progress towards a "theory of everything." Likewise for biology, where revolutionary advances are underway in understanding the genome. But, in terms of easily communicating these discoveries to the public, there is no comparison with astronomy's advantage: the pressing, current questions of astronomy are easy to describe. How did planets form? When and how did the universe begin? Are stars born, and how do they die? Furthermore, often the answers can usually be understood without resorting to complex jargon. These are powerful edges over other scientific disciplines. Added to this, of course, and not to be underestimated, is space science's ability to talk about modern research with spectacular, inspirational images. (4) Excitement and drama: the human adventure is fascinating. Finally the exciting, dramatic and often dangerous *human* exploration of space is a powerful stimulant for interest in space science. Despite the controversies over the international space station, or the costs of a manned mission to Mars, the human element of space helps keeps NASA funding percolating at a high level (although exactly how this funding ends up benefitting space science is a much less straightforward calculation).

4. Space Science is Interesting, Appealing -- and People Support It

Space science is the beneficiary of considerable public largesse in the US. Federal funding of astronomy alone, via NASA and NSF, was about $800M in 1997. NASA's share, in 1997 dollars, has increased from $380M in 1981 as more and more space missions are undertaken; NSF's share has been in the past steady at about $100M (see, for example, the Committee on the Organization

and Management of Research in Astronomy and Astrophysics Report, 1999). Additional Federal funding for space science comes through other agencies including the Defense Department (for example, Air Force or Naval Observatory programs), and is significant but harder to quantify. Finally there is substantial public support in the form of local (state) funds for university telescopes, and/or from individuals and private foundations. It is worth noting, as does the recent National Academy report on astronomy funding, that of ten new generation telescopes being built with US support whose apertures are over 5 meters in diameter, only five receive any Federal funding. Clearly the US public is willing to fund space science at productive levels.

Public support for space science, as measured by the perceptions of its cost-to-benefit ratio, has also been high in the US. Nearly half of all adults sampled -- 48% in 1997 -- said the benefits of "space exploration" far outweighed or slightly outweighed the costs. This figure has been relatively stable over the past ten years. We note that support for scientific research in general, including medical research, is even higher -- averaging about 70% over the past ten years, although for some disciplines the support is less: genetic engineering, for example, received endorsement from only 42% of adults in 1997. It is not surprising that people support medical research, whose practical significance is apparent; more noteworthy is the public's endorsement of space science, whose practical consequences are much less clear.

The *Science and Engineering Indicators* survey asked people whether they viewed themselves as attentive to the various fields of science, generally interested, or neither. (To be attentive in this study the respondent had to indicate he or she was very interested, very well informed, and regularly read about the material.) When one compares the responses to being attentive to that of *support* for science, it becomes clear that the attentive public is the most supportive, both in terms of the strict cost benefit ratio, and also insofar as the perceived advantages (leading to better lives, more interesting work, more opportunities, etc.) outweigh the perceived disadvantages (its effects can

be harmful, change our way of life too fast, or reduce the dependence on faith, etc.) Among the attentive population, two and one-half times as many think of science as positive and promising as compared to those whose attitudes are critical or pessimistic. Among the public who are neither attentive nor particularly interested, this ratio is only one and one-half -- so, about 43% of them are quite pessimistic. When formal education is taken into account, it clearly appears that the more educated the population, the more likely it is to be optimistic and supportive -- about twice as much for college graduates as for those without a high school diploma, and even more so for those with post graduate education. However, increased education (and knowledge, too, we infer) does not always lead to a more supportive community. In the example of nuclear power, the survey showed that support leveled off as more informed people also become more critical. No such tendency was found in the space science sample.

There are at least three dimensions to scientific literacy (Miller, 1998): knowing the vocabulary of science, understanding the nature of scientific discovery, and understanding the impact of science and technology on individuals and society. The surveys revealed an interesting point about this third level of literacy for the group of people who thought of themselves as "very well informed": they were significantly more likely to say they participated in public policy disputes than those who had doubts about their level of understanding. Increasing the knowledge of the public will, if these trends are related, also increase the number who participate in the policy development. It is also true that some of the more knowledgeable public were aware of their limits and did not consider themselves "very well informed," and so to some extent increased knowledge might lead to a group declining o participate; however, better teaching will also educate those who do participate while not being particularly well informed. Overall, then, better education about space science - and we show below that there is considerable room for improved education - should result not only in a

better informed citizenry, but one more likely to participate intelligently the public discourse, and one more optimistic about - and supportive of - space science.

5. The Public's knowledge of Space Science is Surprisingly Limited

5.1 JUST THE FACTS

The NSF's *Science and Engineering Indicators* (*S&EI*) surveys also sampled the public's knowledge of scientific facts by asking 20 questions, three of which were astronomy or space science related: (1) "True or false -- The Universe began with a huge explosion?" (2) "Does the earth go around the Sun or does the sun go around the earth?" (3) "How long does it take for the earth to go around the sun: one day, one month or one year?" The results are disconcerting, if not completely new. Only 32% of all adults answered true to number 1, including fewer than half of those who considered themselves as "attentive" to science topics. Some good news: nearly three-quarters -- 73% -- did know the earth went around the sun, although fewer than half of those without a high school education knew this to be the case. Perhaps most surprisingly, fewer than half of all adults, 48%, knew that the earth circles the sun in one year -- and 28% of those adults with graduate/professional degrees, the most knowledgeable category, did not know this fact.

It is important to place all this in context. For comparison, 93% of all adults in the survey knew that "cigarette smoking causes lung cancer" -- this was the best response to any of the factual questions . Not too far behind, about 83% of the adult public knew that "the oxygen we breathe comes from plants" and that "the center of the earth is very hot." I conclude that is it reasonable to hope that effective education programs might teach something to the 68% of adults unfamiliar with the Big Bang, or the 52% unsure of what a "year" is. The survey also discovered that only 11% of adults (only 28% of college graduates!) could in their own words describe "What is a

molecule?" from which I conclude that, just as the level of general knowledge about space science could be better, it could also be worse. This is important to recognize because there may be a tendency to throw up one's hands in despair, given the tremendous, post-sputnik science education efforts under which many of those in the survey were schooled. These efforts were not obviously failures, but we can do better.

A further conclusion can be derived about the *attentive* public – it was (not surprisingly) also the most knowledgeable. In every science topic the respective attentive public was better informed than the "interested" public, which in turn was much better informed than the general public. Thus there is a clear link between the attentive and interested public, and the knowledgeable public.

5.2 BEYOND THE FACTS: THE BELIEF IN ASTROLOGY AND PSEUDOSCIENCE

It's not only what people don't know that can hurt them. In a recent survey undertaken by York University in Toronto, 53% of first year students in both the arts and the sciences, after hearing a definition of astrology, said they "somewhat" or "completely" subscribed to its principles (an increase of 16 percentage points for science students since the first survey was done in 1991). The students also replied that "astronomers can predict one's character and future by studying the heavens." The *S&EI-2000* study is only a little more sanguine: it found 36% of adults agreeing that astrology is "very scientific" or "sort of scientific," and notes that a roughly comparable percentage believes in UFOs and that aliens have landed on Earth – so, more people than know about the Big Bang. And about half of the people surveyed believe in extra-sensory perception -- more than know that Earth goes around the sun in a year. The *S&EI-2000* study speculates that the dominant role of the media (especially the entertainment industry) in people's awareness has resulted in an increasing inability to discriminate between fiction and reality. People can forget what they learned in high school, while the media, insofar as they do contribute to the "dumbing down" of America,

provide a steady stream of images; public education efforts need to be persistent and competitive as well.

6. Might the Surveys be Wrong or Misleading?

In their book Misunderstanding Science? The Public Reconstruction of Science and Technology, Irwin and Wynne (1996), and the other contributors to the volume, attack the Royal Society's methodology and Report (and by inference other similar studies) for its implicit presumptions about the nature of science and the scientific methods (for example, that science is "a value-free and neutral activity"), and for its presumptions as well about the citizenry (for example, the "assumption of 'public ignorance' " and that 'science is an important force for human improvement.") They emphasize that "in all these areas, social as well as technical judgments must be made -- the 'facts' cannot stand apart from wider social, economic and moral questions." It is perhaps easy to understand their criticisms of surveys of attitudes towards medicine, or nuclear power, where the impact on the individual or the state is more direct than it is for space science. Their underlying proposition however -- "the *socially negotiated* [their emphasis] nature of science" -- applies across the board, and is a much more controversial one. As for the data themselves, they point out that the surveys, as a result of these presumptions, are of questionable value. For example, in the context of the public's knowledge of the facts, they cite studies that show "ignorance [can be] a deliberate choice – and that [it] will represent a reflection of the power relation between people and science." The ESA survey, for example, rather clearly indicated it was sponsored with the aim of ascertaining public support for ESA's programs. Without necessarily agreeing on all these counts, we can still appreciate the legitimate limits of these surveys. As Bauer, Petkova and Boyadjieva (2000) suggest, there are other ways of gauging knowledge. In our

case, for instance, the fact so many people answered incorrectly to the survey's query about the earth's revolution may not really be so damning a statistic; it may not even prove that people really do not know the meaning of a "year." Despite their possible limitations, there is nevertheless an internal consistency to these studies. I believe they demonstrate, at least insofar as "knowledge" is concerned, that things could be worse -- but also that they could be better.

7. Why do Space Science Research?

Copernicus expressed the opinion that the philosopher's "aim is to seek truth in all things." Certainly many researchers today would echo this high-minded sentiment. However Copernicus does not say why a practical-minded public should support that effort, and so it is useful to attempt an understanding of public attitudes towards basic research itself.

7.1 COPERNICUS, NEWTON, BACON, AND JEFFERSON

Gerald Holton (1998, 1999) has put forward a model in which basic scientific research falls into three general categories, each associated with an historical figure who represented that mode of inquiry. The "Newtonian mode," also the Copernican model, is the one in which scholars work for the sake of knowledge itself. Francis Bacon, on the other hand, urged the use of science "not only for 'knowledge of causes, and secret motion of things,' but also in the service of *omnipotence*, 'the enlarging of the bounds of the human empire, to the effecting of all things possible." According to Holton's analysis, this applied, "mission-oriented" approach to research is today the one most often used to justify public support of science. He proposes that there is actually a third way to view research, as exemplified by Thomas Jefferson's arguments to Congress for funding the

Lewis and Clark expedition, namely, the "dual-purpose style of research" in which basic new knowledge is gained but where there is also a potential for commercial or other practical benefit.

The positive public attitudes towards science and space science in part reflect the opinion that basic science research ultimately does drive a successful economy and lifestyle. Since 1992 the *S&EI* studies have tried to quantify these attitudes by asking people whether they thought science (in general, and not space science in particular) was beneficial by making our lives "healthier and easier," "better for the average person," would make work "more interesting," and provide "more opportunities for the next generation." In 1999 over 70% of all adults agreed with all of these assertions. But at the same time more than half of the respondents (to another survey) agreed that "science and technology have caused some of the problems we face as a society." Progress is a mixed bag. More to the point, a dramatic 82% of adults in the 1999 *S&EI* study agreed that, "Even if it brings no immediate benefits, scientific research that advances the frontiers of human knowledge is necessary and should be supported by the Federal Government." Space science research benefits from this general support, but in a more limited way. While 37% of adults thought "too little" money was being spent by the government on "scientific research," only 15% thought so regarding "exploring space," while 46% thought "too much" was being spent on it (by far the highest percent of the three science disciplines queried: exploring space, pollution and health.)

7.2 THE KENNEDY MODEL

It is clear that basic research -- the search for "truth" -- is supported by the public, especially if there might be some practical outcome. While health and profit are obvious inducements to the support of medical, environmental, or applied research, the practical benefit of having more *astronomical* truths is harder to identify. I argue, however, that in fact there are unique, even

practical benefits to space science research, based on two of the "appeals of space science" presented above (section 3.1), namely, the implications for spiritual and personal meaning, and (not unrelated) satisfying a love of adventure and exploration. Following in the example of Holton, I call this perspective on research the "Kennedy Mode." Said President Kennedy, referring to the Apollo program to land on the moon, "No single space project in this period will be more impressive to mankind, or more important for the long-range exploration of space; and none will be so difficult or expensive to accomplish . . . in a very real sense, it will not be one man going to the moon if we make this judgment affirmatively, it will be an entire nation (May 25, 1961)." "We choose to go to the moon in this decade and do the other things, not because they are easy, but because they are hard (Sept. 12, 1962)." While understanding that Kennedy had many political, economic and defense concerns enmeshed in his proposals – all justifications for government research admittedly have complex subtexts associated with them – it is nonetheless significant that he chose to frame a justification for the space program, as exemplified by these quotes, in the clear language of spirit and of challenge. Space is a grand human adventure, not done purely for the sake of curiosity, nor for the sake of economic benefit either, whether strategic or serendipitous. This underlying sense of the important intangibles of space science is quite pervasive. For example, the recent National Academy of Science Committee on Science, Engineering and Public Policy (COSEPUP) report, "Evaluating Federal Research Programs: Research and the Government Performance and Results Act (7)" states, "Knowledge advancement furthermore leads to better awareness and understanding of the world and the universe around us *and our place therein* [my emphasis]..." Our place in the universe is not a reference to astrometric studies of the stellar reference frame and the location of the sun and earth in space, but to personal meaning.

8. Successful Communication -- It takes Effort from Both Sides

There are an incredible number of popular books on space science. A search of Amazon.com in June, 2000, finds 2395 books in print on the topic of "cosmology," about 800 of them (!) published since 1996. Many are not for the general public, but most are, yet even the popular ones are often not very good. A good example of the latter is Stephen Hawking's phenomenal success, "A Brief History of Time" (Hawking, 1988). A movie with the same name, about his life and touching on this material, was made in the early 1990's, and which I had the pleasure of introducing at its Washington, D.C. premier at the Museum. I fielded questions from the audience afterwards, and took the opportunity to pose a few of my own to those assembled, which, like most NASM audiences, was literate and self-selected. When I asked the sellout crowd of over 500 people how many had read the book, virtually every person raised his or her hand. Then I dared to ask how many people understood the book -- and almost no one raised his hand, or the few who did, did so with visible temerity. Despite the talents of this great physicist and communicator, this book was a failure as an effort to teach. Indeed I spent most of the next hour trying to persuade people that they were not stupid, and that most of the material in the book was possible for *even* a layman to understand, though it might take a bit more effort on both the part of the reader and the writer. I noted, since the majority of them had said they were lawyers, that even though I have a Ph.D. I did not expect to understand the details of real estate law after reading a 200 page book, or seeing a movie. Motivation and expectations are important ingredients of learning.

8.1 A SCIENTIFIC UNDERSTANDING OF THE PUBLIC

Irwin and Wynne (1996)) urge that scholars consider "not just the 'public understanding of science' but also the scientific understanding of the public and the manner in which that latter

understanding might be enhanced [because] without such a reflexive dimension scientific approaches to the 'public understanding' issue will only encourage public ambivalence or even alienation." The surveys help towards this goal because they clarify what is meant by "the public understanding," provide context, and can measure trends. To rise to the challenge of increasing the public's understanding of space science, we must be able to evaluate success or failure, using studies including the *S&EI*, yet often the community has felt that simply trying hard was good enough. The statistics suggest we have so far been able to maintain steady levels of "understanding," but made little progress. In this new millennium there are hurdles which will require new approaches. The five "appeals" of space science listed above can facilitate creative new programming, while involving adults, children, and people of all cultures and backgrounds.

8.2 SOME CHALLENGES FACING THE SPACE COMMUNITY

There are some specific difficulties, as well advantages, for space science education efforts. For one thing, the pace of discovery in astronomy is very rapid. There are about 65% more US astronomers today than in 1985 (as measured by the total membership in the American Astronomical Society), and more papers are being published, about 80%more, for example, in *The Astrophysical Journal.* Furthermore very large amounts of data are now being collected thanks in part to the sensitive, large format detector arrays. In 1969, for instance, the Infrared Sky Survey found about 6000 objects, whereas the 2MASSinfrared sky survey has over ~400 million point sources, and over 8 TB of useful data. The Sloan survey will contain 15TB of data. Not least, the topics are increasingly complex. The power spectrum of the cosmic microwave background is a more difficult concept to explain to people than is the recession velocity of galaxies. Finally, television, computers and increased mobility mean that there are new populations of people, with varying educations, backgrounds, and perspectives, who are gaining access to modern space science

information. All of these challenges should be viewed as opportunities as well, chances to incorporate exciting new results and alternative perspectives for what, in agreement with Irwin and Wynne, I think must be a more reflexive educational approach. There is a strong temptation to resort to hyperbole when the significance of a discovery is hard to explain. These temptations should be resisted, because, as survey critics have noted, people may be smarter than polls suggest.

9. "Nothing... [can] be moved without producing confusion"

> "Thus...I have at last discovered that, if the motions of the rest of the planets be brought into relation with the circulation of the Earth and be reckoned in proportion to the orbit of each planet, not only do the phenomena presently ensue, but the orders and magnitudes of all stars and spheres, nay the heavens themselves, become so bound together that nothing in any part thereof could be moved from its place without producing confusion of all other parts and of the Universe as a whole." -- Nicolaus Copernicus, *De Revolutionibus op. cit.)*

Copernicus observed that his model worked well, and furthermore, that like a jigsaw or clockwork, it seemed to fit together so perfectly that the simple notion of the earth circling the sun led to an entire universe with internal order and beauty. I make, by analogy, the same point as regards the public's understanding of space science. A population which can comprehend that the earth revolves around the sun in one year – one of those simple facts – is one which may also comprehend that the scientific method offers a rational, consistent and objective approach to life. And, contrariwise, a public which does not have a grasp of the basics is likely to be one which is susceptible to "confusion," doubting these facts and perhaps the methods used for their discovery

as well. Does it matter that only 48% of adults, not 58%, know the period of the earth's revolution? Perhaps not. But the statistics provide strong evidence that improvement is possible, and likewise that degeneration is possible with increasing numbers of people vulnerable to astrology, belief in alien invaders, or the hope that their lucky numbers will win at the lottery. I have shown that space science is a very popular kind of science, particularly accessible and interesting. These indicators should spur on the space science community to continue, and enhance, its public programming in order to attract and inform new and larger audiences.

The consequences of an improved understanding of space science on attitudes towards space science are not clear. Increased knowledge may be accompanied by increased scepticism about particular missions or experiments, as polls show can happen. Nevertheless it seems likely, to first order, that research programming will benefit from increased civic knowledge. While felicitous, this should not in itself be the reason for improving our educational efforts, for like Copernicus, I believe our "aim is to seek truth in all things as far as God has permitted human reason so to do," and in this enterprise the multitude, our sponsors, are also our partners.

Acknowledgments

The author acknowledges a helpful discussion with Prof. Gerald Holton. This work was supported in part by NASA Grant NAG5-10659 and NAGW-1261. An earlier version of this paper was prepared in conjunction with an invited talk given to the COSPAR-2000 session on "The Public Understanding of Space Science."

The Far Infrared Lines of OH as Molecular Cloud Diagnostics

Howard A. Smith
Harvard-Smithsonian Center for Astrophysics
60 Garden Street
Cambridge, MA 02138
hsmith@cfa.harvard.edu

Abstract

Future IR missions should give some priority to high resolution spectroscopic observations of the set of far-IR transitions of OH. There are 15 far-IR lines arising between the lowest eight rotational levels of OH, and ISO detected nine of them. Furthermore, ISO found the OH lines, sometimes in emission and sometimes in absorption, in a wide variety of galactic and extragalactic objects ranging from AGB stars to molecular clouds to active galactic nuclei and ultra-luminous IR galaxies. The ISO/LWS Fabry-Perot resolved the 119μm doublet line in a few of the strong sources. This set of OH lines provides a uniquely important diagnostic for many reasons: the lines span a wide wavelength range (28.9μm to 163.2μm); the transitions have fast radiative rates; the abundance of the species is relatively high; the IR continuum plays an important role as a pump; the contribution from shocks is relatively minor; and, not least, the powerful centimeter-wave radiation from OH allows comparison with radio and VLBI datasets. The problem is that the large number of sensitive free parameters, and the large optical depths of the strongest lines, make modeling the full set a difficult job. The SWAS montecarlo radiative transfer code has been used to analyze the ISO/LWS spectra of a number of objects with good success, including in both the lines and the FIR continuum; the DUSTY radiative transfer code was used to insure a self-consistent continuum. Other far IR lines including those from H_2O, CO, and [OI] are also in the code. The OH lines all show features which future FIR spectrometers should be able to resolve, and which will enable further refinements in the details of each cloud's structure. Some examples are given, including the case of S140, for which independent SWAS data found evidence for bulk flows.

1 The Far Infrared Transitions of OH

Storey, Watson and Townes (1981) made the first far infrared detection of OH in the interstellar medium: the two 119μm lambda-doubled lines between the ground and first excited states, which they discovered in absorption from Sag B2, and in emission from the shock in Orion KL. Altogether there are 15 far infrared lines between the lowest 8 rotational levels of OH. The lines (each involving six transitions between the hyperfine-split rotational levels) are at wavelengths of (approximately) 28.9μm, 34.6μm, 43.9μm, 48.8μm,, 53.3μm, 65.1μm, 71.2μm, 79.2μm, 84.4μm, 96.3μm, 98.7μm, 115.4μm,

119.9μm, 134.8μm, and 163.1μm. The upper state excitation temperatures for these lines range from 120K to 618K. The dipole moment for OH is large, 1.668 Debye (for comparison the CO dipole moment is 0.112 Debye), and the radiative rates for OH transitions are generally fast. For example, the 119μm fundamental transition rate is about 0.1 sec^{-1}. But the FIR OH transitions also include some cross-ladder lines whose radiative rates are one hundred times weaker, providing a dataset of neighboring, far IR lines which frequently include both optically thin and very optically thick features. The OH analyses have an additional resource from which to draw: the strong hyperfine radio wavelength transitions that OH has in its ground-state, and which have been extensively observed. Maser and/or mega-maser activity is seen in many of the stars and galaxies which ISO observed.

The general properties of interstellar OH are known from thermal OH emission studies done at radio wavelengths, as well as from the far IR observations. Typically OH has the following range of properties: $N_{OH}/N_{H2} = 0.1 - 3 \times 10^{-7}$; $N_{OH}L = 2\text{-}100 \times 10^{15}$ cm^{-2}; T_x = 100 - 275K; and $N_{H2} = 0.1 - 3 \times 10^{7}$ cm^{-3} (e.g., Watson *et al.* 1985; Jones *et al.* 1994). In maser galaxies, such as the ones we observed with ISO/LWS, the OH masers regions typically have somewhat different properties: $N_{OH} / N_{H2} = 10^{-7} - 10^{-8}$; $N_{OH}L \sim 10^{15}$ cm^{-2}; T_x = 40K - 50K; $N_{H2} \sim 0.1\text{-}1 \times 10^{4}$ cm^{-3} (e.g., Henkel and Wilson, 1990). The presence of OH megamasers allow for VLBI observations in AGN, and results indicate that the sizes of the emitting regions are compact: ~ from a few to tens of parsecs. For example, in Arp220, one of the galaxies I discuss below, they seem to surround the AGN, with H_2 densities ~ 10^6 cm^{-3} (Lonsdale *et al.* 1994; Skinner *et al.* 1997).

Four of the relatively strong far IR OH transitions involve the ground state. In warm clouds the molecules absorb the strong IR dust continuum, populating effectively some of the higher lying levels. As was conclusively shown by Sylvester *et al.* (1997), the 18 centimeter radio maser emission in evolved stars is pumped by absorption of the 34μm dust continuum, while in AGN Skinner *et al.* (1997) proved the effectiveness of the IR pumping of mega-masers in Arp220. The presence of a strong far IR continuum affects all of the far IR lines, to varying degrees, and means (besides making the models more complicated) that the set of far IR OH lines also provide a sensitive measure of the local continuum conditions. One final point is worth noting about OH: unlike other some species commonly used as far IR probes of the interstellar medium, like CO, H_2O, or OI, OH emission from PDRs or shocks does not contribute a relatively dominant amount of luminosity to these other processes. In the cases I model below, just the warm gas from a dusty molecular clouds is adequate to explain the strengths we observe. OH, therefore, has a powerful combination of features that makes it a very useful species for dis-entangling cloud properties across a very wide range of conditions.

2 ISO/LWS Observations of Extragalactic OH

The ISO/LWS Extragalactic Science team has seen OH in fifteen galaxies, and has obtained potentially useful limits on approximately one hundred other galaxies observed by ISO. Our observations include a set on the 34.6μm "IR pump" transition from the OH $^2PI_{3/2}$ ground state, which was obtained using the ISO/SWS spectrometer. This line, and the less important 28.9μm line between excited upper states, are the only OH far IR lines not in the LWS wavelength coverage. ISO of course has also seen OH in numerous galactic locations, including Sag A, and Sag B2, and in particular in the evolved star IRC+10420 -- the first source to demonstrate that the 34μm continuum can effectively pump the OH maser lines in these stars. The LWS extragalactic detections of OH are in the following sources: Arp 220, Cen A, IRAS17208-0014, IRAS20100-4156, M82, Mkn 231, Mkn 273, NGC 253, NGC 891, NGC 1068, NGC 1614, NGC 3690A, NGC 4945, NGC 7469, and 3Zw35. Figure 1 shows all the eight OH lines detected in Arp220, along with a sample of the lines detected in other objects to illustrates some of the morphological variety.

2.1 General Characteristics of the Observed Extragalactic OH Lines

Perhaps the most striking observation about the set of extragalactic lines measured is the wide morphological range of behavior they display, even though all arise in infrared bright galaxies with either active star formation, an active nucleus, or perhaps both. In Arp 220, for example, every OH line is seen in absorption except the longest wavelength, 163μm, line which is seen weakly in emission (Fischer *et al.* 1998) . By contrast, NGC 1068, another AGN, has every detected line seen in *emission*, even the strong 119μm transition between ground and the first excited state (Spinoglio *et al.* 1999). NGC 253, a nearby starburst, has some OH lines in emission and some in absorption (Bradford *et al.* 1999), while in M82, the infrared bright, prototype starburst galaxy, the lines' equivalent widths are so small continuum that even with our high signal-to-noise ratio only the 119μm line has been conclusively seen at all, in absorption (Colbert *et al.* 1999). From the analysis of this diverse set of line strengths, several useful preliminary generalizations may be drawn for the different categories, as summarized below.

ULIGs: In the case of Arp 220, the VLBI megamaser studies together with the strength of the 34μm pump absorption provide some strong physical constraints. The OH lies in numerous small clouds which surround the AGN, and which are pumped by the local, warm, far IR continuum. Through further modeling I hope to arrive at a better sense of the shape of that continuum: is it starburst-like, or more AGN like, and is it characteristic of all ULIGs?

AGN: In the case of the bright Seyfert galaxy, NGC 1068, analyses of the strong atomic lines (Spinoglio *et al.* 1999) show the substantial presence of a PDR line emission component, along with the high ionization lines from the AGN component in the ISO beam, and a starburst component, which is seen as well in other AGN. However the [CII]/FIR ratios are strange -- often less than in PDRs. The OH lines, all seen in

emission, might help sort out the density and geometry of the clouds (for example, to see if the PDR regions have smaller than average filling factors) – and provide clues to their relationship to the active nucleus.

Infrared Bright Galaxies: We find that the OH 119 μm ground fundamental transition is always in absorption in these galaxies, as is the 53μm line, while the 163μm feature is always seen in emission. Otherwise there does not appear to be any consistent behavior in the lines from different objects: in some sources they are seen in emission, in others they are in absorption. Saraceno *et al.* (1996) and Benedetti *et al.* (2000), among others, have noted there seems to be a dearth of H_2O emission in some galactic clouds. Also, the [CII] fluxes are very low, perhaps due to low gas heating (but this is not conclusively demonstrated). They note that the neutral oxygen [OI] 63μm line is often abnormally weak and may be self absorbed. Finally, the SWAS satellite found that O_2 is very weak or absent (Goldsmith *et al.* 2000). OH plays a key role in the chemistry of the ISM, is sensitive to the temperatures and radiation fields, and its abundance and distribution should help in the analyses of all these issues.

3 Modeling of the Far Infrared OH Lines

3.1 The Montecarlo Code for Lines; the "DUSTY" Code for Continuum

I used the one-dimensional montecarlo radiative transfer code developed by the SWAS mission (Ashby *et al.* private comm) to model the OH line strengths. This code, a modification of the original Bernes code, adds a treatment of continuum photons from dust mixed in with the gas -- a particularly essential feature for OH, which is pumped in many cases by absorption of 34μm continuum. In addition, the code corrects for some previous errors encountered at large optical depths, also an issue of importance for OH which has a very strong matrix element. Finally, the code includes an ability to handle a wide range of molecules besides rigid rotors. The montecarlo code takes as input a series of concentric shells, each of which is specified as to size, gas and dust temperature, H_2 density, velocity and velocity width, and molecular abundance relative to H_2. The model as a whole also assumes a (specifiable) dust emissivity. In all the modeling, the dust is assumed to be 1% of the gas, and to have the same temperature as the gas everywhere in the cloud. The montecarlo code calculates the populations of the molecular levels in each shell. The output is then fed into a radiative transfer code that calculates the line profiles as seen by an external observer looking at the cloud.

The montecarlo results confirm the fact, noted above, that the OH lines are often optically thick. The peak optical depth at line center for the 119μm line exceeds 100 in some cases. As a result, many of the lines in many situations show self-absorption. As the model is tuned to fit the data by increasing the column density, these features can turn an emission line into an absorption line, one while strengthening the emission from a weaker

neighbor. The full set of nine line intensities, which span a range of wavelengths and optical depths, enable us to derive a rather detailed self-consistent picture of the cloud conditions solely from their intensity ratios, without the need for velocity information. But, as seen in the example below, there is also a wealth of information in the line shapes.

ISO/LWS also observed lines of CO, H_2O, and [OI] in these galaxies, with varying degrees of success. The SWAS montecarlo code can also predict the line emission from these species. In general the model predictions for these lines are in overall agreement with the observations; the uncertainties are due to uncertainties in the ISO line fluxes themselves, in the assumed molecular abundances, and in the amounts of possible line "contamination" from shocks and PDRs in the beam. Overall the results add further confidence to the models. The [OI] 63μm line is clearly self absorbed in several instances, confirming the suspicion that the line intensity is sometimes very weak due to self-absorption (Saraceno *et al.*)

The montecarlo output is not strictly internally self-consistent; the input parameters need not conserve luminosity between shells, for example. To obtain this self consistency, and to guarantee that the final cloud model was also consistent with the observed far infrared continuum flux, I used the DUSTY code (Ivezic and Elitzur, 1997) to model the continuum and generate a set of shell parameters that provided this consistency. Then I iterated the DUSTY model with the montecarlo line outputs. While this technique does not give a unique solution for the cloud structure, it does provide a canonical model consistent with the observations.

3.2 Some Modeling Results

3.2.1 S140 - A Molecular Cloud with Bulk Inflow Motions

Ashby *et al.* (2000) used the SWAS satellite to observe S140, and the SWAS montecarlo code to model the shape of the observed submm H_2O line. They are able to obtain a detailed, if not entirely unique, model of the cloud. From their set of models they conclude, for example, that the cloud radius is 0.44pc, has an inner temperature of ~70K an inner hydrogen density of 1.4x106 cm^{-3} , a radial profile of temperature which varies like $r^{-0.5}$, and a density profile varying like $r^{-0.8}$. They also conclude that "significant bulk flow" is required to explain the H_2O line shape, but because of the small optical depth of the 557 GHz line they could not differentiate between infall and outflow. Although the ISO observations of S140 were only able to set weak limits on the OH lines (Aannestad and Emery, 1998), the detailed nature of the SWAS models made it a useful check. Taking the SWAS cloud parameters for the case of bulk infall motions, I used the montecarlo code to calculate the strengths and line shapes for the full set of OH lines; I calculated the far IR lines of H_2O and the [OI] lines as well, for comparison with the ISO values. The reasonable results obtained from the model of S140, as confirmed with the SWAS (and ISO) observations, provide some confidence in the galaxy modeling. Figure

2 shows the results for three of the OH lines, on the same scale: the 163μm line (top), the 79μm line (middle), and the 119μm line (bottom). It is clear that high spectral resolution observations of the far IR water lines can readily distinguish infall from outflow, because these lines are optically thicker than the submillimeter line.

3.2.2 Arp220 - The Molecular Cloud Component of a Peculiar Ultra Luminous Galaxy

Arp220 is a particular challenge, because so many OH lines are seen, and every one of them (except the line at 163μm) is seen in absorption -- something that happens in no other known object. Arp220 is also unusual in general in that its spectrum is characterized by numerous molecular absorptions; even the [OI] 63μm fine structure line is seen in absorption, while the [CII] 157μm line is found only in weak emission (e.g., Fischer *et al.* 1998). Skinner *et al.* (1997) showed that the 34μm OH absorption could pump the OH megamasers in Arp220, and their analysis supported the model in which many small, dense molecular clouds circulate around the nucleus. Suter *et al.* (1998) attempted to model the OH line absorptions with some less complex radiative transfer models, and were driven to consider some unusual non-LTE situations to explain the observations; .

I used the SWAS montecarlo code successfully to model (to first order) all of the observed OH lines in Arp220. Figure 3 shows a sample of these model line shapes. In order to get absorption in all the lines, including the 79μm line to the ground state $^2PI_{3/2}$ from the lowest level of the $^2PI_{1/2}$ ladder, while still getting weak emisson at 163 μm, it was necessary to have falling within the ISO/LWS beam a combination small dense clouds, and a few large, giant molecular clouds. Iterating with the DUSTY code provides a way to obtain a continuum shape that fits the observed infrared continuum, though there may also be a continuum component in our beam arising from clouds without much OH. It was not necessary in this process to resort to the non-LTE scenario postulated in Suter *et al.*

3.3.3 NGC 253 - The OH Emission from a Nearby Infrared Bright Galaxy

In NGC 253, the two strongest OH lines are seen as emission lines: the 79μm and 163μm features, each of which is about twice as strong as the 119μm fundamental absorption (Bradford *et al.* 1999). Only two other OH lines are also seen in this galaxy, and as a result the model's constraints are weaker than for Arp220. The montecarlo modeling of these OH lines implies that a few giant molecular clouds, with r . 100pc, can explain the observations. The clouds have H_2 densities averaging approximately $3x10^3$ cm^{-3} and an OH abundance relative to H of about $5x10^{-8}$. ISO/LWS also observed the 119μm line in NGC 253 with the high resolution Fabry-Perot, which Bradford (2001) has successfully modeled.

3.3.4 NGC 1068 - OH Emission from AGN

NGC1068 is a remarkable extragalactic source in its OH spectrum, because it is the only galaxy observed in which all the detected transitions are found in emission. The code accurately predicts the observed line flux ratios to 40%. Based on the montecarlo

modeling, it seems the clouds that produce these lines in NGC1068 must be relatively small and dense, and heated from the inside. They are about 0.2pc in radius, with densities of $\#10^4$ cm^{-3} at the outer edges, increasing towards the center with a power law behavior of $(R/Ro)^{1.25}$. The temperature in the outer shells is about 25K, increasing inwards approximately with a power law dependence $(R/Ro)^{1.47}$. The total column density of H_2 in each cloud is $1.5x10^{24}$ cm^{-2}, and the relative abundance of OH in the model is approximately 10^{-7}. OH is taken to be absent in the hotter portions of the cloud, where T>300K. With these high column densities the strong lines of OH are very optically thick, and precise radiative transfer calculations like the present ones are absolutely essential. At a distance of 16.2Mpc, the total number of equivalent number of clouds needed to produce the observed absolute flux in the lines and the continuum is $\sim 3x10^7$. The limits to the observed fluxes in all the weaker lines are consistent with this modeling. It is worth noting in this context that in some galaxies the weaker OH lines in NGC 1068, like the 53μm line, are amongst the strongest, but the montecarlo modeling can successfully account for these differences. The montecarlo code also successfully reproduces the continuum emission seen from NGC 1068 to within a factor of 2-3 in absolute flux density across the entire LWS spectrum. The total mass in such an ensemble of clouds in NGC 1068 is approximately $9x10^9$ $M_\odot$.

4 Conclusions to Date

What general conclusions might we hope to draw from this large set of ISO OH observations? Although the analysis is still underway, it appears that the infrared luminous galaxies can be grouped into three general categories based on the relative strengths of their infrared OH lines: (1) relatively normal galaxies like NGC 253 and M82, from which the OH lines are seen in both emission and absorption, and which are dominated by starburst activity in giant molecular clouds; (2) NGC 1068 and other AGN, whose OH is seen in emission, and whose clouds must be quite small and dense (hydrogen densities up to 10^8 cm^{-3} in the cloud cores); and (3) Arp220, and perhaps other ULIGs with active starbursts as well as an active nucleus, for which a combination of a few giant molecular clouds and a collection of moderately dense cloudlets are required. (The ISO/LWS spectrum of Mkn 231 is much noisier than Arp 220's, but hints at similar behavior in its OH.) While I have made substantial progress using only the intensities of these lines, velocity resolved spectra will enable even further refinements. Future far infrared missions with sensitive, spectroscopic capabilities should find that the set of OH lines can provide wealth of information needed to unravel the structures of complex clouds.

Acknowledgments:

The modeling work reported here was done in close collaboration with the SWAS montecarlo team, especially Matt Ashby and Gary Melnick. The ISO observations and their analysis represents a large effort by the ISO/LWS extragalactic science team, in

particular Jackie Fischer, Chris Dudley, Shobita Satyapal, Luigi Spinoglio, Gordon Stacey, Matt Bradford, Matt Malkan, and Sarah Higdon. I particularly want to thank the Istituto di Fisica dello Spazio Interplanetario (IFSI) in Rome, Italy, and Paolo Saraceno of the host Infrared Group, for their gracious hospitality during a summer visit during which time I did much of this analysis. The research was sponsored in part by NASA Grant NAG5-10659.

References:

Aannestad, P.A. and Emery, R, 1998, *BAAS*, **192**, 1009.

Ashby, M., *et al.*, 2000, *Ap.J. (Letters)*, **539**, L119.

Benedettini, M., Giannini, T., Nisini, B., Tommasi, E., Lorenzetti, D., Di Giorgio, A. M., Saraceno, P., Smith, H. A., and White, G. J., 2000, *A&A*, **359**, 148.

Bradford, C. M., Stacey, G. J., Fischer, J., Smith, H. A., Cohen, R. J., Greenhouse, M. A., Lord, S. D., Lutz, D., Maiolino, R., Malkan, M. A., and Rieu, N. Q., 1999, *The Universe as Seen by ISO*. Eds. P. Cox & M. F. Kessler. ESA-SP 427.

Bradford, C.M., 2001, Ph.D.thesis.

Colbert, James W., Malkan, Matthew A., Clegg, Peter E., Cox, Pierre, Fischer, Jacqueline, Lord, Steven D., Luhman, Michael,Satyapal, Shobita, Smith, Howard A., 1999, *Ap,J.*, **511**, 721.

Fischer, J., Satyapal, S., Luhman, M., Melnick, G., Cox, P., Cernicharo, P., Stacey, G., Smith, H.A., Lord, S., and Greenhouse, M., 1998, in Proceedings of the "ISO to the Peaks Workshop: The First ISO workshop on analytical Spectroscopy", Madrid, Spain.

Goldsmith, P., *et al.*, 2000, *Ap.J. (Letters)*, **539**, L123.

Henkel, C., and Wilson, T.L., 1990, *A&A*, **229**, 431.

Ivezic, Z., and Elitzur,M., 1997, *M.N.R.A.S.*, **287**, 799.

Jones, K.N., Field, D., Gray, M.D., and Walker, R.N.F., 1994, *A&A*, **288**, 581.

Lonsdale, C.J., Diamond, P.J., Smith, H.E., Lonsdale, C.J., 1994, *Nature*, **370**, 117.

Saraceno, P., *et al.* 1996, *A&A*, **315**, L293-L296.

Skinner, C.J., Smith, H.A., Sturm, E., Barlow, M.J., Cohen, R.J., and Stacey, G.J., 1997, *Nature*, **386**, 472.

Spinoglio, Luigi, Stacey, Gordon, and Unger, Sarah J, 1999, *Ap.J.*, **511**, 721.

Spinoglio, L., Suter, J. P., Malkan, M. A., Clegg, P. E., Fischer, J., Greenhouse, M. A., Smith, H. A., Pequignot, D., Stacey, G. J., Rieu, N. Q., Unger, S., J., and Strelnitski, V., 1999, *The Universe as Seen by ISO*. Eds. P. Cox & M. F. Kessler. ESA-SP 427.

Storey, J.W.V., Watson, D.M., and Townes, C.H., 1981, *Ap.J.(Letters)*, **244**, L27.

Suter, J. P., Harvey, V., Cox, P., Fischer, J., Lord, S. D, Melnick, G. J, Satyapal, S., Smith, H. A., Stacey, G., Strelnitski, V., and Unger, S. J., 1998, *BAAS*, **193** 9002.

Watson, D.M., Genzel, R., Townes, C.H., and Storey, J.W.V., 1985, *Ap.J.*, **298**, 316.

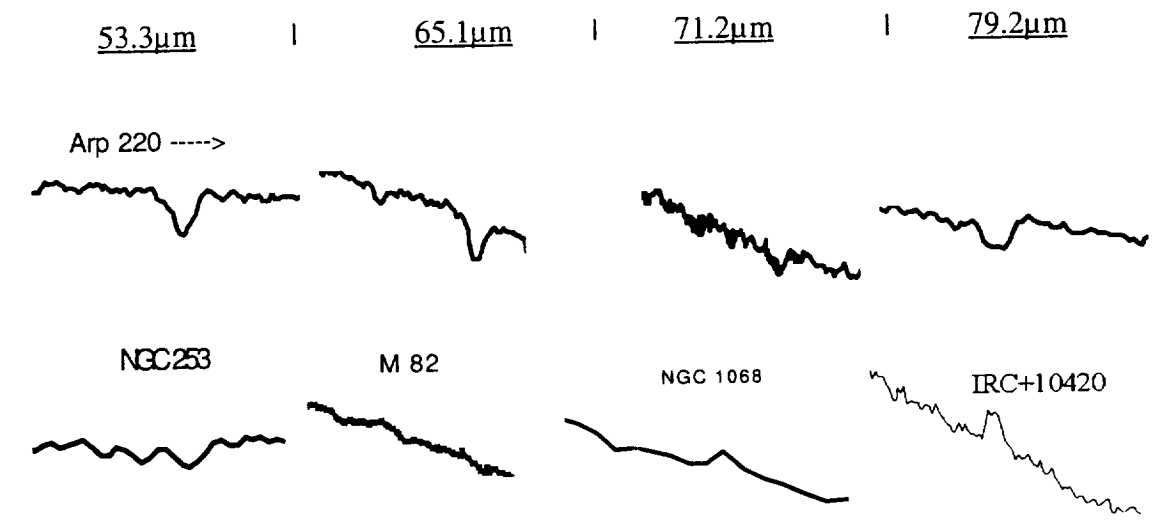

Sample of next four lines:

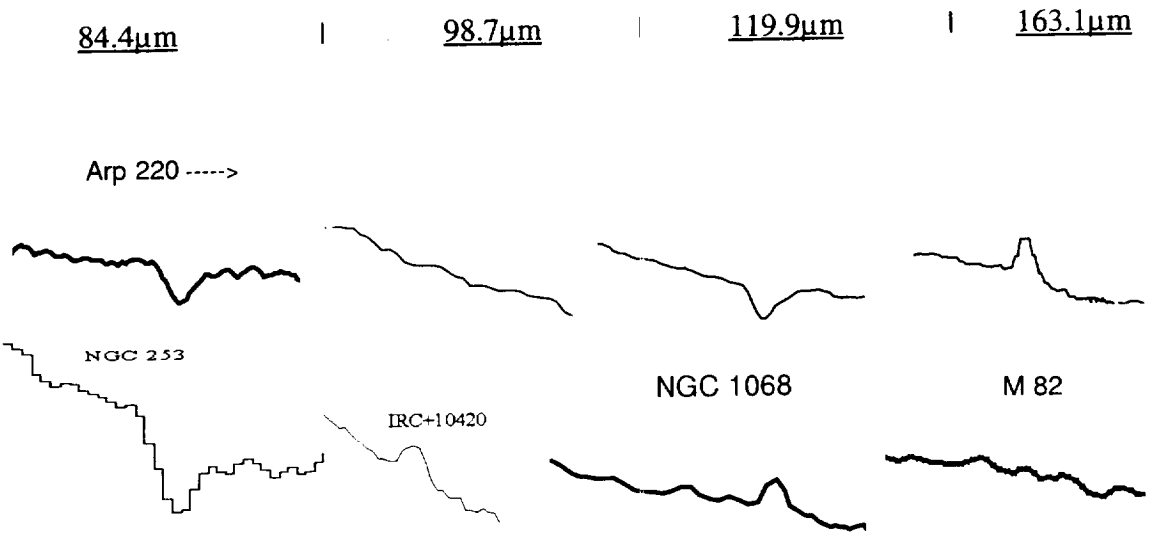

Figure 1: The 8 ISO/LWS OH lines seen in Arp 220 (the 34µm SWS-band line is not shown here). Under each OH line in Arp220, an OH line selected from another other ISO galaxy (or IRC+10420) is shown for comparison at the corresponding wavelength to illustrate some of the variety in the intensities observed.

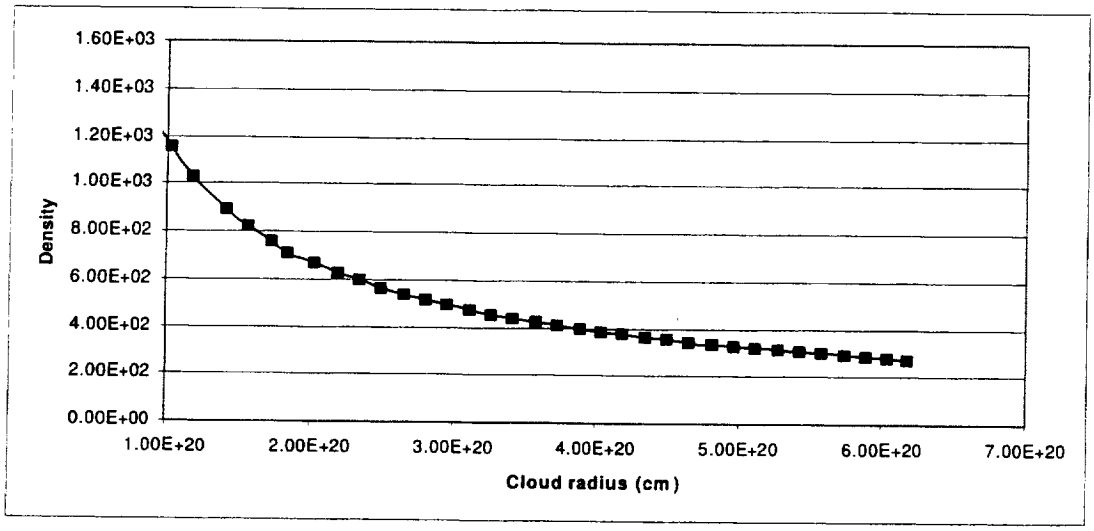

Figure 2: The hydrogen density distribution in a nominal giant molecular cloud in the galaxy NGC 253. This distribution was used in the montecarlo code modeling. The inner 50 parsecs of the GMC has warm, 250K, gas and dust, at constant density, while the bulk of the cloud has much cooler, 35K material.

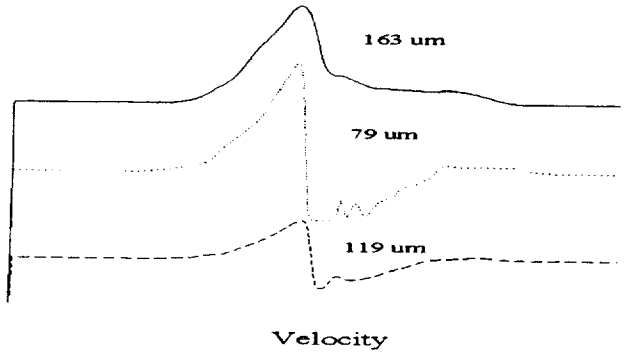

Figure 3: Predicted OH line shapes from infalling gas in S140, based on cloud profiles derived from SWAS data. The figure shows the 163 μm line (top), the 79 μm line (middle), and the 119 μm line (bottom). While all three lines show evidence for infall from their highly asymmetric shapes, only the latter two show characteristic absorption: in the redshifted (near side) material. The velocity range across the figure is ±10 km/sec, reflecting the fact that the maximum infall velocity in the model (and seen by SWAS) was 7.2 km/sec.

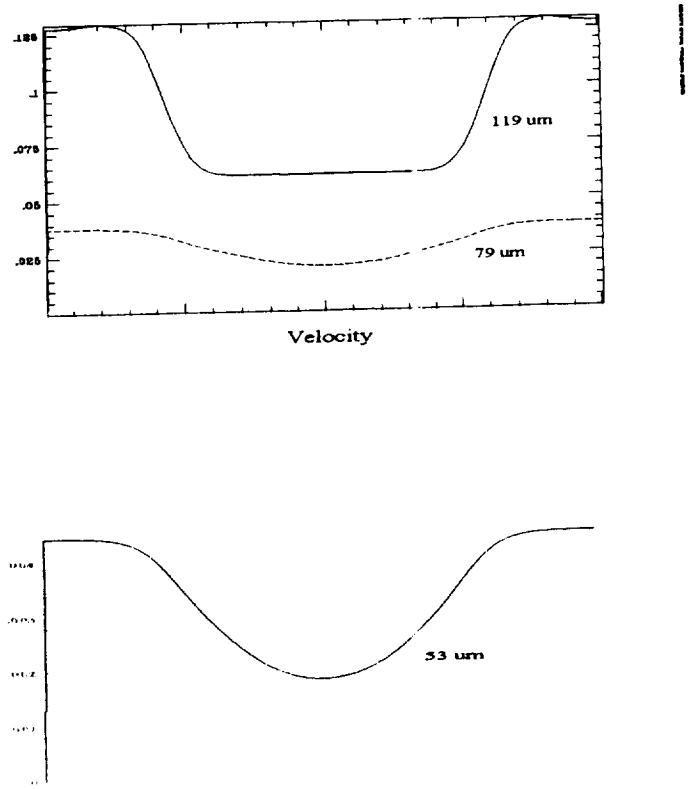

Figure 4: Montecarlo modeling results of three OH lines in Arp 220. The OH lines at 119μm, 79 μm, and 53 μm are displayed. All the OH lines are seen in absorption in Arp 220, except the weakly emitting 163 μm line – the only known object with this property.

DRAFT for Second Workshop on New Concepts for
Far Infrared and Submillimeter Astronomy

IR Fine-Structure Line Signatures of Central Dust-Bounded Nebulae in Luminous Infrared Galaxies

J. Fischer,[1] R. Allen,[1] C. C. Dudley,[1] S. Satyapal,[2] M. Luhman,[3]
M. Wolfire[4] & H. A. Smith[5]

ABSTRACT

To date, the only far-infrared spectroscopic observations of ultraluminous infrared galaxies have been obtained with the European Space Agency's Infrared Space Observatory Long Wavelength Spectrometer. The spectra of these galaxies are characterized by molecular absorption lines and weak emission lines from photodissociation regions (PDRs), but no far-infrared ($\lambda > 40$ μm) lines from ionized regions have been detected. ESA's Herschel Space Observatory, slated for launch in 2007, will likely be able to detect these lines in samples of local and moderate redshift ultraluminous galaxies and to enable measurement of the ionization parameters, the slope of the ionizing continuum, and densities present in the ionized regions of these galaxies. The higher spatial resolution of proposed observatories discussed in this workshop will enable isolation of the central regions of local galaxies and detection of these lines in high-redshift galaxies for study of the evolution of galaxies. Here we discuss evidence for the effects of absorption by dust within ionized regions and present the spectroscopic signatures predicted by photoionization modeling of dust-bounded regions.

---

[1]Naval Research Laboratory, Remote Sensing Division, 4555 Overlook Ave SW, Washington, DC 20375, USA, Jackie.Fischer@nrl.navy.mil

[2]George Mason University, Fairfax, VA

[3]Institute for Defense Analysis, Alexandria, VA, USA

[4]University of Maryland, College Park, MD, USA

[5]Harvard-Smithsonian, Center for Astrophysics, Cambridge, MA USA

1. Background

Prior to the launch of the European Space Agency's Infrared Space Observatory (ISO) in 1995, Voit (1992) showed how mid- and far-infrared fine-structure lines could be used to constrain the electron densities, extinction, and shape and ionization parameters of the central ionizing sources in ultraluminous infrared galaxies (ULIRGs). Moreover, the ground-based work of Roche et al. (1991) showed that the mid-IR spectra of the nuclei of galaxies could be placed into three classes: those with aromatic feature emission, featureless, and those with silicate absorption, typically associated with optically identified H II region, Seyfert 1, and Seyfert 2 nuclei respectively. Building on this early work on optically selected starburst and AGN galaxies, Genzel et al. (1998) constructed a diagnostic diagram of the ratio of high-to-low ionization fine-structure lines vs. the equivalent width of the 7.7 μm aromatic feature emission based on which they concluded that 70 - 80% of ULIRGs are powered predominantly by starbursts and 20 - 30% are powered by a central AGN. They attributed the weakness of the mid-infrared fine-structure lines relative to the infrared luminosity to the effects of extinction.

Far-infrared spectroscopy of a small sample of IR-bright and ultraluminous galaxies taken with the ISO Long Wavelength Spectrometer (LWS) has revealed a dramatic progression extending from strong fine-structure line emission from photoionized and photodissociated gas in the starburst galaxy Arp 299 (Satyapal et al. 2002) to faint [C II]158 μm line emission and absorption in lines of OH, H_2O, CH, and [O I] in the ULIRG Arp 220 (Figure 1; Fischer et al. 1999). With the progression towards weak emission line strengths, no trend in density or far-infrared differential extinction is indicated (Figure 2), i.e. the temperature-insensitive [O III]52 μm/[O III]88 μm line ratio does not show a trend with the ratio [O III]88 μm/FIR ratio as it would in either of these cases and all of the measured [O III] line ratios fall within the range 0.6 - 1.2, consistent with electron densities between 100 - 500 cm^{-3}. The sequence does show a trend toward lines with lower excitation potentials in the ratios [N III]57 μm/[N II]122 μm (Figure 3) and [O III]52 μm/[N III]57 μm (Figure 4). No FIR fine-structure line emission from species with excitation potentials greater than 13.6 eV were detected in Arp 220 or in Mkn 231 (Harvey et al. 1999), the two ULIRGs for which full ISO LWS spectra were taken. Voit (1992) discussed the possibility that even the mid- and far-infrared fine-structure lines would be weak in ULIRGs if they are formed in high ionization parameter regions. In such regions with high ratios of ionizing photon to electron densities, UV photons are preferentially absorbed by dust rather than gas, due to the high column densities of ionized gas in such regions. Bottorff et al. (1998) found that the L_{IR}/H_β ratios in such dust-bounded nebulae are greater than 100 for ionization parameters greater than 10^{-2}, density = 100 cm^{-3}, and stellar temperatures between 30,000 - 50,000 K.

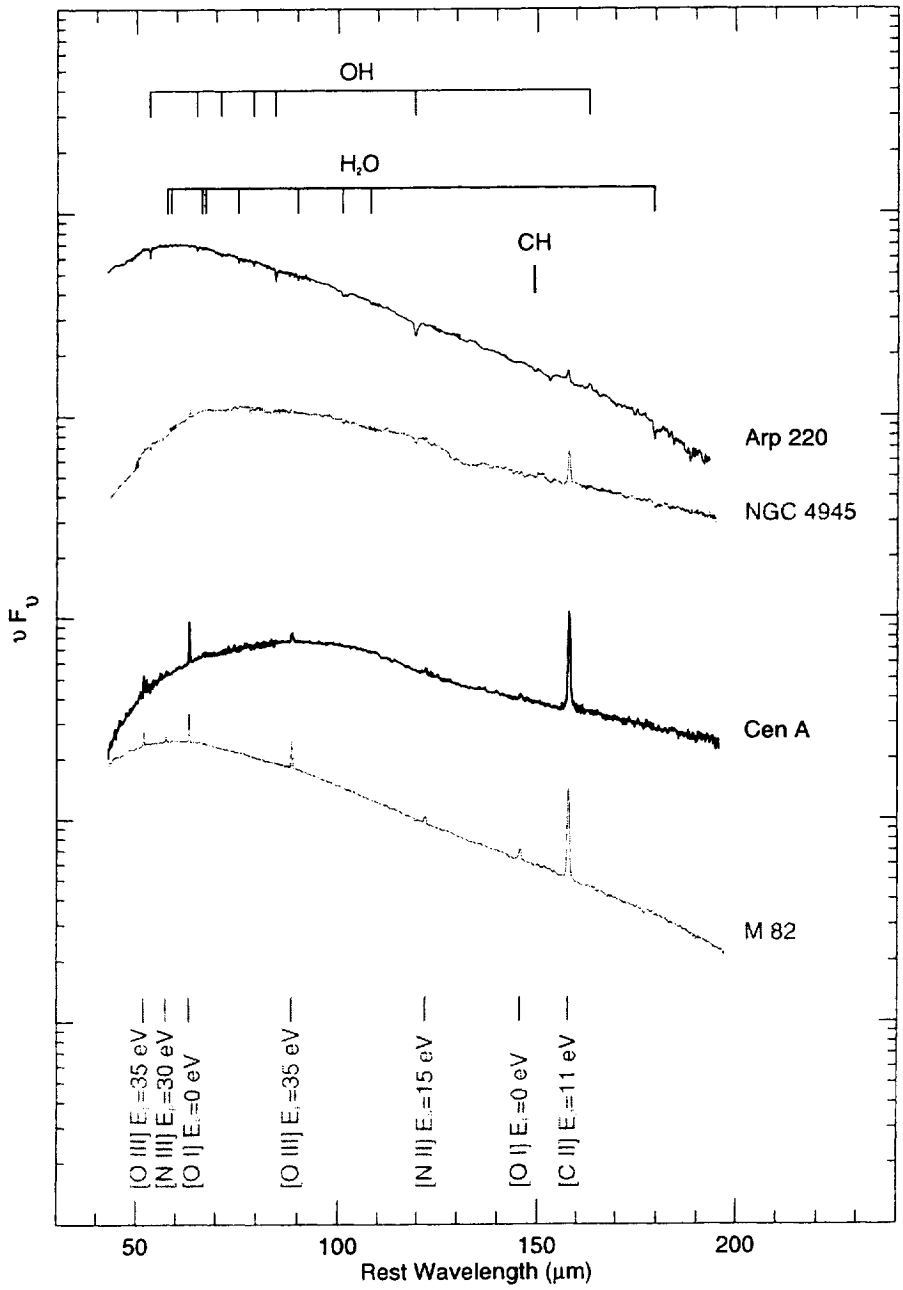

Fig. 1.— The full ISO Long Wavelength Spectrometer spectra of six IR-bright galaxies. The spectra have been shifted and ordered vertically according to the equivalent width of the [O III]88 μm line. The excitation potential, the energy required to create the species, is given in eV at the bottom of the figure. From Fischer et al. (1999).

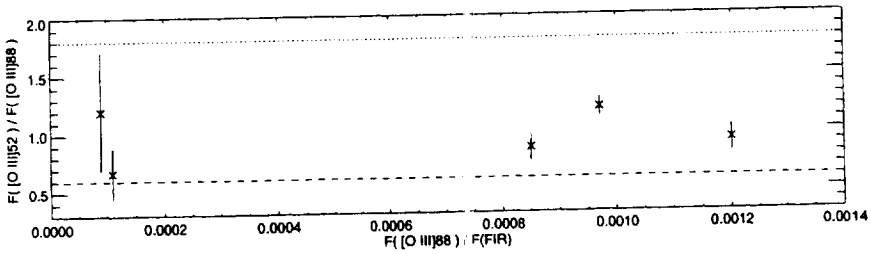

Fig. 2.— The [O III]52 μm/[O III]88 μm line ratio versus the [O III]88 μm line to integrated far-infrared continuum flux ratio for the sample galaxies. The dashed and dotted lines show the [O III] line ratio in the low density limit ($\leq$ 100 cm^{-3}) and for an electron density of 500 cm^{-3}, respectively (Fischer et al. 1999).

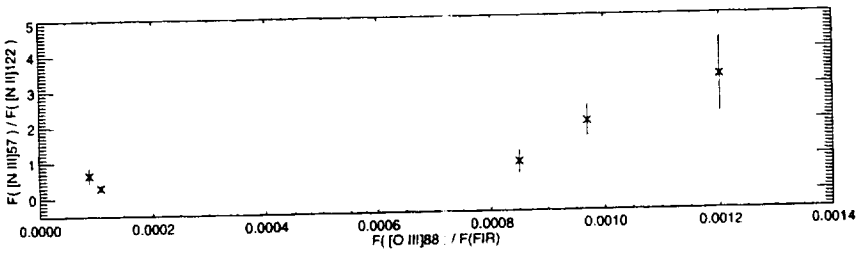

Fig. 3.— As in Figure 2 for the [N III]57 μm/[N II]122 μm line ratio.

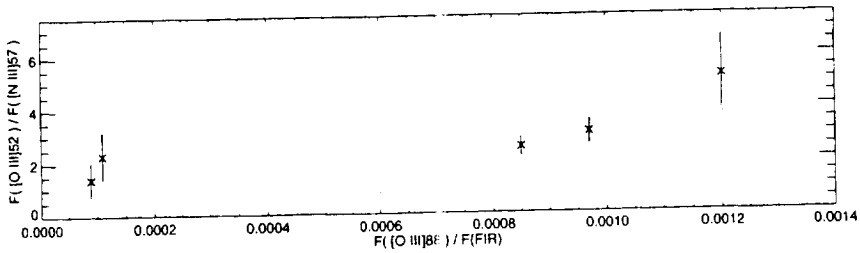

Fig. 4.— As in Figure 2 for the [O III]52 μm/[N III]57 μm line ratio.

Here we present photoionization models with starburst and power law ionization sources to predict the strengths of the fine-structure lines in dust-bounded nebulae and to compare them with the LWS spectra of the infrared-bright galaxies. Due to the weakness of the infrared fine-structure lines from photoionized gas in ULIRGs, ISO mid- and far-infrared spectroscopy produced mostly upper limits. Comparison of photoionization models of dust-bounded nebulae with spectra from future space missions such as SIRTF and Herschel will help to determine the conditions in the photoionized regions of these galaxies. The understanding yielded by these missions can then be used to probe the ionized media in high redshift galaxies by the missions being discussed in this workshop.

2. Photoionization modeling

The photoionization modeling was done using CLOUDY 94.01 (Ferland et al. 1998) for central power law (Figure 5) and instantaneous starburst (Figure 6) ionization sources. For power law models, the "table" power law option in CLOUDY was used. This option produces a continuum with $f_\nu \propto \nu^\alpha$ that is well behaved at both high and low energy limits (10^{-8} - 10^{8} Rydbergs in CLOUDY). An index α = -1.5 was used for the mid-range (10 μm - 50 keV), while the default indices of +2.5 and -2 were used for the low and high ranges, respectively. For the starburst models, we used the instantaneous, Salpeter IMF, 3 and 5 Myr aged burst models of Leitherer et al. (1999) with solar metallicity and standard mass loss. H II region abundances were used in CLOUDY.

With a central ionizing source, the ionization parameter U, defined as the ratio of ionizing photons to hydrogen atoms at the inner face of the cloud, is equal to $Q/4\pi r^2 nc$, where Q is the central Lyman continuum rate, n is the density, and r is the inner radius of the cloud. It was varied from $10^{-3} - 10^{1}$ by setting $Q = 4.5 \times 10^{54}$ sec^{-1} and varying the inner radius from 30 - 1600 pc.

The power law models predict a decrease in the [N III]57 μm/[N II]122 μm and [Ne V]14 μm /[Ne III]15 μm line ratios in the high U cases. For the starburst models, only the far-infrared line ratio decreased at high U, over the range of parameters explored. In both cases the line-to-luminosity ratios drop at high U, as expected. As Figures 5 & 6 show, high densities also produce both lower values of the line ratios and lower line-to-luminosity ratios. Older starbursts can also produce these effects, but are unlikely to power ULIRGs (Satyapal et al. 2002).

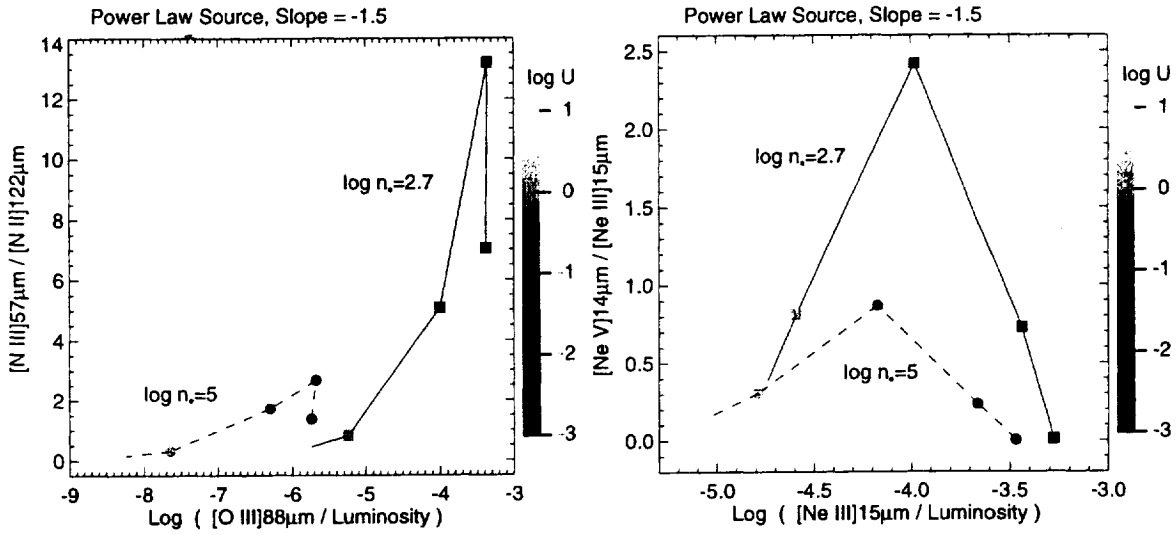

Fig. 5.— Far-infrared (left) and mid-infrared (right) line ratios vs. line-to-luminosity ratios for an AGN-like power law ionizing source for moderate (500 cm^{-3}) and high (10^5 cm^{-3}) densities are plotted for ionization parameters U, for log U = -3, -2, -1, 0, and 0.5 (as shown by the greyscale bar, right). See text for the details of the modeling.

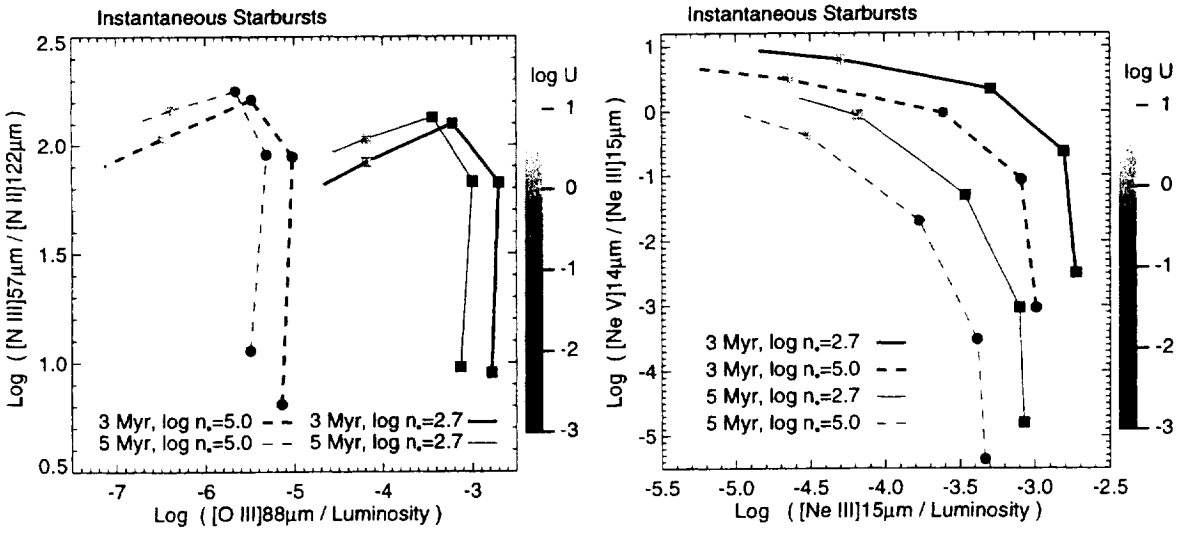

Fig. 6.— Same as Figure 5 (except for log scale in the line ratios), for ionization by instantaneous starbursts of ages 3 and 5 Myrs.

3. The effects of high ionization parameters on photodissociation region diagnostics

The CLOUDY models presented here show that under high U conditions, line emission ratios from ionization states below the dominant stage of ionization at the illuminated face of the cloud, i.e., from constituents deeper in the cloud, are often inverted compared with moderate ionization parameters due to the effects of the strong grain absorption. Some of the other infrared characteristics of ULIRGs are warm 60/100 μm colors, low aromatic feature-to-luminosity and low [C II]158 μm line-to-luminosity ratios, although their aromatic feature-to-[C II] ratios are normal (Dudley et al. 2002; Luhman et al. 2002). These characteristics may be the result of the effects of grains in ionized regions. For example in our own galaxy, Boulanger et al. (1988) find that 60/100 μm colors are higher and small grain emission lower, as traced by the IRAS 12 μm flux, within the California nebula H II region than outside of it.

SIRTF and Herschel studies will greatly improve our understanding of these diagnostics. SAFIR and future spaceborne FIR/submillimeter interferometry will be able to exploit them in the high redshift universe to futher our understanding of the evolution of galaxies.

It is a pleasure to thank Gary Ferland for helpful discussions. This work was supported by the Office of Naval Research and the NASA Long Term Space Astrophysics program.

REFERENCES

Bottorff, M., Lamothe, J., Momjian, E., et al. 1998, PASP, 110, 1040

Boulanger, F., Beichman, C., Desert, F. X., et al. 1988, ApJ, 332, 328

Dudley, C. C., et al. 2002, in prep.

Ferland, G. J., Korista, K. T., Verner, D. A., et al. 1998, PASP, 110, 761

Fischer, J., Luhman, M. L., Satyapal et al. 1999, Ap&SS, 266, 91

Genzel, R. Lutz, D., Sturm, E., et al. 1998, ApJ, 498, 579

Harvey, V.I., Satyapal, S., Luhman, M.L, Fischer, J. et al. 1999, in *The Universe As Seen By ISO*, eds. P. Cox, M.F. Kessler, ESA SP-427, 889

Leitherer, C., Schaerer, D., Goldader, J. D. et al. 1999, ApJS, 123, 3

Luhman, M. L., Satyapal, S., Fischer, J., et al. 2002, ApJ, submitted.

Roche, P., Aitken, D., Smith, C. H., & Ward, M. 1991, MNRAS, 248, 606

Satyapal, S., Luhman, M. L., Fischer, J. et al. 2002, ApJ, submitted

Voit, G. M. 1992, ApJ, 399, 495

Appendix B: SIRTF Observations

1) IRAC Images of an Infrared Bright Galaxy: M82
2) IRAC/IRS Early Release Observations of RCW 108
3) Observations of Interacting Galaxies
4) SIRTF Observations of the Galactic Center
5) Extremely Red Background Objects in the IRAC Survey

M82 ERO

9/20/02

Appendix B

IRAC Images of an Infrared Bright Galaxy: M82 **H. Smith *et al.***

Scientific Justification:
M82 is a bright, nearby starburst galaxy -- a visually dramatic prototype for the wild -- but often concealed -- infrared activity that SIRTF will study in other galaxies located both nearby, and in the remote universe. M82 contains elements of many key cosmic phenomena: a few hundred MY ago tidal interactions between M82 and a neighbor galaxy (probably M81) channeled vast quantities of gas into the dust-obscured central regions of M82, near to where a middle-sized black hole currently resides (about 9 arcsec NW of the bright 2um core; Kaaret 2001). The result was a continuing burst of star formation that progressed outward from the center (at least as suggested by some authors including ourselves). Early remnants of this activity are seen 1 arcmin NE of the center (in M82 "B": deGrijs 2001). This star formation in turn resulted in a string of supernovae, seen clearly in the near IR and the radio, that help drive a "super wind" of hot, million-degree gas blowing from the central regions in a double lobed spray, even while some infall of cooler gas continues. An elongated, doubled-peaked bar (or torus/disk) of gas and dust spans the central 700pc, and is clearly seen and velocity resolved in the infrared (including our own ISO observations) and in submillimeter lines. The ring of ionized gas (star formation) lies closer in, across about 200pc. CO is seen extending as much as 6kpc above and below the disk (Taylor, 2001).

Despite its being intensely studied, M82 still boasts numerous, unanswered scientific puzzles, including: (1) Has the star formation been dominated by outward propagation from the center, as we have argued (e.g., Satyapal et al 1997) but which is by no means certain (e.g., Alonso-Herrero et al, 2001)? (2) Does the IMF in M82 have an upper mass limit less than 100 Mo, and/or is there a deficit of low-mass stars (e.g., *op cit*)? (3) What role, if any, does the black hole play in local star formation, or otherwise in contributing to the IR? ISO spectra (Colbert *et al.* 1999; Fig. 2) find clear PAH emission of moderate strengths; its spatial distribution will be revealed by 4-color IRAC images to tell us more about the locations of SNR, the warm IR-pumped OH "kilo-masers," the central bar, and the clusters of star-burst activity detected in the H and FeII lines.

Technical Feasibility of the Observations: We propose a 3x3 raster IRAC image (14.8'x14.8' prime field) centered on the nuclear region, with 290" offsets, 12-sec frames, and 5-point cycle dithers, in High Dynamic Range (HDR) mode (see below) for a total time of 1716 seconds (Spot 6.1, with 6sec/frame corrections for HDR mode). The map will be done as a chained set of two sub-maps; the second sub-map, which covers the nuclear region, will be done last to minimize possible residual memory effects from the bright core. The source is available 22Feb03-8May03 (becoming available again on 8Oct). The resultant 5-sigma sensitivities (in μJy) are roughly 13/16/44/51 in Bands 1- 4, respectively.

Data Reduction Plan: Possible saturation in the peak pixels is a concern. ISOCAM and ISOSWS spectra (Fig.2) found an average per/IRAC-sized pixel flux at the 8μm PAH peak (IRAC band 4) of about 90mJy; ISOCAM images show this flux is spatially peaked at the center with about 190mJy per IRAC-sized pixel. Thus, IRAC's higher spatial resolution is likely to find

even higher values. We have therefore used HDR mode observations, with 0.6 second frame times, whose maximum unsaturated flux densities of approximately 780/620/1780/1500 mJy (Bands 1- 4, respectively; SIRTF SWGM 5/06/02) are, we believe, reasonably safe.

Conflicts and/or Collaborations: IRAC observations of M82 are not in the GTO program, but are included in large maps of the SINGS (Kennicutt) Program. A member of SINGS (R. Kennicutt) is a part of this team, as is a member of the SSC.

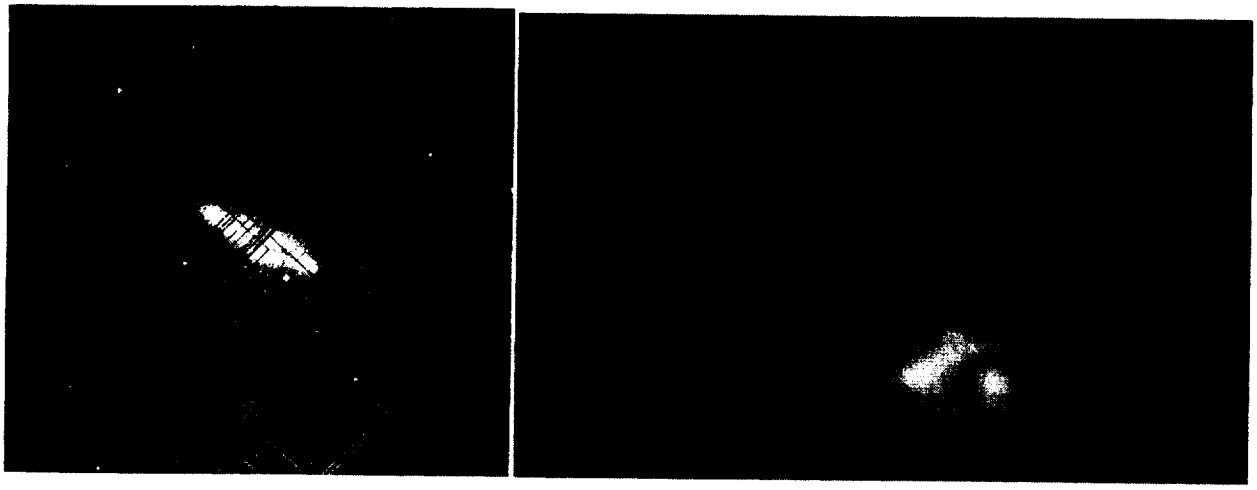

Figure 1a: M82 DSS-band image (25'x25') overlayed with our proposed 3x3 dithered IRAC fields. Figure 1b: The central ~500 pc (32") of M82 in [FeII 1.64um] (red) and Br gamma (green), as imaged by us with a 1.3" beam through a near-IR Fabry-Perot. The colors trace the relative contributions of SNR and Lyman continuum producing stars, respectively. The image is consistent with the notion that M82 contains radially propagating starburst activity. The asymmetry in [FeII] suggests the super wind has broken out of the galactic disk in the south (Greenhouse *et al.* 1997).

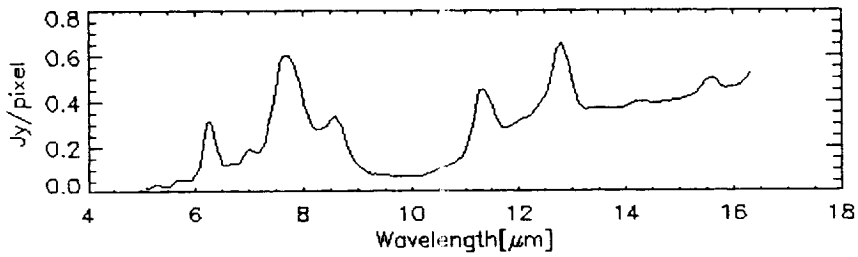

Figure 2: The ISOCAM CVF spectrum of M82 (averaged over the central1600 pc), showing in particular the PAH emission features. The PAHs are almost certainly not uniformly distributed, and the high spatial resolution, high contrast, color- color images which IRAC will obtain will directly shed light on the geometry and physics of the uv excitation and star formation activity.

References:

Alonso-Herrero, Rieke, Rieke and Kelly, *A&SS*, **276**, 1109, 2001
Colbert, J., .. Smith, H.A., et al, *Ap.J.*, **511**, 721, 1999.
Davies *et al. MNRAS*, **293**, 189, 1998
deGrijs, O'Connell and Gallagher, *A..J.*, **121**, 768, 2001
Elmouttei, Krause, Haynes and Jones, *MNRAS*, **300**, 1119, 1998.
Genzel, R., *et al.* ApJ, **498**, 479, 1998
Greenhouse, M.... Smith, H A., et al, *Ap.J.* , **476**. 105, 1997
Kaaret et al, MNRAS, **321**, L29, 2001
Maiolino, Krabbe, Thatte, and Genzel, *Ap.J.* **493**. 650, 1998.
Matt, G. *et al.*, A&A, **341**, L39, 1999.
Satyapal, S., ...Smith,H.A., et al, *Ap.J.* , **448**, 611, 1995
Satyapal, S., ...Smith, H.A., et al, *Ap.J.* , **483**, 148, 1997
Smith, D., and Wilson, A., *Ap.J.*, **557**, 180, 2001
Taylor, Walter and Yun, *Ap.J.L*, **562**, L43, 2001.
Wilson, A. *et al. ApJ*, **120**, 1325, 2000

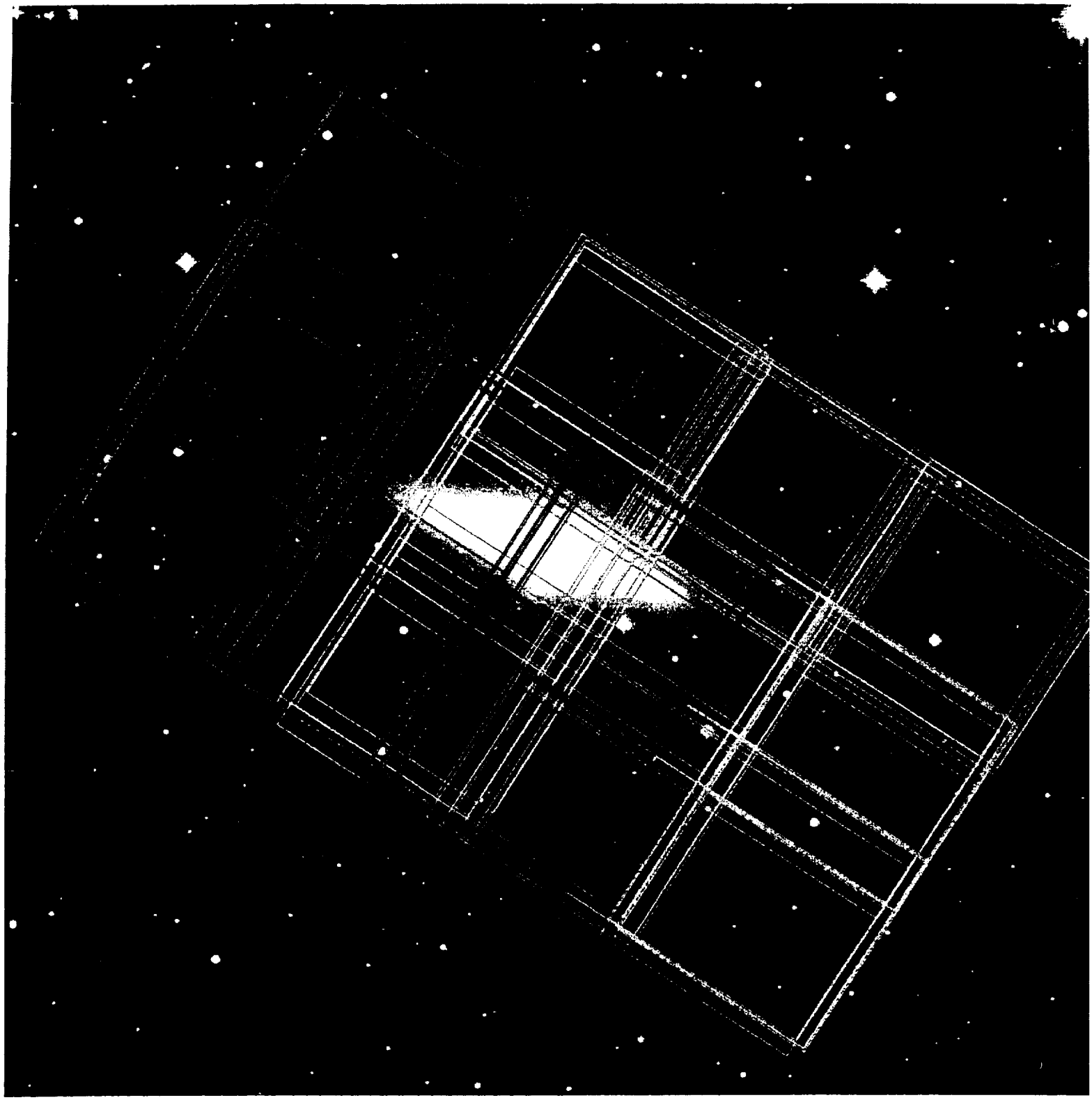

Appendix B

RCW108 ERO

Appendix B

IRAC/IRS EARLY RELEASE OBSERVATIONS OF RCW 108: A Dust Shrouded High-Mass Star Forming Region with Exceptionally Strong Thermal Water Emission

Gary Melnick, Edwin Bergin, Howard Smith, Thomas Megeath, Lori Allen, Giovanni Fazio, James Houck, and Bernhard Brandl

Scientific Justification

At a distance of 1.3 kpc, the emission nebula RCW 108 (Rodgers, Campbell, and Whiteoak 1960, *M.N.R.A.S.*, 121, 103), also known as G336.5-1.5, lies at the heart of an optically-obscured, but highly IR-luminous region in the southern Ara Constellation that is the site of active high-mass star formation (see Fig. 1). In addition, with the sole exception of Orion BN/KL, RCW 108 is the source of the strongest thermal water emission detected by NASA's Submillimeter Wave Astronomy Satellite (SWAS) in more than 3.5 years of observations.

Loosely surrounding RCW 108 is the young OB association Ara OB1, which is dominated by two early O-stars (HD 150135 and HD 150136) whose ionizing radiation generates much of the extensive nebulosity seen in RCW 108. A complex range of physical processes are thought to operate in the RCW 108 cloud; these processes must be disentangled to produce a coherent picture of current star formation in this region, and the subsequent influence the recently formed stars have on the surrounding cloud. The IRAC 4-band maps will be essential to the task, and will provide dramatic images which should illustrate to the public the unique capabilities of SIRTF in studying molecular clouds and the process of star formation. The high spatial resolution will help us to unravel the various regions of activity present. IRAC images will pierce the extinction of the cloud to reveal a dense field of background stars; measurements of the extinction to these background stars will be used to map out all but the densest parts of the structure of the RCW 108 molecular cloud. These images will also show extended nebulosity from the diffuse PAH emission which is produced by the interaction of the "dark" molecular cloud with UV photons originating in the young, hot stars both internal and external to the RCW 108 cloud. Finally, the IRAC images will detect protostars embedded in this cloud; the protostars will be identified by the IRAC photometry together with the IRS spectra. These data will provide a first-ever snapshot of current star formation in this region.

The SWAS water map of RCW 108 is consistent with there being a compact ($\lesssim 4'$) emitting region in which water is either abundant, warm, or both. The narrow width of the H_2O line (FWHM ~ 4 km s^{-1}; see Fig. 2) suggests that the emission arises in relatively quiescent gas, such as a photodissociation region (PDR) or hot core. Unfortunately, the distribution of water within the $4'$ SWAS beam is unknown. With its higher spatial resolution (than SWAS), an IRS image could establish the distribution of warm water vapor. As listed in Table 1, there are eight transitions of $H_2{}^{16}O$ within the IRS wavelength range with upper level energies below 1000 K that may be detectable. ISO conducted no Long-Wavelength Spectrometer (LWS) observations of RCW 108 and the archive contain data only for the 32–37 μm portion of the Short-Wavelength Spectrometer (SWS) range. Three candidate $H_2{}^{16}O$ transitions lie between 32 and 37 μm. Though ISO set only upper limits on their line fluxes (see Table 1), SIRTF/IRS will be able to improve on the ISO results by more than a factor of 50, greatly enhancing the prospect of a water detection. The relative locations of water (IRS), protostars and PAH emission (IRAC) and other tracers (e.g., H_2) will allow us to establish the source of the powerful water emission. Such observations demonstrate the synergy between IRAC and IRS.

In addition to quiescent gas, single position ISO observations of RCW 108 demonstrate the presence of shock excitation of atomic and molecular species, as inferred by detections of H_2 S(3) 9.66 μm and Fe II 24.0 μm. The presence of H II regions, photodissociation regions (PDR), and fast shocks within the RCW 108 complex is indicated by the ISO detections of the Fe III, He II, S III, Si II, Fe II, and Ne III lines (see Table 1). In addition,

other emission lines in the IRS band (*not* studied by ISO toward RCW 108) include SI 25 μm and H_2 S(0) 28 μm which are additional tracers of PDRs, fast shocks, and cooler molecular gas. With the exception of the H_2 9.66 μm line, all of the above lines are observed simultaneously in the IRS Long-Hi mode.

Communication of Results to the Public

This Orion-like region in the southern hemisphere is a compelling ERO candidate for two reasons. First, RCW 108 is a strong infrared source with a complex underlying spatial structure of embedded luminous protostars, wisps of gas, and dust lanes. Because RCW 108 is largely obscured at visible wavelengths, the contrast between the best optical image of this source – which is almost entirely devoid of features – and the rich SIRTF/IRAC image will be stunning. A preview of these contrasting images is shown in Fig. 1 in which an optical and a coarse (20″) resolution 8 μm-image are shown side-by-side. Comparisons of this kind will also highlight the power of the infrared to penetrate dust-concealed regions of high interest in a way not possible with the most powerful optical instruments. Second, the known presence of very strong thermal water emission from this source presents a prime opportunity to showcase not only SIRTF's spectroscopic capability, but also SIRTF's ability to study a molecule of great astrobiological interest through observations of as many as eight water transitions between 25 and 37 μm.

Source Availability/Alternate Target

RCW 108 will be visible by SIRTF from 23 February through 11 April 2003, making it a suitable ERO target for a launch through early February. If the launch were to slip past early February, then we propose to combine the proposed IRAC observations of RCW 38 with a set of IRS observations similar to those proposed here for RCW 108. RCW 38 is visible by SIRTF between 19 March and 28 June. If the launch date were to slip to between 8 May and 23 July 2003, then RCW 108 would once again become visible.

Technical Feasibility

The $22' \times 20'$ IRAC map would be made with a 2-second frame time and 3-point cycling. The total time required is 27.0 minutes. The large map will provide the most impressive visual image of this complex and beautiful region. RCW 108 has an MSX peak flux (Band 4) of about 60 mJy per sq. arcsecond, and will not saturate with the 2-second frame time. We expect a point source sensitivity (5σ) at 3.6 and 4.5 μm of 15.0 and 14.5 magnitudes, respectively, which are well matched to the 2MASS K-band sensitivity.

The proposed IRS observations for the ERO consist of a total of 36 pointings in the Long-Hi mode. This will give a spatial coverage, with coarse sampling, of a $2' \times 2'$ region. To avoid saturation on RCW 108 IRS 29 we have split the IRS step and stare observations to sample a region just above and below the point source. This is shown on Fig. 2; the cross shows the position of IRS 29. This avoids the strongest region of emission as delineated by the MSX Band E (~ 25 μm) image (not shown). The required observing time is 32.2 minutes (6-second ramp per pointing with 2 cycles for redundancy).

Data Reduction

The IRAC data will be processed to completion by Tom Megeath and Lori Allen. The IRS data will be processed to completion by Bernhard Brandl. The SWAS data products will be prepared by Edwin Bergin and Gary Melnick. All references to ISO results will be handled by Howard Smith.

Conflicts

Neither RCW 108 nor RCW 38 presents a conflict with other SIRTF programs. (The GLIMPSE Legacy project covers $\pm$ 1° about the Galactic plane; RCW 108 lies $-1.5°$ below the plane.)

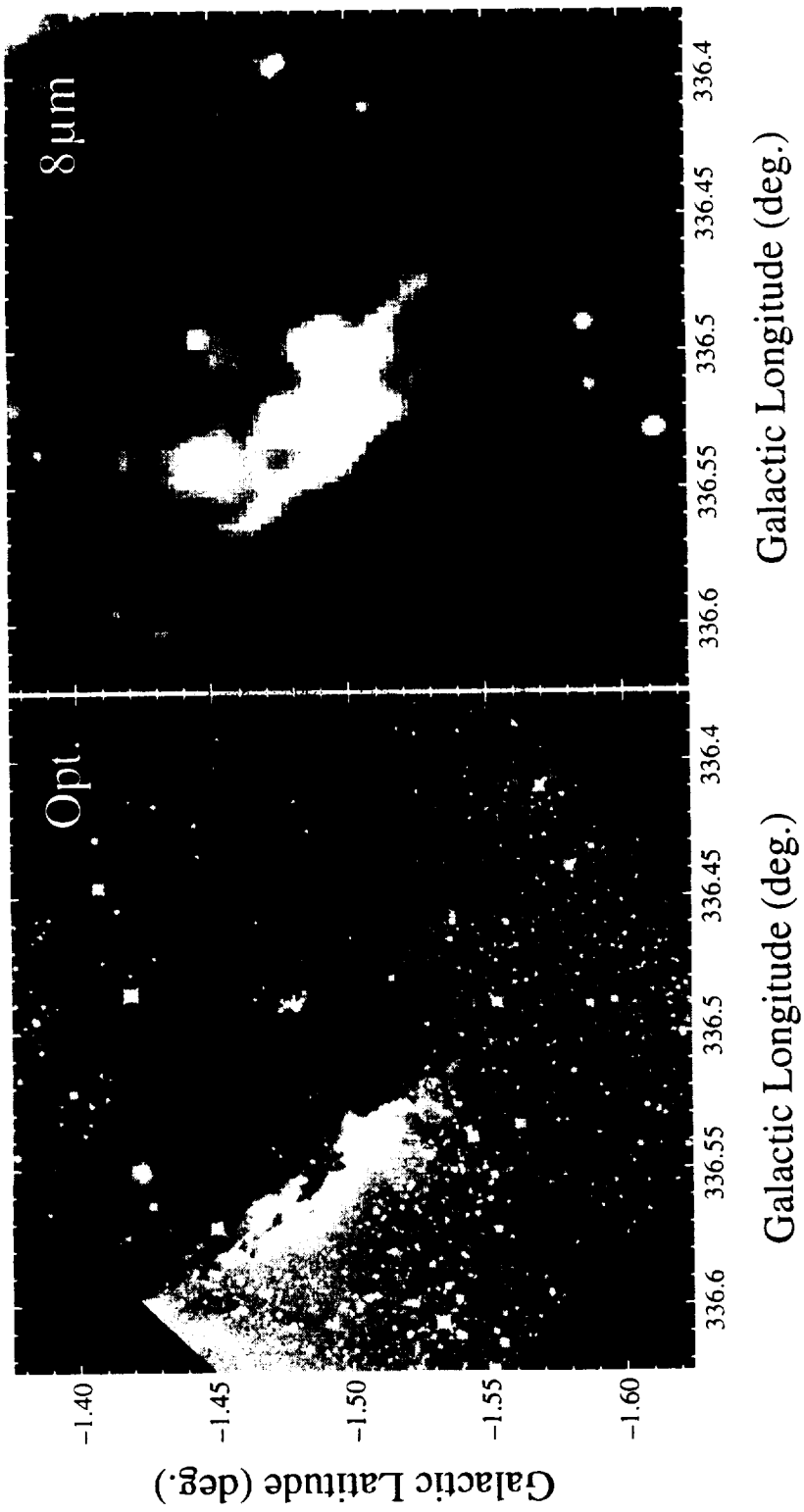

Fig. 1. Optical (*left panel*) and infrared (*right panel*) image of the Ara constellation centered on RCW 108 in each image. The proposed $22' \times 20'$ IRAC map would cover an area larger than shown. The optical image was obtained with the red filter of the Digital Sky Survey. The infrared image was obtained with the MSX Band A, centered at 8 μm, with a spatial resolution of 20″ (Price, S. D., Egan, M. P., Carey, S. J., Mizuno, D. R., & Kuchar, T. A. 2001, *Astron. J.*, 121, 2819).

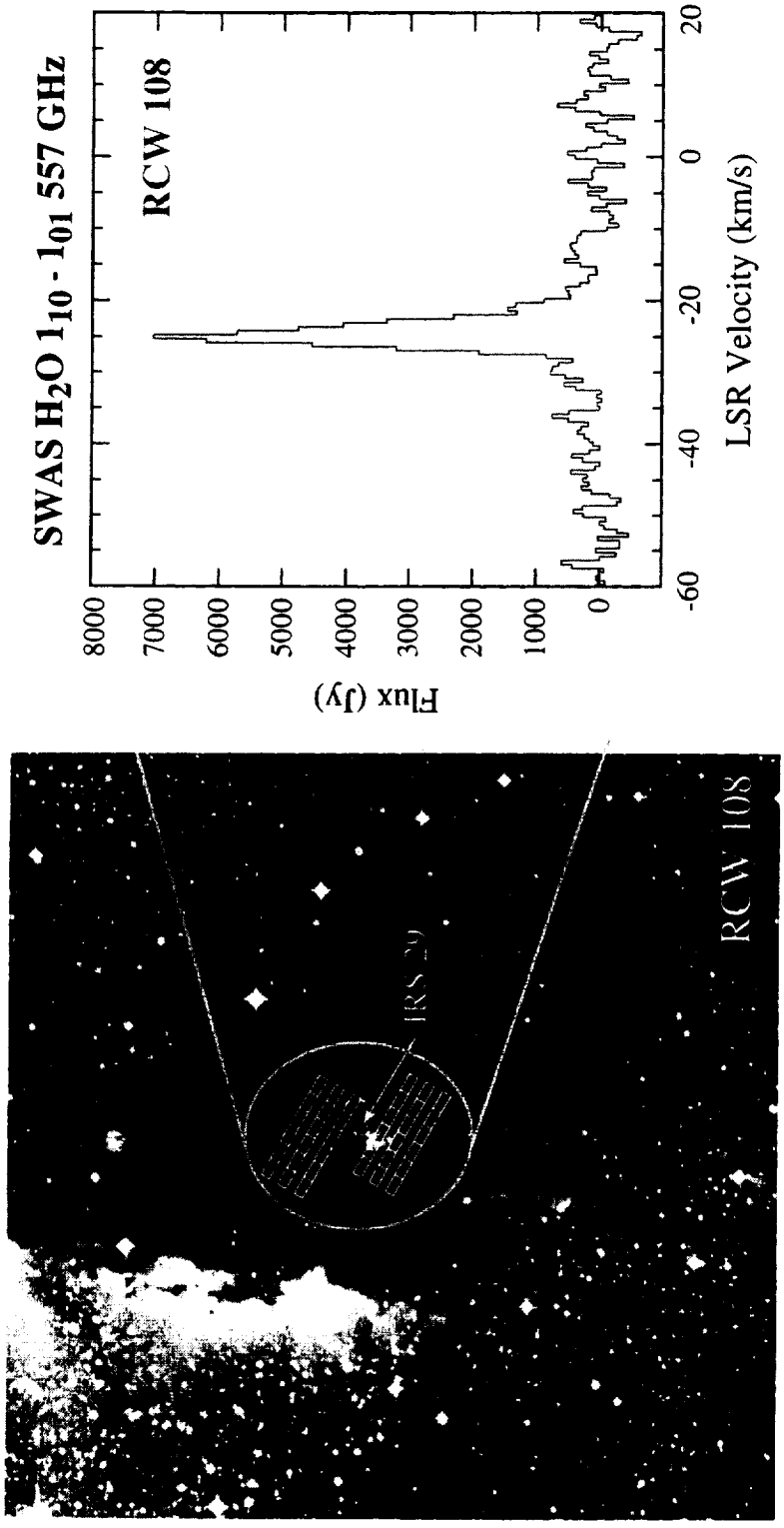

Fig. 2. Optical image of the RCW 108 region showing the positions of IRS spectra we propose to obtain along with the position of the (saturating) source, IRS 29 (denoted by an ×). As shown, this position will be avoided. Within the period of source availability the map orientation angle will change only slightly and no pointing will coincide with the position of IRS 29.

TABLE 1. $H_2{}^{16}O$ Lines Available to the IRS with Upper-Level Energies < 1000 K Plus ISO-Detected Lines Between 32 and 37 μm

Wavelength (microns)	$H_2{}^{16}O$ Transition						Temp. Above the Ground State Lower Level (K)	Upper Level (K)
36.212	6	2	4	- 5	1	5	469.98	867.33
35.471	5	3	3	- 4	0	4	319.51	725.16
35.275	5	4	2	- 5	1	5	469.98	877.89
31.772	4	4	1	- 3	1	2	215.22	668.10
30.899	6	3	4	- 5	0	5	433.90	899.57
29.885	5	4	2	- 4	1	3	396.41	877.89
28.914	4	4	0	- 3	1	3	204.72	702.37
25.940	5	4	1	- 4	1	4	289.28	843.98

ISO-Detected Lines from RCW 108 Between 32 and 37 μm †‡

Species	λ (μm)	Flux (10^{-19} W/cm^2)
Fe III (or He II 19-17)	33.04	10.5 ± 0.1
S III	33.48	185 ± 0.8
Si II	34.82	194 ± 0.8
Fe II	35.35	6.8 ± 0.1
Ne III	36.01	2.4 ± 0.1

† These data were retrieved from the ISO archive and have not appeared in press. RCW 108 was not observed at other wavelengths available to the ISO Short- and Long-Wavelength Spectrometers.

‡ The ISO-established upper limit to the 35.275, 35.471, and 36.212 μm $H_2{}^{16}O$ lines is 2×10^{-19} W cm^{-2} in a 33×20″ beam. The 1σ IRS sensitivity to a point source is 4×10^{-21} W cm^{-2} in a 4.5 × 5.5″ pixel and a 6-second integration. (The IRS 1σ sensitivity improves to about 10^{-21} W cm^{-2} between 22 and 30 μm.)

Interacting Galaxies ERO

Appendix B

Scientific Justification

Galaxy interactions are not only spectacular but also intrinsically interesting. When galaxies interact with each other, the gravitational forces can profoundly change the physical state of the stellar and gas contents of the objects involved, thereby completely altering their appearances and subsequent evolution. What types of interaction may trigger star formation? Do spirals merge to form ellipticals? Are mergers producing central black holes in the new galaxy? These are just some of the hotly debated topics at the forefront of today's extragalactic research.

Recently, the breathtaking progresses in galaxy formation studies and observational cosmology have provided even more impetus to study galactic interactions as an almost universal phase in cosmic evolution. In a hierarchical model, smaller galaxies form first and the present-day giant galaxies are products of subsequent interactions and mergers. Observations have shown that a large proportion of the galaxies found at high redshifts are experiencing rapid star formation, while at the same time bearing traces of recent interaction (e.g., Abraham *et al.* 1996). Learning the details of galaxy interactions will be an important stepping stone to understanding the extragalactic universe as we observe it today.

Previous space missions have also discovered that interacting galaxies tend to be much brighter in the infrared, and contain a lot more dense gas and dust than their counterparts in isolation (Sanders *et al.* 1991; Lisenfeld *et al.* 2000). In fact, when sorted by absolute (bolometric) luminosities, almost all of the brightest (a.k.a. ultraluminous) galaxies are interacting pairs or mergers (Soifer *et al.* 1987; Sanders and Mirabel 1996). Lately, detailed numerical work has emerged to model what happens to the stars and interstellar medium when galaxies collide. This further highlights the importance of direct observations of nearby samples in validating the theoretical model. Among these, high resolution, high sensitivity infrared imaging plays a pivotal role (James *et al.* 1999; Thompson *et al.* 1999; Scoville *et al.* 2000).

Because of the high dust content in these galaxies, images of the visual band are incapable of revealing the detailed structures, especially in their central regions where most of the activities take place. IRAC, on the other hand, can penetrate deep into the dust-shrouded nucleus and pinpoint the precise locations of star formation. Combining IRAC imaging with observations of other wavelengths, one can also expect to address the relationship of star formation in these galaxies to the gravitational interactions that are the underlying mechanism for all the activities.

NGC 6240 is one of the best-known ultraluminous infrared galaxies (ULIRGs) in the nearby universe. It is widely recognized as a merger with large amount of dust and molecular gas found near its center, where a double nucleus structure can be seen (Wang *et al.* 1991; Sugai *et al.* 1997; Tacconi *et al.* 1999). Recent studies with NICMOS/WFPC2 and the VLT have shown that this is probably a typical case where two disk galaxies are merging, triggering a burst of star formation, and evolving towards a giant early type galaxy (Scoville *et al.* 2000; Gerssen *et al.* 2001; Genzel *et al.* 2001). Narrow band emission line (Hα) imaging (see Fig. 1b) shows a highly distorted morphology and extended tidal filaments, yet it is hampered by severe obscuration. This galaxy has been the focus of extensive studies in many wavelengths as well as numerical modeling.

NGC 2623 is also a well-known, luminous interacting galaxy with a text-book morphology of extended tidal tails in a favorable orientation (Toomre and Toomre 1972; Joy and Harvey

1987). Its central region is filled with much dust and cold molecular gas (Casoli *et al.* 1988), and stellar velocity dispersions suggest on-going formation of an early type galaxy (Shier and Fischer 1998). This relatively nearby galaxy bears almost all the characteristics of a merger system as we discussed here. The comparison of IRAC images with that observed in the visual wavelength (see Fig. 2b) should be dramatic.

Communication of results to the public

It is no coincidence that the front-page news from the Hubble and other new astronomical facilities have repeatedly used images of interacting galaxies as their best illustrations. At NASA's latest press conference (April 2002) highlighting new results from the Advanced Camera for Surveys (ACS), for example, two out of the five images released to the public were interacting galaxies. SIRTF ERO images of NGC 6240 and NGC 2623 should be just as spectacular and once again raise the public's fascination about astronomy.

In interpreting the importance of interacting galaxies to the public, the ACS team chose to draw a connection to the future of our own environment. The press release material reads: "...In several billion years, our own Milky Way Galaxy is expected to collide with the Andromeda galaxy". Although this could be viewed as a publicity-drawing statement, scientifically it is not at all unfounded, and we might consider using a similar description as well. Basically, the message is that these have more importance than just pretty pictures. They form part of our understanding of the evolution of matters in the universe.

Because IRAC images are likely to show details in the dusty central parts of the interacting galaxies that no one has ever seen before, the images would be especially striking when viewed side-by-side with optical ones, to illustrate the penetrating power of the infrared — thus the true value and uniqueness of SIRTF instruments. For this we have intentionally selected candidates that are very luminous, extended, and known to have high dust contents. HST and Chandra images of NGC 6240 are already available in the public domain.

Technical feasibility

We propose to observe NGC 6240 and NGC 2623 as our primary targets, and reserve NGC 3690 (=Arp 229) and NGC 4038/4039 (the Antennae) as our backup targets in case of a SIRTF launch date slip. In NGC 6240 and NGC 2623, we find that the observations can be done with five-point dithering of a few pointings, all with 12 sec frames (see Table 1, and Fig. 1a, 2a). Based on the luminosities of these galaxies, the estimated surface brightness distribution, and the spectral energy distribution as measured by ISO, we find that the sensitivity of IRAC can ensure a signal-to-noise ratio of at least 5 for even the relatively low surface brightness regions of the tidal disrupted arms, at the longer (6 and 8 micron) wavelengths. The S/N ratio at shorter wavelengths should be even higher. Since there is no extremely bright point source, we do not anticipate any problem with array saturation.

The SPOT6.0 AOR times are estimated to be 12 and 18 minutes for NGC 6240 and NGC 2623, respectively. So the total time for this program is 30 minutes.

Data reduction plan: The Co-Is of this program are members of the IRAC instrument team and of the SIRTF Science Center, and are familiar with various aspects of the IRAC data calibration and reduction. We are also experienced in similar data reductions of ground-based observations and archival research from other space-borne facilities. Assuming no major instrument performance problem, we expect to be able to reduce the data and have presentable results within a week.

Conflicts/collaborations: These galaxies are part of our own IRAC Team's GTO program on interacting galaxies, although the observing strategies and emphasis there are somewhat different. Members of the GTO team are also on this ERO program.

Comments on the alternative targets: NGC4038/4039 (the Antennae) is one of the best known merger galaxies in the sky. Because of its unique and striking morphology, it has always been used as the poster shot to illustrate the beauty of nature. Its HST images have made the front pages of all major news publications, and has been an icon for amateur astronomers. NGC 3690 (Arp 229) is another well-known ultraluminous infrared galaxy that could well serve as a substitute for NGC 6240. It is a clear merger case and has received much attention and observational/theoretical studies since its infrared brightness has been discovered by IRAS. Neither of these two galaxies would fit well in the current ERO time window, but they make good backup targets in case of a SIRTF launch delay.

Table 1. The basic parameters of the proposed observations

Object	RA	Dec (J2000)	Map	Dither	Frametime	Visibility (2003)	Comments
NGC6240	16:52:58.89	+02:24:03.4	1x2	5	12sec	Feb 20 – Apr 7, Aug 5 – Sep 20	primary
NGC2623	08:38:24.08	+25:45:16.9	1x3	5	12sec	Mar 27 – May 9, Oct 23 – Dec 2	primary
NGC4038/4039	12:01:53.70	+00:52:44.9	2x4	5	12sec	Jun 1 – Jul 15	backup
NGC3690	11:25:42.00	+00:50:17.0	1x2	5	12sec	Mar 25 – Jun 1, Nov 6 – Dec 31	backup

References

Abraham, R. G., Tanvir, N. R., Santiago, B. X., Ellis, R. S., Galzebrook, K., van den Bergh, S. 1996, MNRAS, 279, L47
Casoli, F. *et al.* 1988, A& A, 192, L17
Genzel, R. *et al.* 2001, preprint, in astro-ph0106032
Gerssen, J *et al.* 2001; in *The Central kpc of Starbusrt and AGN*
James, P. *et al.* 1999, MNRAS, 309, 585
Joy, M. and Harvey, P. M. 1987, ApJ, 315 480
Lisenfeld, U. Isaak, K. G., and Hills, R. 2000, MNRAS, 312, 433
Ohyama, Y. *et al.* , 2000, P.A.S.J., **52**, 563
Sanders, D. B., *et al.* 1991, ApJ, 370, 158
Sanders, D. B. and Mirabel, I. F. 1996, in *Ann. Rev. A&A*, **34**, 749
Scoville, N. Z., *et al.* 2000, AJ, 119, 991
Shier, L. M. and Fischer, J. 1998 ApJ, 497, 163
Soifer, B. T. *et al.* 1987, ApJ, 320, 238
Tacconi, L. J. *et al.* 1999, ApJ, 524, 732
Thompson R. I. *et al.* 1999, AJ, 117, 17
Toomre, A. and Toomre, J. 1972, ApJ, 178, 623
Wang, Z., & Scoville, N. Z., and Sanders, D. B. 1991, ApJ, 368, 112

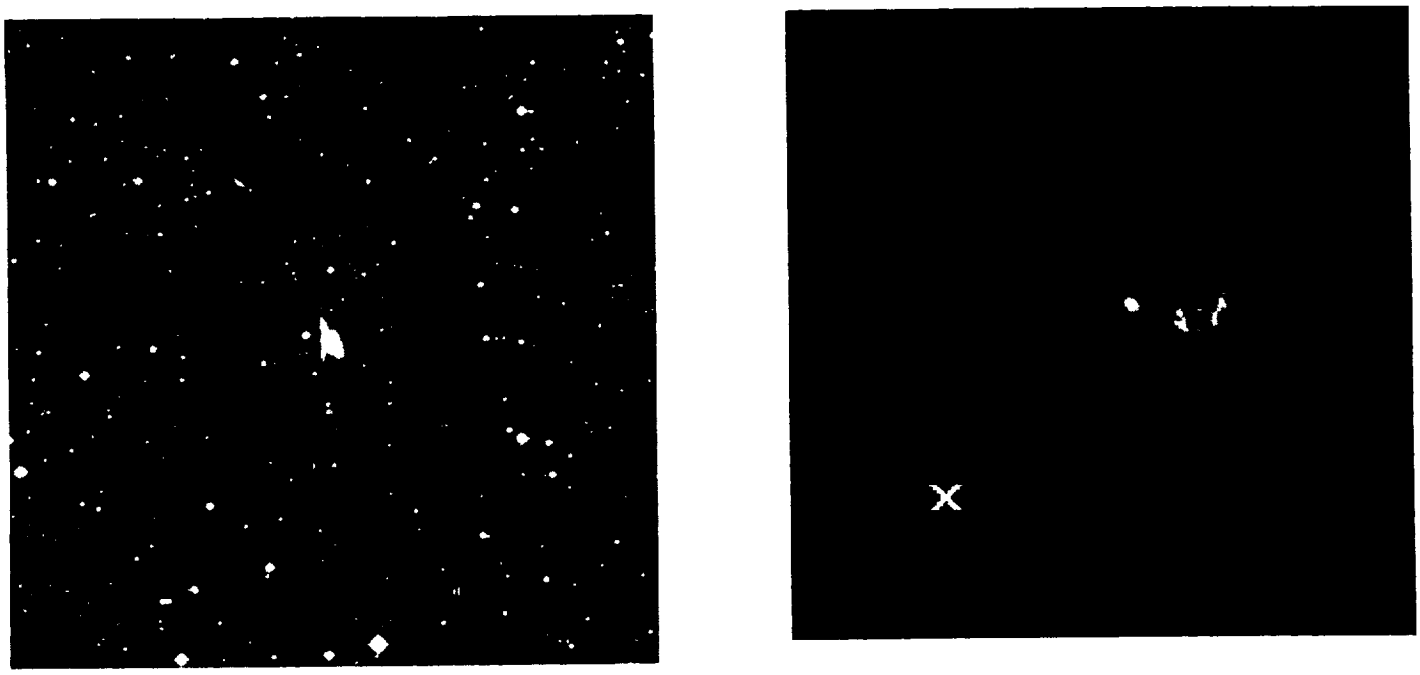

Figure 1 — Left: the DSS image of NGC 6240 with the planned pointing of IRAC FOVs superimposed (a), and right: a close-up of the Hα+[NII] image covering the nuclear region of the galaxy (b), based on NICMOS observations. A possible massive black hole location is marked by an "X".

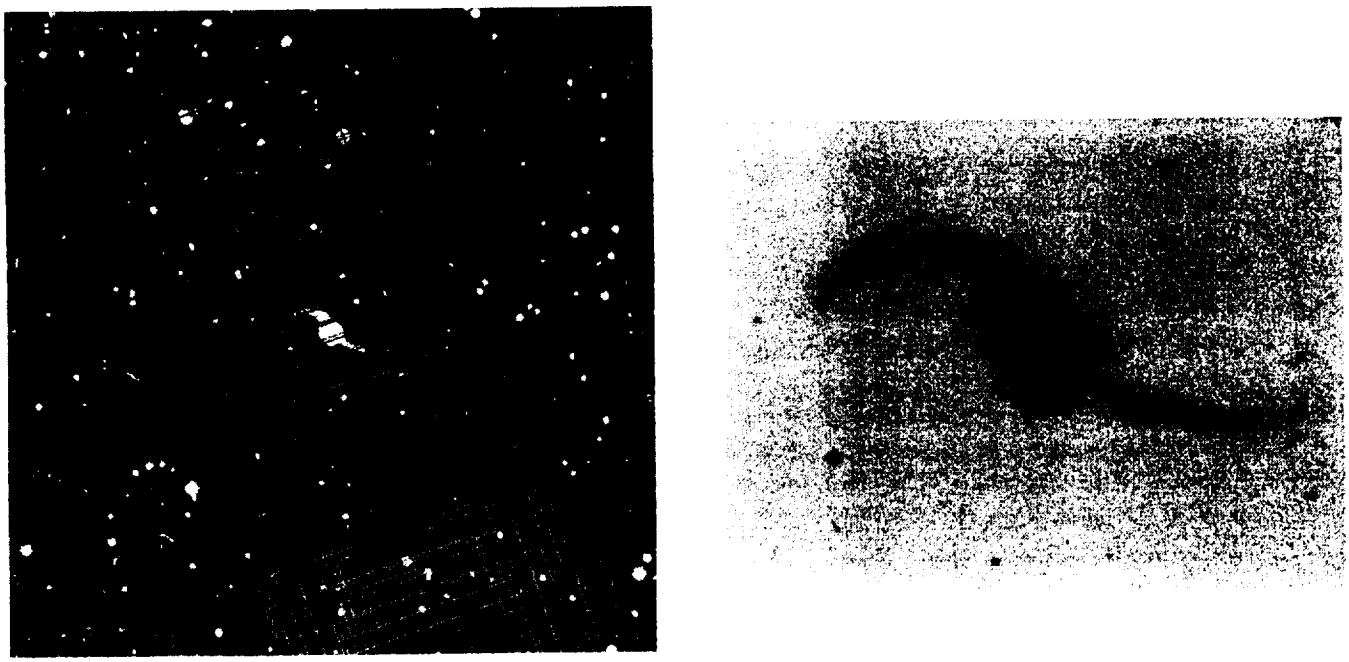

Figure 2 — Left: the DSS image of NGC 2623 with the planned 1x3 mapping of IRAC FOV superimposed (a), and right: a close-up visual image of the galaxy (b). The scale of this image is about 3x2 arcmin.

Galactic Center ERO

Appendix B

SIRTF-ERO-Galcen-final.doc 5/23/02

Proposal Title:	Faint Extended Structure in the Galactic Center
Proposal Type:	IOC
Hours Required:	0.5
Principal Investigator:	Dan Gezari - gezari@stars.gsfc.nasa.gov NASA/Goddard Space Flight Center - Code 685 Greenbelt, MD 20771
Co-Investigators:	Giovanni Fazio (SAO) Bill Hoffman (UA) Howard Smith (SAO) Harvey Moseley (GSFC) Eli Dwek (GSFC) Rick Arent (GSFC) Farhad Yusef-Zadeh (NWU) Randall Smith (CfA)

Abstract:

The region within 30 arcmin of the Galactic Center contains an extraordinary collection of astronomical sources. No other region in the Galaxy shows such a diversity of exotic objects and interdependent astrophysical processes. Surprisingly, the small-scale (~1 arcsec) structure of the infrared emission in the Galactic Center region is known in only a very tiny fraction of the region of interest (the 25 x 25 arcsec field of view centered on Sgr A*). In contrast, the entire Galactic Center has been surveyed over a large area with 1-2 arcsec resolution in radio emission (VLA), the near infrared (2MASS), and recently the X-ray (Chandra). Radio interferometry has revealed an extraordinary system of non-thermal filaments quite unlike any other radio sources observed in the Galaxy. Higher spatial resolution observations would reveal the unobserved details of the faint, fine structure, and show whether the filaments originate in clusters. This has implications for the nature of the star formation process in the nucleus of our galaxy. If SIRTF does not observe the Galactic Center, it is likely that high spatial resolution (2 arcsec), deep (~5 mJy), mid-infrared observations of this important and well-observed region may not be obtained for a decade.

Science Category: Galactic - other

Scientific Justification:

The region within 30 arcmin of the Galactic Center contains an extraordinary collection of astronomical sources. No other region in the Galaxy shows such a diversity of exotic objects and interdependent astrophysical processes (see Figures 1 and 2). Extended complex infrared source structure in the central galactic plane has been imaged at 8, 12, 15 and 21 um by the MSX survey, but with only with moderate (18 arcsec) spatial resolution. IRAS mapped the Galaxy at 12, 25, 60 and 100 um with 2 arcmin resolution. While ISO (Figure 3) had the same pixel size as MSX at 15 um, it did not observe the central 5 x 10 arcmin field of view at all because of concerns over saturation and confusion in large pixels. Surprisingly, the small-scale (~1 arcsec) structure of the infrared emission in the Galactic Center region is known in only a very tiny fraction of the region of interest, where the brightest of sources (>1 Jy arcsec^{-2}) can be detected with big ground-based telescopes. These bright mid-infrared sources are concentrated in the central parsec (the 25 x 25 arcsec field of view centered on Sgr A*).

In contrast, the entire Galactic Center has been surveyed over a large area with 1-2 arcsec resolution in radio emission (VLA), in the near infrared (2MASS), and recently in the X-ray (Chandra). However, because of a lack of infrared data with comparably high resolution, a detailed comparison with the radio thermal/non-thermal, plasma, molecular line, and near-infrared (stellar) emission components - and analysis of their underlying and inter-dependent physical processes - can not yet be made. If SIRTF does not observe the Galactic Center, it is likely that high spatial resolution (2 arcsec), deep (~5 mJy), mid-infrared observations of this important and well-observed region may not be obtained for a decade.

Radio interferometry has revealed an extraordinary system of non-thermal filaments quite unlike any other radio sources observed in the Galaxy, as well as completely independent thermal emission component which is not unlike the very brightest mid-infrared emission from warm dust. Higher spatial resolution observations would reveal the unobserved details of the faint, fine structure, and show whether the filaments originate in clusters. This has implications for the nature of the star formation process in the nucleus of our galaxy. One of the most interesting structural features of some of the isolated filaments is that they show kinks, which may be places where dense molecular gas clouds are interacting with the filaments. The interaction of the molecular cloud and the filament should be detected in the mid-infrared. Most recently the Chandra survey has observed the 2-10 KeV X-ray emission with high spatial resolution and detected point sources as well as diffuse, extended structures. The diffuse X-ray component may be associated with the radio filaments, and the filaments may originate in the luminous cluster stars. Comparison (Figure 1) of the Chandra diffuse X-ray emission distribution with 90 cm radio continuum (LaRosa et al. 2000) and 25 um mid-IR continuum MSX images (Price et al. 2001) shows that the diffuse X-ray emission is generally correlated with the radio Arches and Quintuplet clusters, as well as Sgr A and Sgr B2. Shocked stellar winds from the massive clusters may produce the hot, extended gas detected in diffuse X-ray emission (Yusef-Zadeh et al. 2002). Stellar clusters near the Galactic center are a record of the history of star formation in this unique region. At present, four young (10-20 Myr) clusters have been discovered within a projected distance of 35 pc (15 arcmin) of the center of the Galaxy - the IRS 16, Sgr A East, Arches and Quintuplet clusters. All show emission line stars and are associated with thermal ionized and molecular gas clouds.

Communication to the Public: The Galactic Center images obtained with SIRTF/IRAC will show complex, faint, extended infrared source structure with an order of magnitude higher resolution than is presently available. The comparison of detailed structure and new sources in this rich field, using the existing near-infrared, radio, X-ray images and in the new, dramatically different IRAC infrared images (which will be the first large scale infrared images of the Galactic Center with equally high spatial resolution), will provide numerous opportunities to discuss exotic astrophysical processes in the nearest galactic nucleus. For ERO, press release and public outreach purposes, limited regions of saturation in the Galactic Center images will not be objectionable, and should not be significant in very detailed wide-field infrared images. The images should show spectacular new detail, most of it away from the brightest central known sources. The new image data will provide the opportunity to present and compare the exotic sources, analyze their interactions, and describe their associated physical processes, resulting in much appealing educational and publicity material.

Observational and Operational Strategy: The Galactic Center is observable: March 8 - April 19, and August 24 - October 9. These periods are well within the SIRTF windows of opportunity. We would observe a 30 x 20 arcmin (l,b) region of the Galactic Center (with Sgr A* positioned l = -10 arcmin from center), which would include Sgr A*, the Sgr A West complex, the non-thermal arches and filaments, and several very luminous star clusters. To cover this area we would make a 2-cycle dithered 6 x 4 maps. The observations would be made in 12 second frame times and High Dynamic Range (HDR) mode (0.6 second frames), avoiding saturation in all but the central IRAC field (where some saturation may occur at the strongest compact sources; 0.6 sec frames saturate at approximately 780/620/1780/1500 mJy (Bands 1-4, respectively). Saturation will only be a serious concern in parts of the 5 arcmin IRAC array field centered on Sgr A*. Image data from saturated regions such as Sgr A West will still have qualitative value, and scientific results in adjacent regions will not be compromised. Two sets of dithered mosaics in all 4 bands can be obtained in a total time of 1703 seconds.

Data Reduction Plan: Collaborators H. Smith, H. Moseley, and R. Arent have extensive knowledge of SIRTF/IRAC data processing procedures and reduction algorithms, and collaborators D. Gezari, W. Hoffmann, and E. Dwek have extensive experience in infrared image processing methods and the interpretation of mid-infrared observational data. The ERO observational data will be reduced and interpreted promptly, and detailed comparisons will be made with other existing high resolution surveys by collaborators F. Yusef-Zadeh for radio interferometry and R. Smith for X-ray.

Collaborations and Resolution of Conflicts: There are no conflicts with other instruments or observations. F. Yusef-Zadeh (NWU) is an expert outside collaborator for comparison of the ERO data with radio interferometry observations. R. Smith (CfA) is an expert outside collaborator for X-ray observation comparisons.

Gezari, D. Y., private communication, (1985)
LaRosa, T. et al., AJ, 119, 207 (2000)
Morris, M. and Serabyn, E., Ann. Rev. Ast. Ap., 84, 645 (1996)
Price, S. D., et al., Ap. J., 121, 2819 (2001)
Wang, Q.D., Gotthelf, E. & Lang, C., Nature, 415, 148 (2002)
Yusef-Zadeh, F., Morris, M. and Chance, D., Nature, 310, 557 (1984)

Figure 1: Multi-wavelength close-up of complex structure and diverse process in the central ~30 arcmin field of view near Sgr A* (Wang, Gotthelf and Lang 2002). False color image shows 20-cm radio VLA (red), 25 um MSX (green) and 6.4 keV Chandra Xray (blue).

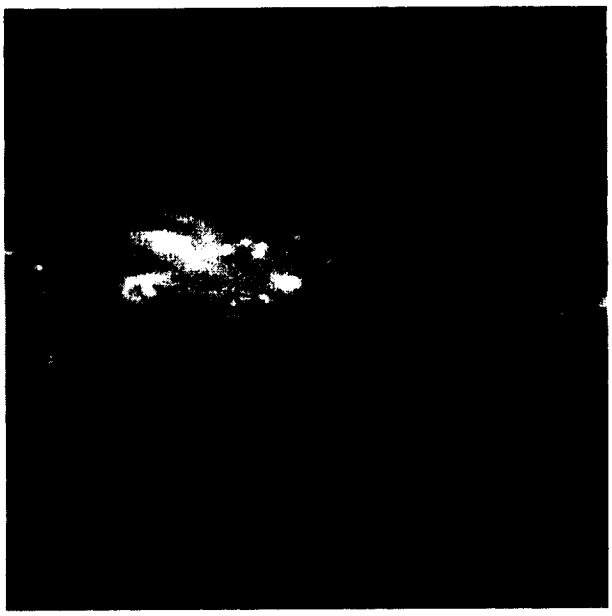

Figure 2: The Midcourse Space Experiment (MSX) observed the entire galactic plane (10 x 360 degrees) at 8, 12, 15 and 21 um, but with only 18 arcsec resolution (Price et al., 2001). This 4-color image of the central 2 x 2 degrees shows large-scale extended features including the Sgr A, B, and D complexes. The circular arcs at l = 0.2, b = 0.0 are the thermal radio filaments. The Quintuplet cluster and the Sickle HII region are also detected. These compled structures would be imaged by SIRTF/IRAC with 2 arcsec resolution.

Figure 3: ISO observed most of the central galactic plane at 7 um, but not the central ~10' x 5' region containing the Galactic Center source complex and Sgr A* (omitted because of saturation and confusion). A special "ISOGAL" survey mapped a 12 deg .sq. region of the galactic plane (45 degrees away from the Galactic Center) to a limit of 8 mJy with ISOCAM at 15 um with 6" pixels (~15 arcsec resolution).

"ERO" & "HERO" BACKGROUND OBJECTS IN IRAC SURVEYS

- Howard Smith 6/19/02

1. Introduction

Special attention should be paid to the serendipitous discovery of numerous Extremely Red Objects (EROs) and Hyper-EROs (HEROs; Totani 2001) in the IRAC fields, because of their importance to the question of how the first and subsequent generation of stars aggregate, galaxy formation and evolution processes in the early universe, implications of CDM cosmology scenarios as they affect galactic structure clustering, and, not least, because of the uniquely powerful contributions which IRAC will make to this investigation.

ERO galaxies (I-K>4) may either be massive, dusty elliptical galaxies assembled at z~1 from mergers of older galaxies (the "hierarchical models"), or more primordial objects formed at earlier epochs, subsequently evolving passively into the older elliptical population we see (the "evolutionary models"; Cimatti, et al 2001). EROs do appear to be highly clustered, with between about .05 and 0.2 arcmin^-2 for [K] <19, and their colors lend credence to evolutionary models with original formation times at z~3 -- but hierarchical models with a flat CMD cosmology and omega(lambda)=0.7 appear to be more consistent with their surface density distributions (Martini, 2001). Based on such estimates, the "Shallow Survey" might expect to see thousands of "EROs."

The picture has become more complex as the small sample of known EROs has increased, and as more spectroscopic data are obtained. It is increasingly clear that while 50%-80% are evolved ellipticals, perhaps 20-40% are dusty starburst galaxies, with a sizable fraction being dusty quasars, Seyferts, or other transition-type system. Most appear to be IRBs (log L(IR)>11). HERO galaxies (J-K>3-4) are even more extreme objects, perhaps comprised of the class of primordial ellipticals themselves.

2. The SED and IRAC color-color plot

The first Figure, adapted from Graham Smith et al, shows the nominal SED for an ERO based on observations, and estimates from Arp220 (I have fiddled with the latter a bit based on our ISO measurements.) The second figure shows an ERO diagnostic figure (from Pozetti, 2000), in which I have included brown dwarfs and Hyper-EROs. Unfortunately – or fortunately for us – there is a particular dearth of information in the IRAC B3 and B4 bands. Much will depend on the details of the dust and PAHS in these sources. But, simply using the rough curve given here, redshifting it, and looking at the flux densities at the nominal IRAC band centers, I find the IRAC color-color diagram as in the third figure. The main conclusion, based again on the very simple SED above, is that at z>2 the color change is particularly noticeable, as the slope of the SED at about 1.5microns picks up the warm dust component to make a big change in the IRAC colors. (Normal elliptical and spirals, of course, have values all <1 in this plot.)

3. Detectability

I re-estimated the detectability of some sources. One of the ERO objects in the plot for which there are data is J164023; it lies at z=1.05, and has an observed K band flux of 63uJy, rising as per the Figure below. The fluxes for this object, at SIRTF wavelengths, and extrapolating using Arp220's SED, are very roughly: (+- a factor of two):

B1	150	microJy
B2	170	"
B3	210	"
B4	540	"
24um	1000	"

These flux densities should be relatively easy to see. The 24um flux is only about 2 to 4 times the IRAC B4 flux. At z= 4 the B4 flux from a J164023 would be about 4 uJy. For comparison, for Arp220 at z=4 its B4 flux would be about ~1 uJy (that's micro -not milli: I made a mistake in my earlier email, typing "m" for "u"!-- its rest frame [H] band flux is about 145 mJy). If these objects are indeed very dusty ellipticals or spirals there may not be many beyond z= 2-3, and the z=4 case is just a limiting example.

References

G. Smith et al, astro-ph 108039, 2001
Cimatti et al, astro-ph 111527, 2001
Martini, ApJ 121, 2301, 2001
Pozzettl and Mannucci, MNRAS 317, L17, 2000
Totani et al, astro-ph 0108145

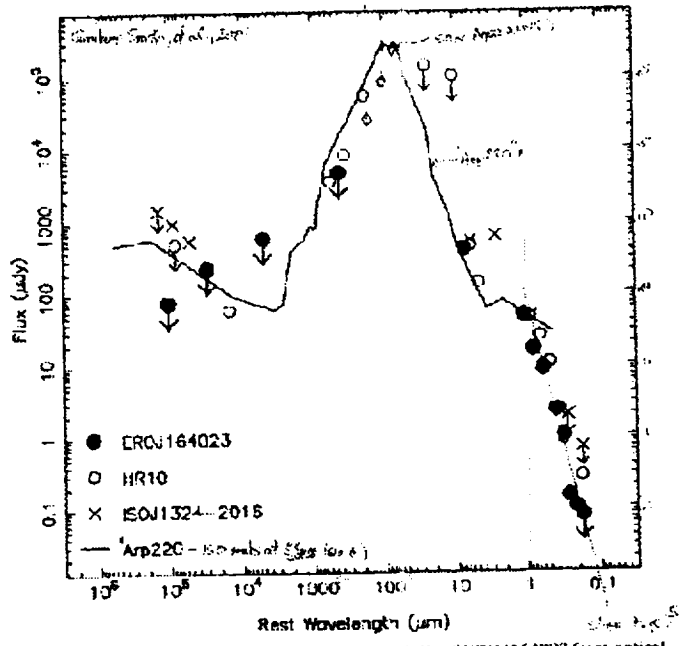

FIG. 4. —The rest frame spectral energy distribution (SED) of ERO J164023 from optical to radio wave-bands. For comparison, we show the SEDs of HR10 (Dey, Elbaz et al. 2001), ISO J1324–2016 (Pierre et al. 2001) and Arp220 (Hughes et al. 1998) The flux densities of ERO J164023 have all been corrected for gravitational amplification (§1). The SEDs of all four galaxies have been normalised to the observed *K*-band flux of ERO J164023.

Color - color diagnostic for "ERO's"

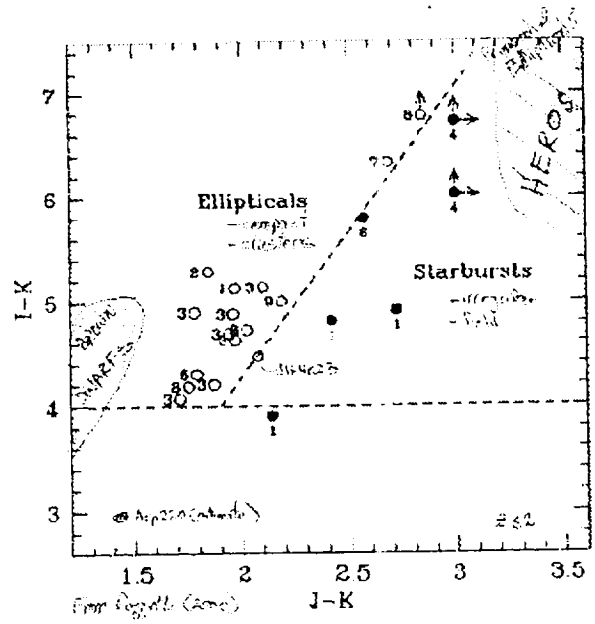

Appendix B

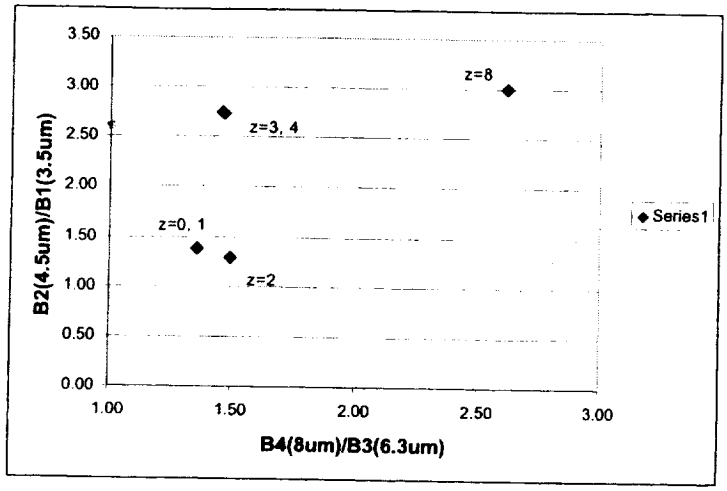

IRAC color-color plot for presumptive ERO at varying z

Appendix C: Postdoctoral Scientists' Research Statements

1) "Recent Research: The Starburst-AGN Connection in LIRGs" (Kewley)
2) "Galaxy Mergers: The Gas, Star Formation and AGN Interplay" (Kewley)
3) Design of IR Filters for Astronomy: "Micro-Program, Transmission Line Theory and Design of Filters in the 20 to 60 μm Region" (Sternberg)

Recent Research: The Starburst-AGN Connection in LIRGs

Lisa J. Kewley

1. Introduction

The main focus of my research so far has been to understand the processes at work in Luminous Infrared Galaxies (LIRGs). LIRGs have been an intense subject of research since the discovery of a large number of such galaxies by the IRAS satellite in 1983. The concensus view is that LIRGs represent mergers of gas-rich galaxies. The merger fraction increases with infrared luminosity and approaches 100% for samples of the most luminous ($L_{IR} > 10^{12} L_{\odot}$) galaxies (*eg.* Sanders et al. 1988). LIRGs derive their power from either rapid star formation or an active nucleus or a combination of the two. Despite numerous studies in the area, the nature of their ultimate energy source is still a vigorous issue of debate. My thesis research furthers our understanding of LIRGs in a number of directions, from the nature of compact radio cores in LIRGs, to detailed theoretical modelling of starbursts and Active Galactic Nuclei (AGN) which allow a number of important characteristics of galaxies to be determined including the relative contribution of AGN and star formation to the optical energy budget. This research is described in Section 2. I have developed a number of ongoing projects which have stemmed from my thesis work and these are described in Section 3 along with additional projects and collaborations I am currently involved in.

2. The Starburst-AGN Connection in LIRGs

My Ph.D. research is based on the study of a large sample of 285 LIRGs. High resolution long-slit optical spectroscopy was obtained using the Double Beam Spectrograph at the MSSSO 2.3m telescope for ~ 230 objects in this sample for comparison with my detailed theoretical starburst and AGN models.

2.1 Theoretical Starburst Modelling

To model the starburst galaxies, rather than using a blackbody ionizing radiation field as has been done previously, I generated the ionizing radiation fields using the new generation of stellar population synthesis models. The ionizing radiation fields were then used in detailed self-consistent photoionization models; MAPPINGS (Sutherland & Dopita 1993). These models include self-consistent treatment of dust physics and the depletion of various elements out of the gas phase. I explored a large range of parameter space with these models including metallicity, ionization parameter, burst scenario (instananeous vs. continuous), stellar tracks, and stellar atmospheres. The standard optical diagnostic diagrams (see Fig. 3 of Research Proposal) were used for the comparison of these models first with HII regions from the literature and secondly with the starbursts in my sample. The results of this analysis can be found in Kewley et al. (2000a) and (Dopita et al. 2000), but are described briefly below:

- HII regions are best modelled by instantaneous burst models (0 Myr) which may be a selection effect; the most luminous and hence the youngest HII regions have been observed.
- Infrared starburst galaxies are best modelled by continuous burst models (star formation continuing for atleast a few Myr). This is consistent with merger scenarios for LIRGs in which a tidally triggered starburst continues over the dynamical timescale of the merger ($\sim$100 Myr).
- Starburst galaxies have a relatively hard EUV ionizing radiation field, as traced by the optical diagnostic diagrams which are primarily sensitive to the EUV regime. The EUV spectrum in these models is determined by the Wolf-Rayet stars, and is modelled better by the PEGASE (Fioc & Rocca-Volmerange 1997) stellar population synthesis models in which planetary nebulae nuclei (PNN) atmospheres are used, rather than the STARBURST99 (Leitherer et al. 1999) models with their detailed Wolf-Rayet atmospheres. The Wolf-Rayet atmospheres should be more applicable to starburst galaxies than PNN atmospheres, but the dilemma can be resolved if continuum metal opacities are incorporated into the STARBURST99 models.
- Shock models with spherical precursor regions were generated to explore the contribution by mechanical energy from supernovae to the optical emission. I found that this is only a few percent and that these models predict a lower limit in the [OIII]/Hβ line ratio, consistent with observations.

2.2 New Optical Classification Scheme

The commonly used classification scheme was a semi-empirical boundary line derived by Veilleux & Oster-

brock (1987) (VO87). Based on the theoretical modelling described above combined with powerlaw and shock models for the AGN, I developed for the first time theoretical boundary lines which may be used to classify starbursts, Seyferts and Low Ionization Narrow Emission-line Regions (LINERs). Classification using both schemes of the objects in my sample were compared with samples of non-warm LIRGs and non-LIRG LINERs. The results of this study are in press (Kewley et al. 2000f), the main results follow:

- My theory-based classification scheme compares favourably against the previous VO87 semi-empirical scheme upon comparing the number of ambiguously classified objects (6% c.f. 17%).
- Many infrared galaxies previously classified as LINERs lie on a mixing sequence between starbursts and AGN, and are likely to be composite in nature. Non-infrared LINERs behave differently on the optical diagnostics to infrared LINERs, and their line ratios are consistent with shock excitation in a gas-poor environment.
- I find that 70% of the galaxies in our sample are classified optically as starburst, 17% are Sy2, 4% are Sy1, and 0.4% are LINERs. A further 2% of our sample are certainly composite galaxies.

2.3 Obscured AGN in LIRGs

To determine the fraction of my sample which harbours obscured AGN, VLBI observations were taken for a subsample of $\sim$ 60 objects using the Parkes-Tidbinbilla Interferometer. The analysis of this data is published in Kewley et al. (2000c) and the main results are:

- 80% of optically classified Active Galactic Nuclei (AGN) type galaxies contain compact radio sources, while 37% of optically classified starburst galaxies contain compact radio sources.
- The compact radio luminosity function has a bimodal distribution, indicating two populations in our sample. The majority of the higher radio luminosity class ($L > 10^4 L_\odot$) are AGNs, while the majority of the lower radio luminosity class ($L < 10^4 L_\odot$) are starbursts.
- On the basis of supernova models and their core luminosities, the compact radio emission in all but two starburst galaxies may be due to complexes of extremely luminous supernovae such as those seen in Arp 220. NGC 4691 and MCG-5-31-7 are likely to harbour obscured AGN.
- Using FIR color-color diagrams, I found that globally the energetics of 92% of the galaxies in our sample are dominated by starburst activity, including 60% of galaxies which contain AGN on the basis of their optical classification. The remainder are energetically dominated by their AGN in the infrared. This shows that the optical technique for classifying the nuclear energy source is more sensitive as a consequence of the higher spatial resolution that can be obtained.
- For starburst galaxies, electron density increases with dust temperature, consistent with the idea advocated by Hwang et al. (1999) that in merging galaxies, the later phases of the merger contain more compact starburst regions.

This work demonstrates that although the incidence of AGN activity within a given infrared luminosity class is similar to that found in earlier studies, the AGN is rarely the dominant power source for the infrared luminosity. This result is similar to findings by Genzel et al. (1998) and Veilleux, Sanders & Kim (1999) for samples of ultraluminous $L_{FIR} > 10^{12}$ $L_\odot$ IRAS galaxies.

3. Ongoing Projects

3.1 Compact Radio Sources: Obscured AGN or Compact Radio Supernovae?

As an extension of the VLBI section of my thesis research, I am carrying out further investigations into the nature of the compact radio sources in the starburst galaxies from my sample in collaboration with R. Norris at the Australia Telescope National Facility (ATNF). We have obtained 13cm radio images of the objects with compact radio sources to determine their core-to-total flux ratio, and allow searches for jets and other extended radio structure associated with AGN activity. We have also carried out a preliminary investigation into the nature of the starburst compact radio cores using the Australian VLBI network. We have imaged two starbursts with the strongest core fluxes to attempt to resolve individual supernovae. If we find that we cannot, future work in this area could include imaging with larger VLBI networks, infrared or X-ray spectroscopy.

3.2 Optical vs. Infrared AGN Fraction

Recently, new empirical near- and mid-infrared diagnostics have been developed to determine the relative contribution of starburst and AGN activity to the infrared emission (*eg.* Genzel et al. 1998, Lutz et al. 1998, Laurent et al. 2000). A number of LIRGs

in my sample have been observed by Laurent et al. (2000) in the mid-IR, and this has made for a useful comparison between the relative contribution of starburst and AGN activity derived from the mid-infrared and optical diagnostics, described fully in Kewley et al. (2000d). I have found that the majority of these objects have a consistently higher derived AGN fraction ($\sim 20 - 30\%$) in the IR than in the optical, including NGC 253 which contains multiple compact radio sources thought to be radio supernovae rather than an AGN (Turner & Ho 1985, Antonucci & Ulvestad 1988). The difference in AGN fraction derived is most likely due to scatter on the IR diagnostic diagrams. Through my detailed modelling of starbursts, I showed that the scatter on optical diagnostic diagrams is largely due to metallicity variations, and I predict that a similar scatter occurs on the IR diagrams due to dust properties as well as metallicity and ionization parameter variations. The range of this scatter is currently unknown and addressing this issue using stochastic dust emission modelling with MAPPINGs composes part of my research proposal. One object, NGC 1808 in the above sample has a much larger AGN fraction than found in the optical (70% c.f. 0%) and could be a candidate for an obscured AGN, although it is unclear at this stage how reliable the 70% IR AGN fraction is.

3.4 The COLA Project

An extension of my interest in the starburst-AGN connection is the COLA (Compact Objects in Low-power AGN) project. The COLA project is an Australian-US collaboration to study the relationship between AGN, particularly low-power ones and their host galaxies. We are carrying out a multiwavelength study of distance-limited samples of AGN and non-AGN galaxies. Data obtained so far includes optical spectra, VLBI, CO, HI, and imaging at various wavebands. Further details can be found in Marston et al. (1999) and at www.atnf.csiro.au/ rnorris/COLA/index.html. The project is currently at the analysis stage and I have been involved with the CO, radio and morphology analysis to date.

3.5 X-Ray Luminous Starburst Galaxies

X-ray luminous starburst galaxies, if found in significant numbers, may have an impact on the infrared background radiation. These galaxies produce extremely high amounts of radiation in the X-rays, and have previously been thought to contain AGN, although recent results from Chandra indicate that a fraction if not all of the power source could be from X-ray binaries and supernovae (Fabbiano, Zezas, private comm.). M. Ward (U. Leceister), A. Zezas (CfA) and I have taken optical spectroscopy of this sample and found that $\sim 25\%$ were X-ray luminous starbursts. Further study of these objects is needed to determine whether they contain optically obscured AGN which may be contributing to their X-ray flux. Once the scatter in the IR diagnostic diagrams has been modelled as described above, these diagnostics will be very useful in this study.

3.6 Interference Excision in Radio Astronomy

Before I began my Ph.D. thesis, I worked for six months at the Defence Science and Technology Organisation on interference excision for radar arrays. Many interference excision techniques have been developed over the last few decades in the fields of defense and communications, but until very recently, they have not been applied to radio astronomy. With the developments in telecommunications over the last decade, it is becoming essential to develop interference excision techniques for use in radio astronomy, which I have been doing with R. Ekers and B. Sault at ATNF. The main outcome of this work has been the successful application of a least squares power minimisation routine to remove satellite interference from radio spectra obtained using the Australia Telescope Compact Array (Kewley et al. 2000e). This technique is currently only applicable to narrow-band observations with a linear array, but I would like to extend it for use over broad-band observations and for arrays of any architecture in the future. While this is a vastly different area of research to my thesis and other ongoing projects, its nature appeals to the engineer in me.

Galaxy Mergers: The Gas, Star Formation and AGN Interplay

Lisa J. Kewley

1. Introduction

Over the last decade, studies of merging galaxies have provided unparallelled insight into the physics of merging and the importance of galactic interactions in the past. We now understand that galaxy interactions are fundamental to galactic evolution, and may well be the dominant process by which galaxies form and evolve.

The most widely supported merger scenario is based on the Toomre (1977) sequence in which two galaxies lose their mutual orbital energy and angular momentum to tidal features and/or an extended dark halo and coalesce into a single galaxy. Tidal interactions and associated shocks are thought to trigger star formation (*eg* Bushouse 1987, Kennicutt et al. 1987, Liu & Kennicutt 1995) which heats the surrounding dust, producing strong FIR radiation. The detailed relationship between the star formation and gas motions remains poorly understood.

Luminous Infrared Galaxies (LIRGs) provide a fertile ground for the study of star formation in mergers, and therefore LIRGs have been the intense subject of research since the discovery of a large population of such galaxies by the IRAS satellite. The consensus view is that LIRGs represent mergers of gas-rich disk galaxies. Studies of these systems are complicated by the presence of large quantities of dust, particularly in the nuclear regions.

In addition to triggering star formation, gas flows in mergers may also feed an AGN. The link between an AGN, the gas, and star formation either on a nuclear or a global scale is unknown. One possibility is that star formation is initially triggered by tidal interactions and as the merger progresses, gas is funnelled towards the merger nucleus and activates nuclear starbursts and AGN, further increasing the infrared luminosity. Circumnuclear star formation is observed in many galaxies with AGN, eg. NGC 1068 and it is possible that circumnuclear star formation is a vital component of AGN feeding.

Previous studies of star formation and its link to AGN activity have been hindered by a lack of knowledge as to the relative importance of these two processes to the global emission. As part of my thesis, I used detailed models combined with optical diagnostics to allow the possible range of contribution by an AGN to the optical emission to be determined for the first time (Kewley et al. 2000a, 2000f). This is very useful for non-dusty mergers, but in some, dust can completely obscure an AGN in the optical. In such cases, infrared diagnostic diagrams must be used but it remains to put these on a firm theoretical basis.

Clearly, a detailed study of the processes occurring in mergers must involve the study of the interplay between star formation, gas kinematics, and AGN activity. This is the objective of my proposed research.

2. Gas Kinematics and Star Formation

Frequently, searches for correlations between the integrated star formation rate (SFR) and the global kinematic properties of the merger such as nuclear separation, or velocity dispersion have yielded negative results (*eg.* Kennicutt et al. 1987). However, these studies were plagued by selection effects, projection effects, and AGN contributions to the optical line or infrared continuum emission.

Our ability to model the emission properties of merging galaxies is now much improved. New developments in stellar population synthesis models allow the star formation history to be inferred, and in combination with optical spectroscopy, the age of the stellar populations can be determined for systems (or regions) without large quantities of dust. Used in combination with N-body and hydrodynamic merger models (Barnes & Hernquist 1996), these models can also be used to provide estimates of merger age (*eg.* Hibbard 1995). These new techniques have so far only been applied to a few isolated galaxies or small samples. The role of the AGN has not been taken into account, and so far the new techniques have not been used to compare LIRG and non-LIRG mergers on a systematic basis, where they may provide valuable insights into the relationship of gas-rich mergers and LIRGs.

Part of my long-term research objective is to study the detailed relationship between gas kinematics and star formation history of merging galaxies. I will endeavour to shed light on the key questions;

How do the stellar populations within a galaxy correlate with the gas kinematics? How do these change as the merger progresses?

By comparing the gas kinematics and stellar populations in LIRG mergers with non-LIRG mergers, I aim to provide insight into the following;

Is the relationship between gas kinematics, stellar populations and merger evolution different for LIRGs and non-LIRGs?
Are LIRG mergers found at a particular stage along an evolution sequence? If so, what were they previously, and what will they evolve into?
How significant are mergers compared with the entire LIRG population over the whole L_{IR} range?
I propose to select three samples ($\sim$ 25 objects each) consisting of; LIRG mergers, Non-LIRG mergers, and a control sample of isolated LIRGs and non-LIRGs. The control sample ensures that any star formation and gas properties found are definitely merger related.

Mergers will be selected on the basis of their tidal features (tails, plumes, bridges) or multiple nuclei. From Figure 1, above $10^{10.5}$ $L_{\odot}$, the infrared luminosity function shows a clear excess of FIR galaxies, and therefore is a natural lower cutoff for the LIRG mergers. The relatively coarse resolution of IRAS raises the possibility that some multiple nuclei galaxies have only their combined FIR flux measured, resulting in misclassifications as LIRGs. The radio-FIR correlation and NVSS images will help resolve this until higher resolution infrared images become available.

I will select LIRG mergers from my thesis sample which overlap with COLA objects (described in my recent research). Non-LIRG mergers and the control sample will be selected from catalogues such as the Arp atlas, Strauss et al. and Fisher et al. (1992,1995) (S+F) catalogues. The final selection will be determined according to which mergers are available in the HST WFPC archive. Many systems have been observed with HST, and this data is vital for studying the gas and star formation distribution within these objects, especially close to the nuclear regions.

Gas kinematics and stellar populations of each sample will be studied using a combination of optical and near-infrared long-slit spectroscopy, CO, HI imaging, and data available in the literature and HST archive. The optical and near-infrared emission lines give the distribution and velocity of the ionized gas. HI and CO observations give the distribution of the cold gas. These will be compared with the distribution of the stellar populations determined by the blue continuum and emission line ratios (young), and the Balmer absorption lines, red and near-infrared continuum (old). The 2 Micron All-Sky Survey (2MASS) will aid studies of the old stellar populations, particularly in dusty systems. Hα and L_{IR} provide estimates of the SFR in non-dusty and dusty systems respectively, once the contribution from an AGN has been properly accounted for.

Merger ages will be estimated using a combination of nuclear separation and dynamical merger models (Barnes & Hernquist 1996) to limit the range of possible ages, which are further constrained using the stellar continuum and Balmer line equivalent widths (Dottori 1981) in combination with stellar population synthesis models (*eg.* Gonzalez Delgado, Leitherer & Heckman 1999). A few of the most interesting mergers will be used for follow-up observations which could include integral field spectroscopy, VLBI, HST WFPC2, SIRTF, or Chandra.

It is likely that there will be dust obscured regions in or near the nuclei of many of the LIRG mergers in my sample but this should not pose a problem. This is demonstrated by Figure 2, an image of Antennae galaxies (NGC 4038/4039) by Mirabel et al. (1998). HST has resolved all but one of the star formation knots seen with ISO. This knot produces $\sim$half the infrared emission, and is clearly in a very dust extinguished region. The spatial extent of such regions is small compared with the total extent of the entire merger, and much can be learned by studying the kinematics of the gas and the star formation distribution outside these regions which are easily observable at optical and near-infrared wavelengths.

The final question outlined above will be answered by calculating near- and far- infrared merger luminosity functions using DSS, 2MASS and IRAS data for the S+F catalogue. Incompleteness in the S+F catalogue and the morphological merger selection criteria will be accounted for with space density calculations (Schmidt 1968, Felten 1976) and by redshifting the images to the redshift limit of the sample and repeating the selection process. If the current star formation and AGN fraction traced by the LIRG infrared excess is from mergers, the merger luminosity function plus a Schecter (1976) or lognormal function (Isobe & Feigelson 1992) should give the infrared luminosity function, providing selection effects have been dealt with. The NIR emission is dominated by the old stellar population. If the NIR merger luminosity function shows a similar excess, then the initial burst of star formation triggered by the merger probably occured atleast 1×10^8 years ago. The timescale of the merger is thought to be 1×10^8 years, so its possible that if an excess is observed, it will be due to evolved mergers.

3. AGN activity, star formation and gas properties.

Here, I will be building on my theoretical modelling experience in order to estimate the AGN contribution to compare with the star formation, gas properties (distribution, kinematics), and age of the mergers.

In the late stages of the merger, gas may be accreted to the central regions to power an AGN (Barnes & Hernquist 1996), possibly obscured from view in the optical. The relationship between the merger and AGN activity is poorly understood. While some studies have found that the incidence of AGN is higher in interacting galaxies than in isolated galaxies (*eg* Veilleux et al. 1995), others have found a deficiency of AGNs in advanced mergers and strongly interacting systems (*eg.* Keel et al. 1985, Bushouse 1986).

Recently, new near- and mid-infrared diagnostics have been developed to determine the relative contribution of starburst and AGN activity to the infrared emission (*eg.* Genzel et al. 1998, Lutz et al. 1998, Laurent et al. 2000). These are empirical, and it remains unknown how properties of the galaxies such as metallicity, ionization parameter, and dust composition affect the derived AGN contribution to the total IR emission.

I have used detailed photoionization and shock models (MAPPINGS) combined with stellar population synthesis models to determine the effect of various parameters on optical diagnostic diagrams (Kewley et al. 2000a, 2000f, Dopita et al. 2000). I found that the scatter between different galaxies on these diagrams is largely due to metallicity variations, and that particular diagrams may be used to determine metallicity, ionization parameter and the possible range of starburst vs AGN contributions to the optical emission, as shown in Figure 3.

To study the impact of a merger on AGN activity, the contribution of an AGN to the total emission must be determined and it is therefore essential to generate detailed theoretical models for the infrared diagnostic diagrams to quantify the effects of metallicity, ionization parameter, and dust properties, with a view to answering the questions:

What is the AGN contribution to the infrared and optical emission? and how are these affected by merger age and gas kinematics?

MAPPINGS computes self-consistent bolometric dust models. I will incorporate the detailed IR emission spectrum of stochastically heated dust grains, the physics for which has been formulated by Guhathakurta and Draine (1989). Infrared grids of models for a range of intrinsic parameters will be calculated to quantize their effect on the infrared diagrams, such as that shown in Figure 4. This, combined with the near- and mid-infrared spectroscopy of my samples, will allow the relative contribution by AGN and star formation activity to be found for these galaxies. This is useful in a number of ways. It will enable the SFRs to be calculated without contamination from AGN contribution in composite galaxies (within a reasonable range of expected AGN contributions). The AGN contribution to the infrared can be compared with other properties of the merger such as merger age and gas kinematics to study the effect of the merger on AGN activity. The optical and the infrared AGN contributions can be used to identify galaxies with obscured AGN for further study.

4. Conclusion

This research has the potential to contribute significantly to our understanding of merging galaxies. Obtaining this understanding is essential for studies of mergers both nearby and in the early universe. The systematic study of the gas kinematics and stellar populations in the infrared and non-infrared merger samples as a function of merger age will greatly aid our understanding of merging galaxies, and the characteristics required for a merger to become infrared-bright. Determining the AGN contribution to the infrared and optical emission in galaxies will allow the merger impact on AGN activity to be studied in further detail and more reliable SFRs to be determined for composite galaxies. In addition, putting the infrared diagnostic diagrams on a theoretical basis will be extremely useful to the astronomical community and may prove to be useful in finding the metallicity, ionization parameter and other properties of dusty galaxies. Finally, the infrared merger luminosity function will tell us how important mergers are in the infrared.

Due to the multiwavelength nature of this study and its combination with detailed theoretical modelling, the Harvard-Smithsonian Center for Astrophysics is the ideal location to pursue this research at. Staff at CfA with expertise in the areas covered by this research include M. Ashby, L. Allen, L. Hernquist, J. Huang, J. Huchra, and H. Smith. In addition, CfA has access to much of the facilities required to carry out the observational aspects of this research: optical, infrared spectroscopy at the 1.5m or 6.5m Multiple Mirror Telescope, and 2MASS from the 1.3m telescope.

References

Antonucci,R.R.J. & Ulvestad,J.S. 1988, ApJS,330,L97.
Barnes, J. E., Hernquist, L. 1996, ApJ, 471, 115.
Bushouse, H. A. 1986, AJ, 91, 255.
Bushouse, H. A. 1987, ApJ, 320, 49.
Dopita, M. A., Kewley, L. J., Heisler, C. A., & Sutherland, R. S. 2000, ApJ, 542, 224.
Dottori, H. A. 1981, Ap&SS, 80, 267.
Felten, J. E. 1976, ApJ, 207, 700.
Fisher, K. B., Huchra, J. P., Strauss, M. A., Davis, M., Yahil, A., Schlegel, D. 1995, ApJS, 100, 69.
Fioc, M., & Rocca-Volmerange, B. 1997, A&A, 326, 950
Genzel, R. et al. 1998, ApJ, 498, 579.
González Delgado, R. M., Leitherer, C. & Heckman, T. M. 1999, ApJS, 125, 489.
Guhathakurta, P. & Draine, B. T. 1989, ApJ, 345, 230.
Hibbard, J. E. 1995, PhDT. "The Fate of Gas in Merging Disk Galaxies".
Hibbard, J. E. & Vacca, W. D. 1997, AJ, 114, 1741.
Hwang, C.-Y., Lo, K. Y., Gao, Y., Gruendl, R. A., Lu, N. Y. 1999, ApJ, 511, L17.
Isobe, T. & Feigelson, E. D. 1992, ApJS, 79, 197.
Kennicutt, R. C. et al. 1987, AJ, 93, 1011.
Kewley, L. J., Dopita, M. A., Sutherland, R. S., Heisler, C. A., Trevena, J. 2000a, ApJ, *submitted*.
Kewley, L. J., Heisler, C. A., Dopita, M. A., Lumsden, S. 2000b, ApJS, *in press*.
Kewley, L. J., Heisler, C. A., Dopita, M. A., Sutherland, R. S., Norris, R. P., Reynolds, J., & Lumsden, S. 2000c, ApJ, 530, 704.
Kewley, L. J., Dopita, M. A., Sutherland, R. S. 2000d, ApJL, *submitted*.
Kewley, L. J., Sault, R., Bell, J., Gray, D., Ekers, R. D. 2000e, *in prep.*.
Kewley, L. J., Dopita, M. A, Sutherland, R. S., Heisler, C. A., Trevena, J. 2000f, RMxAC, 9, 163.
Laurent, O. et al. 2000, A&A, 359, 887.
Liu, C. T. & Kennicutt, R. C. 1995, ApJS, 100, 325.
Leitherer, C. et al. 1999, ApJS, 123, 3.
Lutz, D., Spoon, H. W. W., Rigopoulou, D., Moorwood, A. F. M., & Genzel, R. 1998, A&A, 505, L103.
Marston, A. P. et al. 1999, AAS, 194, 110.
Mirabel, I. F., et al. 1998, A&A, 33, L1.
Sanders, D. B. et al. 1988, ApJ, 325, 74.
Schecter, P. 1976, ApJ, 203, 297.
Schmidt, M. 1968, ApJ, 151, 393.
Strauss, M. A., Davis, M., Yahil, A., & Huchra, J. P. 1992, ApJS, 83, 29.
Sutherland, R.S. & Dopita, M.A. 1993, ApJS, 88, 253.
Toomre, A. 1977, ARA&A, 15, 437.
Turner, A. M., 1997, PhDT, "Stellar Populations in Merging Galaxies".
Turner, J.L. & Ho,P.T.P. 1985,ApJ,299,L77.
Veilleux, S., Kim, D. -C., Sanders, D. B., Mazzarella, J. M., & Soifer, B. T. 1995, ApJS, 98, 171.
Veilleux, S., & Osterbrock, D.E. 1987, ApJS, 63, 295.
Veilleux, S., Sanders, D.B., & Kim, D.-C. 1999, ApJ, 522, 139.

Figures

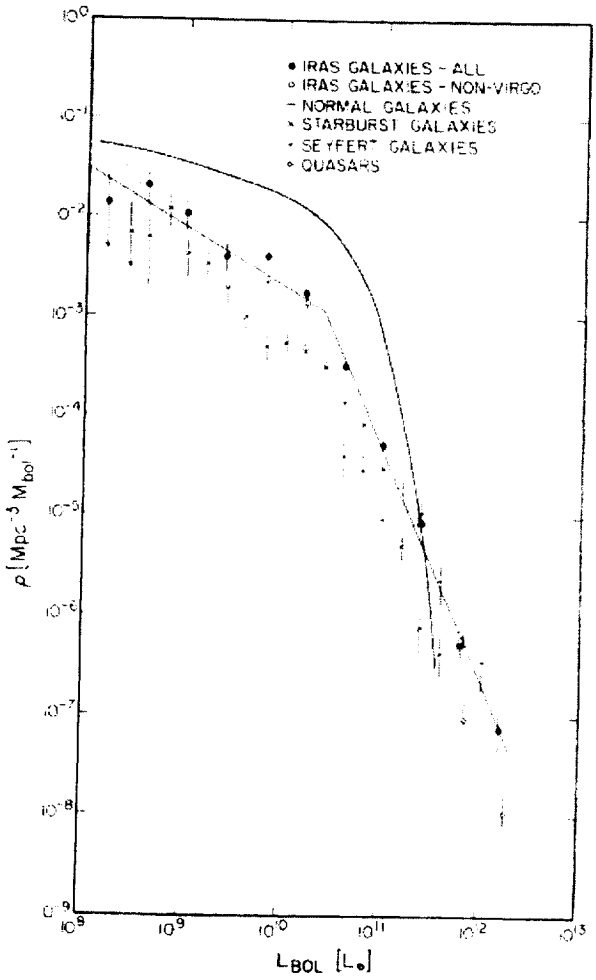

Fig 1: (left) Luminosity function for infrared and normal galaxies from Soifer et al. (1987). L_{BOL} is based on L_{FIR} (60μm - 100μm)

Fig 2: (below) Ground-based (top right), HST image (V & I band), and ISO contours (12-17 μm) of the Antennae galaxies (Mirabel et al. 1998).

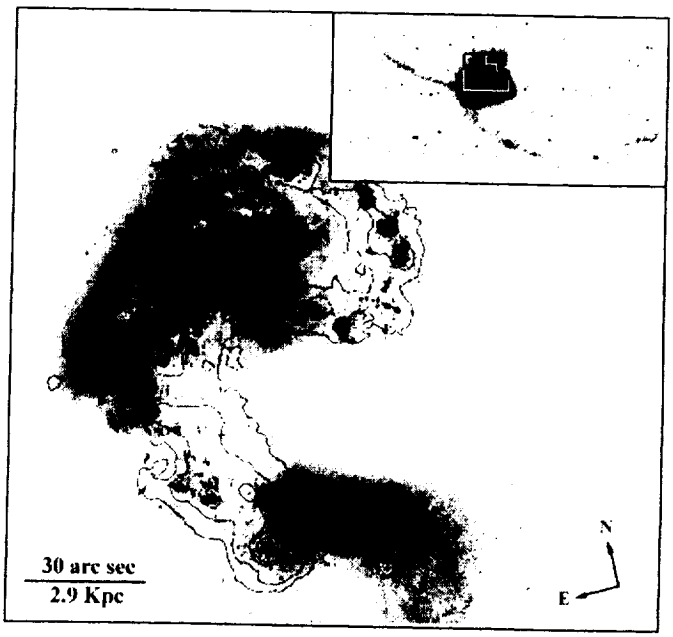

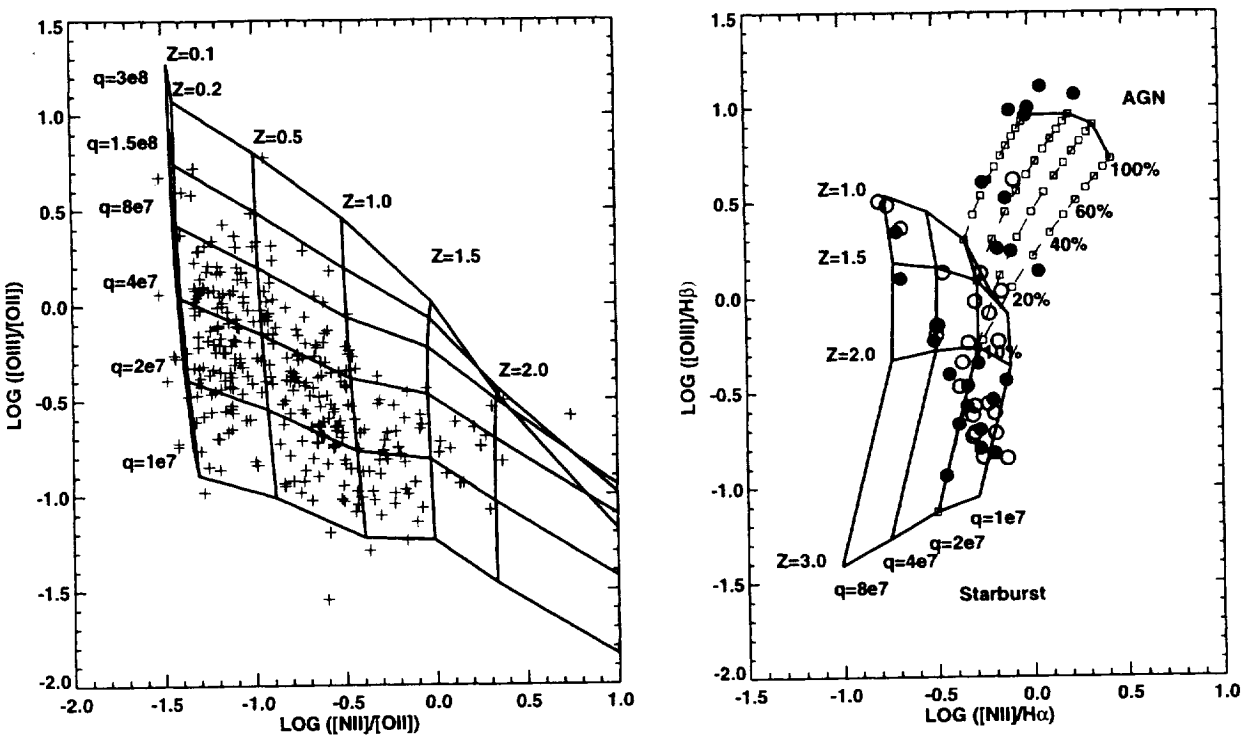

Fig 3: (a) left: This diagnostic diagram separates ionization parameter and metallicity. The grid is for instantaneous star formation, and is plotted against HII regions described in Dopita et al. (2000).
(b) right: Grids for continuous star formation, and for AGN (fast shocks or powerlaw ionizing radiation field) are shown along with mixing lines of constant metallicity and data on IR galaxies. The filled circles distinguish objects with compact radio sources described in Kewley et al. (2000c). All galaxies have metallicities greater than solar (Kewley et al. 2000f).

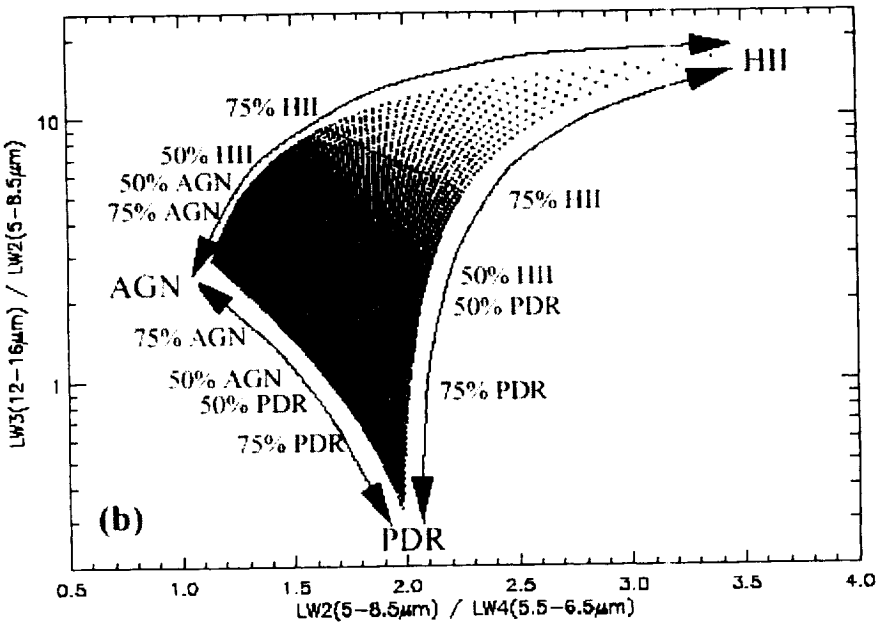

Fig 4: The diagnostic diagram of flux ratios (12-16μm)/(5-8.5μm) vs. (5-8.5μm)/(5.5-6.5μm), for determining contributions of AGN, HII region-like, and photo-dissociation regions (PDR) to the infrared emission. (Laurent et al. 2000).

Micro-Program, Transmission Line Theory and Design of Filters in the 20 to 60 μm Region.

1. Thin and Thick Metal Meshes as Filters for the Astrophysical Community

The astrophysical community needs for space missions in the infrared filters with a fixed resonance wavelength and a width of the transmission band of about 10% to 15%. One of the applications is emission measurements on astro-physical objects, such as galaxies. There is a great need or better filters and a US based capability (SOFIA, NGST, and SAFIR, etc). Filters using metal meshes, as a Fabry-Perot type filter, are used in the far infrared, from 60 to 1000 microns. These filters can not be made in the 20 to 60 micron region because of increasing manufacturing difficulties of the small geometrical pattern required as reflector plates and critical spacer thickness in the shorter wavelength region.

In the 20 to 60 micron region, inductive cross shaped meshes will be used as two coupled oscillator filters at distance of ¼ wavelength for minimum interaction. The geometrical pattern necessary for the mid infrared spectral region may well be fabricated and the spacing of the meshes is considerable less critical with respect to changing the resonance wavelength as in a Fabry-Perot filter. Cross shaped meshes on polyimide or polypropylene may be manufactured and the geometrical design parameters can be obtained from Micro-Stripes calculations. In a special geometrical arrangement, with metal meshes facing one another, the final resonance wavelength can be determined by transmission line theory. Free standing inductive metal meshes show an advantage. They have a smaller width of band for the same design parameters used for the thin meshes on dielectric substrates. The question which of the two mesh filters, the meshes on substrate or the free standing meshes, are better for space applications has to be determined after they have been manufactured and the transmittance studied. The main problems are the quality of the meshes and the substrates, absorption by the substrates and metal losses, as well as mechanical sturdiness.

While full wave propagation method is desirable, most often, the complexity of the structures dictates approximation methods. Two main simulation programs will be used throughout my post doctorate stay, Micro-Stripes, and Transmission line theory.

1. The Micro-Stripes Program

Micro-Stripes is a powerful software program ideal for the design of filters in the mid infrared spectral region. Micro-Stripes provides 3D electromagnetic analysis of arbitrary geometries results in time/frequency domain. The simulator uses the Transmission Line method (TLM). The TLM method is based on establishing a network of transmission lines that represents the physics of the problem, and finding equivalence between the electrical solutions of that network and the physical parameters of the problem. The directional output is simply a record of the ingoing and outgoing signals at the port. These signals are resolved by comparing E and H fields at two points, one on

each side of the reference plane. The arrangement is closely analogues to monitoring the signals in a waveguide by attaching a directional coupler.

In order to construct the computational mesh, a workspace needs to be defined, followed by the construction of the mesh. Each mesh is actually defined by a small rectangular homogenized cell and each cell is entirely empty or entirely filled with the same metal or dielectric. Accuracy is defined as a greater amount the number of cells (greater accuracy means longer calculation time). Micro-Stripes simulator works in the time domain. Depending on the size of the problem, it can take as much as several seconds of computer run- time to simulate each nano-second in real time.

The Micro-Stripes program needs for the calculation of the transmittance the geometrical parameters, the thickness and refractive index of the dielectric substrates and the surface impedance of the metal mesh. The calculation of the resonance wavelength and resonance width are accurate within a few percent for single metal meshes, free standing or on a dielectric substrate. Since Micro-Stripes works with a set-up similar to a waveguide, the openings of two meshes are either lined up or shifted, one with respect to the other.

2. Transmission Line Theory

Transmission line theory assumes that two meshes may have just a little shift or rotation with respect to the other and assumes no lined up opening of the meshes. Therefore transmission line theory is used for the determination of the optimum distance of a two mesh filter.

One mesh needs for the calculations three important parameter, the resonance wavelength, the width of band and the loss parameter. The transmittance of a mesh with resonance wavelength λ_R of a single mesh, corresponding to the frequency $\omega_0 = g/\lambda_R$, is obtained from Micro-Stripes calculations and used as parameter.

A shift of the resonance wavelength by the factor $(n_1^2 + n_2^2)^{1/2}/2$ is implemented for the case of a metal meshes with an interface of two dielectrics of refractive index n_1 and n_2. This shift is lower when the mesh is on a dielectric substrate. The width of resonance band parameter A1 is obtained by adjusting the transmission line transmittance curve to the Micro-Stripes transmittance curve. The loss parameter a1 is taken as 0.001 from the literature. The transmission line theory does not include the dependence of the resonance wavelength on small thicknesses of the dielectric spacer. It assumes a shift as given by the above formula for a mesh on the interface of two dielectrics with refractive index n_1 and n_2